

Dissertation zur Erlangung des Doktorgrades
der Fakultät für Chemie und Pharmazie
der Ludwig-Maximilians-Universität München

**Blocking the “Don’t eat me” checkpoint
in acute myeloid leukemia —
development of a novel antibody format**



Nadine Moritz

aus

Steyr (Österreich)

2016

Erklärung

Diese Dissertation wurde im Sinne von § 7 der Promotionsordnung vom 28. November 2011 von Herrn Prof. Karl-Peter Hopfner betreut.

Eidesstattliche Versicherung

Diese Dissertation wurde eigenständig und ohne unerlaubte Hilfe erarbeitet.

München, am 26.1.2016

.....

(Nadine Moritz)

Dissertation eingereicht am 26.1.2016

1. Gutachter: Herr Prof. Dr. Karl-Peter Hopfner

2. Gutachter: Herr Prof. Dr. Klaus Förstemann

Mündliche Prüfung am 16.3.2016

During the work of this thesis, the following patent application was published:

LMU Munich, Hopfner K.P., Moritz N., Fenn N., Subklewe M. (09.11.2015): “Novel Molecule Combining Specific Tumor Targeting and Local Immune Checkpoint Inhibition.”
EP15193711.7

Parts of the present thesis will be submitted for publication:

Moritz N., Ernst A., Krupka C., Fenn N., Lauber K., Subklewe M., Hopfner K.P.: manuscript
in preparation

TABLE OF CONTENTS

1. SUMMARY	1
2. INTRODUCTION	3
2.1. ANTIBODY THERAPY OF CANCER	3
2.1.1. HISTORY OF ANTIBODY THERAPY	3
2.1.2. STRUCTURE AND FUNCTION OF MABS	5
2.2. IMMUNE CHECKPOINTS	7
2.2.1. CANCER IMMUNOTHERAPY MARKET	8
2.2.2. COMBINATION THERAPY	9
2.3. LEUKOCYTE SURFACE ANTIGEN CD47	13
2.4. SIGNAL REGULATORY PROTEIN A	16
2.5. THE “DON’T EAT ME” CHECKPOINT IN ACUTE MYELOID LEUKEMIA	18
2.6. CONVENTIONAL AML THERAPY	21
2.7. ANTIBODY THERAPY FOR AML	22
3. AIM OF THE THESIS	25
4. MATERIALS AND METHODS	27
4.1. MATERIALS	27
4.1.1. TECHNICAL EQUIPMENT	27
4.1.2. SOFTWARE	28
4.1.3. OLIGONUCLEOTIDES	28
4.1.4. AMINO ACID SEQUENCES	30
4.1.5. BUFFERS	31
4.1.6. ANTIBODIES	32
4.2. MOLECULAR BIOLOGY METHODS	33
4.2.1. MOLECULAR CLONING	33
4.2.2. POLYMERASE CHAIN REACTION (PCR)	34
4.2.3. SITE-DIRECTED MUTAGENESIS	35
4.3. PROTEIN BIOCHEMISTRY METHODS	36
4.3.1. PERIPLASMIC PROTEIN EXPRESSION IN <i>E.COLI</i>	36
4.3.2. PURIFICATION OF POLYHISTIDINE-TAGGED PERIPLASMIC PROTEINS	36

4.3.3.	EXPRESSION OF LICADS IN HUMAN FREESTYLE™ 293-F CELLS	37
4.3.4.	PURIFICATION OF POLYHISTIDINE-TAGGED LICADS FROM FREESTYLE™ 293-F CELL SUPERNATANT	37
4.3.5.	EXPRESSION OF LICAD PROTEINS IN SCHNEIDER 2 CELLS	38
4.3.6.	PURIFICATION OF POLYHISTIDINE-TAGGED LICAD PROTEINS FROM S2 CELL SUPERNATANT	39
4.3.7.	DISCONTINUOUS POLYACRYLAMIDE GEL ELECTROPHORESIS (SDS-PAGE)	39
4.3.8.	WESTERN BLOT ANALYSIS	40
4.3.9.	SMALL ANGLE X-RAY SCATTERING (SAXS)	40
4.4.	CELL CULTURE METHODS	41
4.4.1.	CELL LINES AND MEDIA	41
4.4.2.	MAINTENANCE OF CELLS	43
4.4.3.	siRNA MEDIATED TRANSIENT KNOCK DOWN OF CD47 IN FREESTYLE™ 293-F HEK CELLS AND TRANSFECTION OF CONTROL PROTEINS	44
4.4.4.	GENERATION OF CD47 AND CD33 FLP-IN™ CHO CELL LINES	44
4.4.5.	ISOLATION OF PERIPHERAL BLOOD MONONUCLEAR CELLS (PBMCs) FROM WHOLE HUMAN BLOOD	45
4.4.6.	EXPANSION OF HUMAN NK CELLS FROM WHOLE HUMAN BLOOD	45
4.4.7.	CELL STAINING AND ANALYSIS OF SURFACE MARKER	46
4.4.8.	BINDING STUDIES	46
4.4.9.	K _D DETERMINATION OF LICADS	46
4.4.10.	CYTOTOXICITY ASSAY	47
4.4.11.	PREFERENTIAL LYSIS OF CD47 ⁺ CD33 ⁺ TARGET CELLS	48
4.4.12.	CD14-POSITIVE SELECTION OF MONOCYTES	49
4.4.13.	PKH67 STAINING OF MONOCYTES AND THP-1 CELLS	50
4.4.14.	PKH26 STAINING OF MOLM - 13 AND THP-1 CELLS	50
4.4.15.	GENERATION OF THP-1 MACROPHAGES	50
4.4.16.	GENERATION OF M2 MACROPHAGES	50
4.4.17.	PHAGOCYTOSIS ASSAY	51
4.4.18.	NK CELL MEDIATED CYTOTOXICITY OF <i>EX VIVO</i> EXPANDED AML CELLS	52
5.	RESULTS	53
5.1.	CLONING AND EXPRESSION OF LICADS IN FREESTYLE™ 293-F CELLS	53

5.1.1.	EXPRESSION OF SIRP EX. α CD16. α CD33, SIRPIG. α CD16. α CD33 AND SIRPIG.SIRPIG. α CD16. α CD33	54
5.1.2.	EXPRESSION OF SIRPIG_CV1. α CD16. α CD33 AND α CD47. α CD16. α CD33	57
5.2.	SIRNA MEDIATED TRANSIENT KNOCK DOWN OF CD47 IN FREESTYLE™ 293-F CELLS	58
5.3.	CLONING AND EXPRESSION OF LICADS IN <i>DROSOPHILA MELANOGASTER</i> SCHNEIDER 2 CELLS	59
5.4.	SMALL-ANGLE X-RAY SCATTERING OF SIRPIG.αCD16.αCD33 AND SIRPIG.SIRPIG.αCD16.αCD33	62
5.5.	BINDING STUDIES OF LICAD PROTEINS	64
5.6.	GENERATION OF CHO FLP-IN™ CELLS STABLY EXPRESSING CD33 AND CD47	66
5.7.	BINDING STUDIES OF LICAD PROTEINS ON CHO CELL LINES	67
5.7.1.	K _D DETERMINATION OF LICAD PROTEINS ON CHO CELL LINES	69
5.8.	BIOLOGICAL FUNCTIONALITY OF LICAD PROTEINS	72
5.8.1.	CYTOTOXICITY ASSAY WITH <i>IN VITRO</i> IL-2 EXPANDED NK CELLS	72
5.8.2.	CYTOTOXICITY ASSAY WITH PRIMARY NK CELLS	73
5.8.3.	LICAD DEPENDENT PHAGOCYTOSIS	77
5.8.4.	PREFERENTIAL KILLING OF CD33 FLP-IN™ 293 HEK CELLS	82
5.8.5.	NK CELL MEDIATED LYSIS OF AML PATIENT BLAST SAMPLES	88
6.	<u>DISCUSSION</u>	<u>91</u>
6.1.	GENERATION AND EXPRESSION OF LICADS, A NOVEL TRISPECIFIC ANTIBODY FORMAT	92
6.2.	LICADS EXHIBIT LOW BINDING AFFINITY TO CD47	94
6.3.	LICAD MOLECULES ARE ABLE TO RECRUIT NK CELLS AND INDUCE TUMOR CELL CYTOTOXICITY	96
6.4.	LICADS INCREASE PHAGOCYTIC UPTAKE OF TUMOR CELLS IN MACROPHAGES	98
6.5.	LICADS PREFERENTIALLY KILL CD47/CD33 POSITIVE TUMOR CELLS	100
6.6.	LICADS INDUCE NK CELL MEDIATED KILLING OF PRIMARY AML PATIENT SAMPLES	101
6.7.	FUTURE DIRECTIONS FOR LICAD MOLECULES	102
7.	<u>REFERENCES</u>	<u>I</u>
8.	<u>ABBREVIATIONS</u>	<u>XIX</u>
9.	<u>ACKNOWLEDGEMENTS</u>	<u>XXIII</u>

SUMMARY

SUMMARY

Over the last decades, immunotherapy has become a mainstream approach in the treatment of cancer. Hopes within the scientific community were raised in particular by the groundbreaking success of blocking immune checkpoints, which tightly regulate the activity of immune effector cells by monoclonal antibodies (mAbs). Signal regulatory protein α (Sirp α) is a receptor mainly expressed on immune cells of the myeloid lineage such as macrophages or dendritic cells (DCs). It constitutes an immune checkpoint by binding its ligand CD47, which is ubiquitously expressed on all human cells. Interaction of Sirp α and CD47 inhibits signaling within the immune cell and leads to the “Don’t eat me” signal. In preclinical studies it has been shown that inhibition of the Sirp α -CD47 interaction by mAbs against CD47 leads to an increased phagocytosis of acute myeloid leukemia (AML) cell lines. Additional targeting of tumor cells by another tumor specific mAb even further increased the effect of tumor cell eradication.

This work presents the creation and *in vitro* analysis of a newly-developed antibody derivative, which specifically targets AML cells and simultaneously inhibits the Sirp α -CD47 interaction on CD16 expressing effector cells. We recombinantly linked either the naturally occurring Sirp α extracellular domain or an anti-CD47 single chain fragment variable (scFv) to a central anti-CD16 scFv and a C-terminal anti-CD33 scFv, yielding a molecule that we named a **local inhibitory Checkpoint Antibody Derivative** (liCAD). In order to express different liCAD molecules a new insect cell expression system was successfully established. We could obtain pure, monomeric proteins through a 3-step purification procedure and were able to detect binding of all individual binding domains.

Subsequent *in vitro* data supported our hypothesis that the local blocking of CD47 on natural killer (NK) cells as well as macrophages induces tumor cell killing and phagocytosis, respectively. We could also show that the low affinity interaction of the extracellular domain of Sirp α within the liCAD with CD47 on cells leads to a preferential killing of CD47/CD33 double positive cells compared to CD47 single positive cells. In addition, liCAD molecules

SUMMARY

were tested on primary AML patient samples, where we could also show increased activation of NK cells compared to control constructs.

1. INTRODUCTION

1.1. Antibody therapy of cancer

1.1.1. History of antibody therapy

The idea of a magic bullet, as phrased by Paul Ehrlich in the beginning of the 20th century, that could target specifically different antigens on cells was realized in 1975, when Kohler and Milstein developed a procedure to efficiently produce monoclonal antibodies (mAbs) through a technique called “hybridoma technology” (Kohler and Milstein, 1975). Strong hopes have been put into these very stable molecules, which seemed to be ideal reagents for imaging and therapy. The initial excitement was soon replaced by disappointment, however, when serious problems were observed while using these proteins as therapeutics. The first attempts to use these molecules in therapy had the major drawback that they were of mouse origin and were therefore recognized as foreign when administered to patients leading to graft versus host disease. Furthermore, antibodies were not properly recognized by the patient’s immune system, resulting in severely restricted biological efficacy (Chames et al., 2009).

The advent of antibody engineering made it possible to create chimeric mAbs in which mouse variable domains, which bind the antigen on the target cell, are fused with human constant domains (Neuberger et al., 1985). These antibodies are 70% human and therefore exhibit considerably lower immunotoxicity. An even less immunogenic molecule could be generated by the development of a technology called “complementarity-determining region (CDR) grafting” (Jones et al., 1986). In these humanized antibodies, the CDRs (also referred to as hypervariable loops) of a human antibody are replaced by the hypervariable loops of a murine antibody, resulting in an 85-90% human antibody.

INTRODUCTION

Since the approval of the first chimeric mAb in the late 1990, the rate of product approvals and sales of monoclonal antibody products has increased dramatically (as shown in Figure 1) and at this point in time, most of the approved mAbs used in clinical therapy are either chimeric, humanized or, more recently, fully human (Ecker et al., 2015).

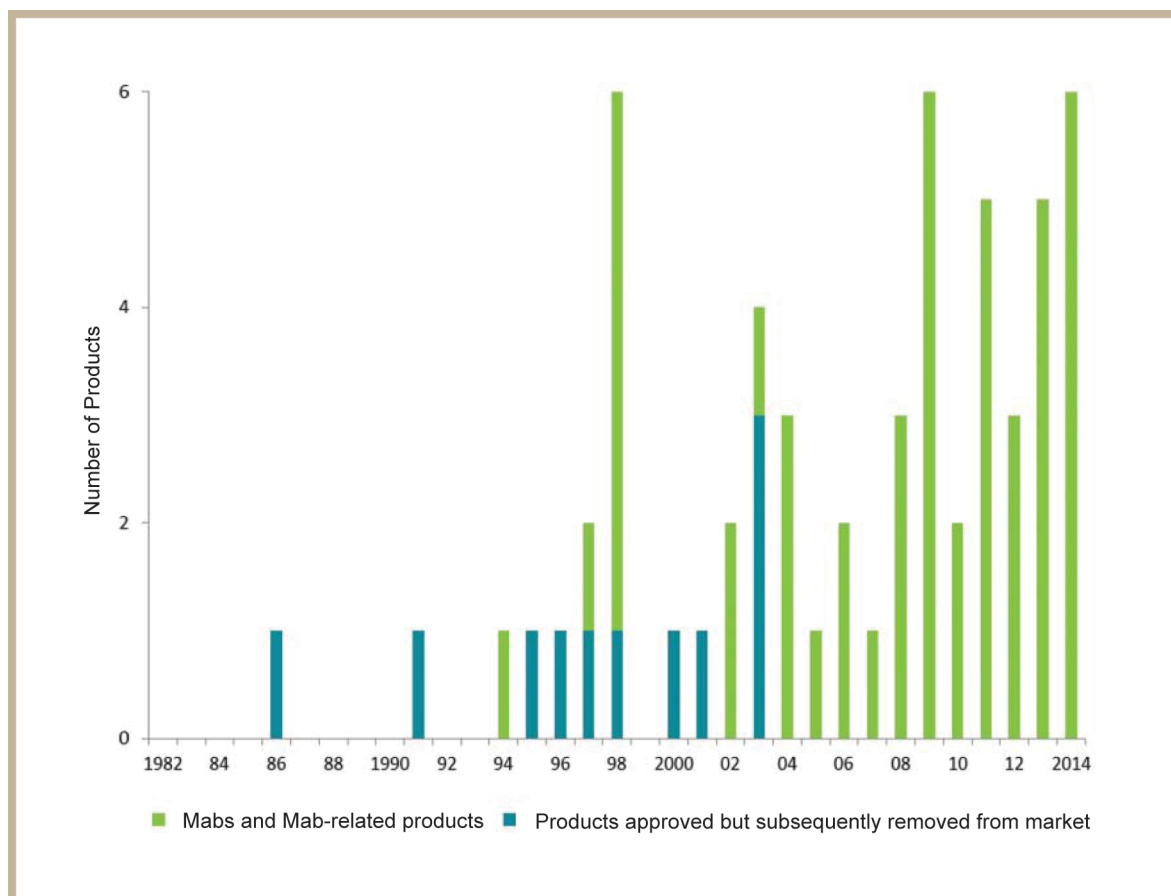


Figure 1 Annual approval of mAbs for therapy in the US and Europe. Overview of mAbs and derivatives that are either approved and on the market (green) or were approved and subsequently withdrawn from the market (blue). Figure taken from (Ecker et al., 2015).

Impressive results were obtained in cancer therapy and the use of mAbs is now one of the most successful and important strategies for treating patients with blood cancer and even solid tumors.

INTRODUCTION

1.1.2. Structure and function of mAbs

In cancer immunotherapy the immunoglobulin G (IgG) format is by far the most promising of the five-existing immunoglobulin classes, due to its ability to bind to and activate Fc gamma receptors (FcγR), and thus induce an immune response.

Monoclonal IgG antibodies are large proteins with a size of 150 kDa. They form homodimers with two identical heavy chains (of approximately 50 kDa each) and two identical light chains (of approximately 25 kDa each). From a structural point of view, the heavy chain is formed from four tandem immunoglobulin folds whereas the light chain is formed from two (depicted in Figure 2A).

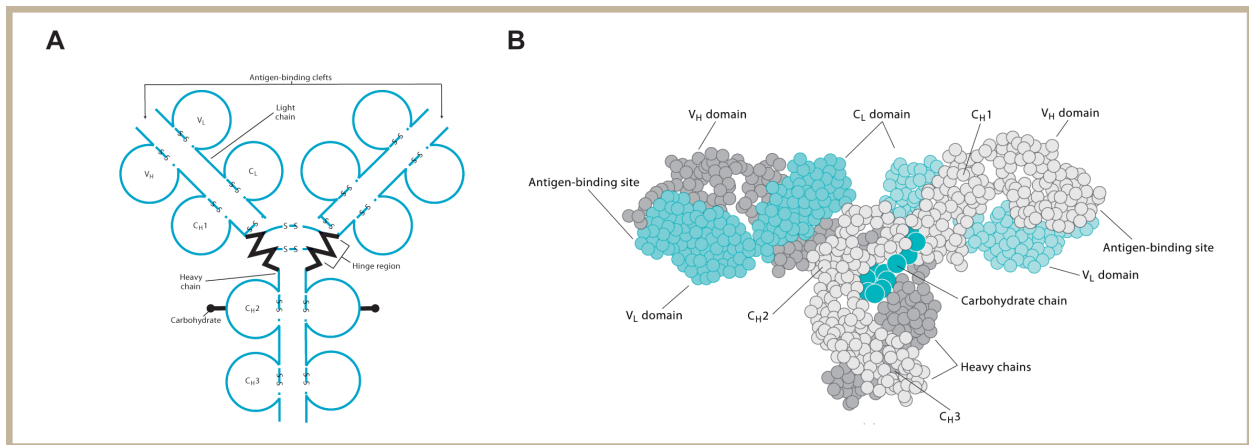


Figure 2 Structure of an IgG antibody. (A) Schematic representation of an IgG antibody with N-terminal variable domains followed by three or one constant domains in case of heavy and light chain, respectively. V_H/V_L and C_{H1}/C_L form the Fab fragment (fragment antigen binding) whereas C_{H2} and C_{H3} constitute the Fc fragment (fragment crystallizable). (B) X-ray crystallography revealed the Y-shaped three-dimensional structure of the IgG molecule. Each sphere represents an amino acid. Light chains are shown in blue and heavy chains are shown in grey. V_H , variable domain of the heavy chain. V_L , variable domain of the light chain. C_H , constant domain of the heavy chain. Figure adapted from “Immunology: Understanding the immune system” (Elgert, 1998).

Each fold consists of two anti-parallel β -sheets with an intra-molecular disulfide bond. Uniqueness is conferred upon the antibody by three loops, which are highly variable in length and sequence that connect the β -sheets within the N-terminal domains of each chain.

INTRODUCTION

The six hypervariable loops or complementarity-determining regions (CDRs) form a unique surface that specifically recognizes and binds the antigen (Maynard and Georgiou, 2000).

Figure 3 summarizes the natural effector functions of an antibody. In the simplest mode of action, the mAb binds and interferes with the activity and interaction of its binding partners, resulting in blockade of the receptor, receptor internalization or the induction of apoptosis. Whereas the Fab fragment of an antibody is responsible for antigen binding, the Fc part is responsible for not only its long half-life but also for its effector functions, including antibody-dependent cellular cytotoxicity (ADCC), complement-dependent cytotoxicity (CDC) as well as antibody-dependent cellular phagocytosis (ADCP).

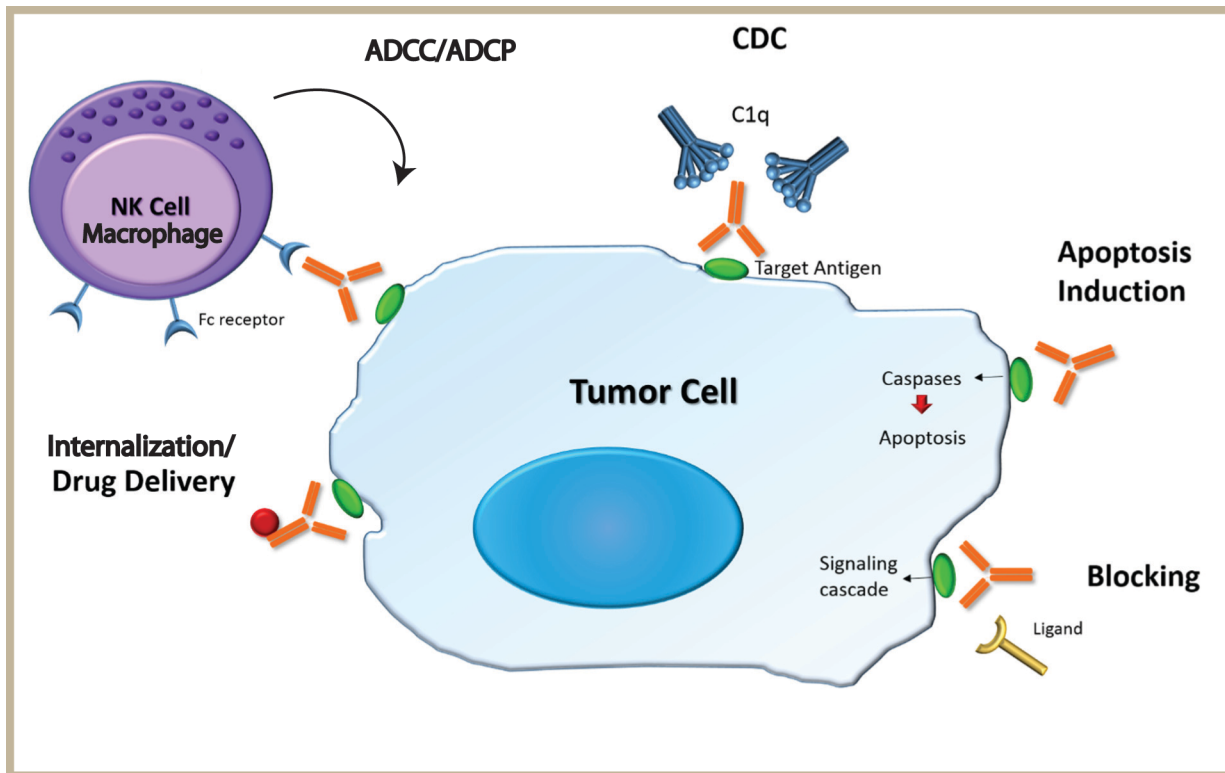


Figure 3 Major functions of antibodies important in cancer immunotherapy. mAbs can induce antibody dependent cell-mediated cytotoxicity (ADCC) by inducing the release of cytotoxic granules in effector cells (e.g. NK cells) or antibody-dependent phagocytosis (ADCP). Other effector functions of mAbs include complement-dependent cytotoxicity (CDC), which starts with the binding of C1q to the antibody triggering the complement cascade, and the induction of apoptosis by activation of capsases. In addition, mAbs can block receptor/ligand interactions, preventing signaling cascade activation, or specifically deliver drugs into tumor cells by receptor internalization. Figure adapted from (Loureiro et al., 2015).

INTRODUCTION

One of the most important effector functions for mAbs is the induction of ADCC as well as CDC as shown by the first mAb approved for cancer therapy, rituximab (Weiner, 2010). A more recent discovery is the application of mAbs that modulate immune cell function such as e.g. T cells by blocking so called immune checkpoints.

1.2. Immune checkpoints

When the immune system is responding to a pathogenic infection under normal physiological conditions, immune checkpoints prevent healthy cells and tissues from damage by maintaining self-tolerance (Pardoll, 2012).

In case of T cells, for example, a reasonable activation depends first on the interaction of the T cell receptor (TCR) with the corresponding antigen and also on the regulation of the balance between co-stimulatory and co-inhibitory receptors on the immune cell. Recently, it has been discovered that the expression of immune checkpoint ligands can be dysregulated by tumor cells as a mechanism of escaping tumor immune surveillance. The importance of immune checkpoint inhibition was emphasized by the *Science* magazine, which awarded cancer immunotherapy the “breakthrough of the year 2013”, mainly due to the great success of mAbs against the cytotoxic T-lymphocyte antigen 4 (CTLA-4) and programmed death-1 (PD-1) (Cousin-Frankel, 2013).

Not only T cells are regulated by immune checkpoints, however. In the case of natural killer (NK) cells there also seems to be a balance between activating and inhibiting signals via corresponding receptors that induce potentially harmful effector functions. Indeed, increasing experimental evidence supports the idea that NK cell activation is under the control of different checkpoints. One of the most promising targets under close investigation are the killer cell immunoglobulin-like (KIR) receptors. KIRs bind to MHC class I on cells and transfer an inhibitory signal within NK cells. Blocking these receptors facilitates activation of NK cells and, potentially, destruction of tumor cells by the latter (Moretta et al., 2004).

Macrophages as well as dendritic cells (DCs) are other possibly important immune cell populations that could be targeted by checkpoint inhibition. Macrophages express all classes of Fc receptors and a number of studies have shown that ADCP is a major mechanism during

INTRODUCTION

antibody therapy. It has been recognized that the interaction of CD47 with the myeloid receptor signal regulatory protein alpha (SIRP α) serves as a myeloid-specific immune checkpoint that limits the response of macrophages to antibody therapies (Weiskopf and Weissman, 2015). Therefore, blocking of CD47 or SIRP α might be another powerful strategy to induce immunotherapy.

1.2.1. Cancer immunotherapy market

As mentioned above, two of the most prominent inhibitory receptors studied extensively in the last years are cytotoxic T-lymphocyte antigen 4 and programmed death-1, both of which are negative regulators of cytotoxic T cell activation.

The first immune checkpoint mAb approved for malignant melanoma by the Food and Drug Administration (FDA) in 2011 was an antibody against CTLA-4 called ipilimumab (trade name Yervoy; Bristol-Myers Squibb), which has subsequently been approved in more than 40 countries. CTLA-4 counteracts the activity of the T cell co-stimulatory receptor CD28, most likely by outcompeting common binding partners CD80 (or B7.1) and CD86 (also known as B7.2) (Schwartz, 1992), and subsequently delivers an inhibitory signal to the T cell (Schneider et al., 2006). The second prominent checkpoint receptor is PD-1, which is mainly expressed on T cells in peripheral tissues during inflammatory response to infection and to prevent autoimmunity (Freeman et al., 2000; Ishida et al., 1992). It binds to PD-1 ligand 1 (PD-L1) and PD-1 ligand 2 (PD-L2) and consequently inhibits kinases that are involved in T cell activation by the phosphatase SHP-2 (Freeman et al., 2000; Latchman et al., 2001). So far, two anti-PD-1 specific mAbs have been approved by the regulators for malignant melanoma. Nivolumab (trade name Opdivo; Bristol-Myers Squibb) was approved in July 2014 in Japan and later by both the FDA and the European Medicines Agency (EMA). Pembrolizumab (trade name Keytruda; Merck & Co.) gained accelerated FDA approval for advanced and unresectable malignant melanoma in September 2014 (Webster, 2014).

CTLA-4 and PD-1 represent two of the most prominent recently targeted checkpoints, but there are certainly various immune checkpoint receptors expressed on different effector cells, resulting in potentially different mechanisms of checkpoint inhibition and mobilization of the

INTRODUCTION

immune system. Two further examples of inhibitory receptors on activated T cells are Lymphocyte activation gene 3 (Lag 3) and T cell membrane protein 3 (Tim3). The blocking of these receptors by mAbs is of great scientific interest and represents a novel strategy of unleashing the power of T cells to eradicate tumors (Grosso et al., 2009; Sakuishi et al., 2010; Zhu et al., 2005). BMS-986016 (Bristol-Myers Squibb) for example is an anti-Lag 3 antibody that is currently being tested in a phase I clinical trial. Another class of inhibitory receptors that are not only expressed on T cells but also on NK cells are KIRs. Their importance is well studied in NK cell activation as mentioned above and with BMS-986015 (Lirilumab; Bristol-Myers Squibb) a first mAb against a KIR is currently enrolled in a phase II study (Pardoll, 2012; Webster, 2014).

Market researchers predict that the immune checkpoint inhibitor market will experience enormous growth to approximately 7 billion US\$ by 2020 across the seven major markets (US, France, Germany, Italy, Spain, UK and Japan) (Webster, 2014).

1.2.2. Combination therapy

Even though the advent of checkpoint inhibitors has revitalized the hope of successful antibody therapy to treat cancer, many clinical studies have revealed that many patients do not respond appropriately, if at all, to monospecific therapy (Chen et al., 2010). Considering the fact that cancer is often a multifactorial disease, in which tumors acquire mutations, it is not surprising that targeting a single tumor target does not appear to be sufficient to eliminate cancer cells (Spasevska et al., 2015).

As outlined previously, the blockade of CTLA-4 and PD-1 has been proven to potently induce the T cell response to tumors when applied as single therapy. It has already been demonstrated in a pre-clinical B16 melanoma model that inhibition of both checkpoints in parallel leads to better killing of tumor cells because of the increased number of infiltrating T cells (Curran et al., 2010). Strikingly, clinical studies revealed that combining both mAbs led to an even higher overall response rate in advanced melanoma patients (Larkin et al., 2015; Tsai and Daud, 2015).

INTRODUCTION

The immune system may be effectively stimulated by approaches other than the dual blockading of checkpoints. Advances in antibody engineering have facilitated the generation of novel antibody formats that can bind two or more different epitopes on tumor cells or immune cells or both. Different approaches to using these so called bispecific antibodies (bsAbs) are currently being used. Some antibodies are designed to target two different epitopes or antigens on tumor cells and thereby inhibiting two signaling pathways. In contrast, others are capable of binding immune cells and tumor cells, and thus link effector cells such as T cells, NK cell or macrophages with cancer cells, inducing the destruction of the latter. So far two main groups of bsAbs have been of great scientific interest: IgG-like bsAbs and small single chain fragment variable (scFv)-based bsAbs (Spasevska et al., 2015).

The first successful Ig-like bsAbs to be generated and enter both clinical trials as well as clinics were TriomAbs[®] (Figure 4). TriomAbs[®] are mouse/rat chimeric antibodies, which are generated by somatic fusion of two hybridoma cell lines to form quadromas (Lindhofer et al., 1995). In 2009 the EMA approved catumaxomab (trade name Removab; Fresenius Biotech), a trifunctional bsAb against Epcam and CD3, for the treatment of malignant ascites in patients with EpCAM positive carcinomas in cases where standard therapy is not available or no longer feasible (Chames and Baty, 2009). Catumaxomab surprisingly interacts with human activating Fc gamma receptors (FcγRI and FcγRIII) but not inhibiting Fc gamma receptors (FcγRIIB) and is thereby able to activate T cells as well as DCs, NK cells and macrophages (Zeidler et al., 2000; Zeidler et al., 1999). Nonetheless, side effects are frequently associated with catumaxomab and other strategies to produce less immunogenic molecules are therefore being widely studied.

Progress in genetic engineering has made it possible to generate fully human molecules with even higher yields of functional bsAbs. Techniques such as the “knob-into-holes” approach, the common light chain approach, CrossmAb approach or the Dual-Variable-Domain Ig (DVD-Ig) approach pin hope on advanced and closer traditional IgG molecules for effective immunotherapy (Figure 4). One promising example is RO5520985 (Roche), a CrossmAb bsAb against Angiopoietin 2 (Ang2) and vascular endothelial growth factor (VEGF) that has shown in pre-clinical studies superior anti-tumor effects when compared to mAbs against

INTRODUCTION

those factors alone (Kienast et al., 2013). This molecule is currently being tested in a phase I study for administration to patients with advanced solid tumors (Hidalgo et al., 2014).

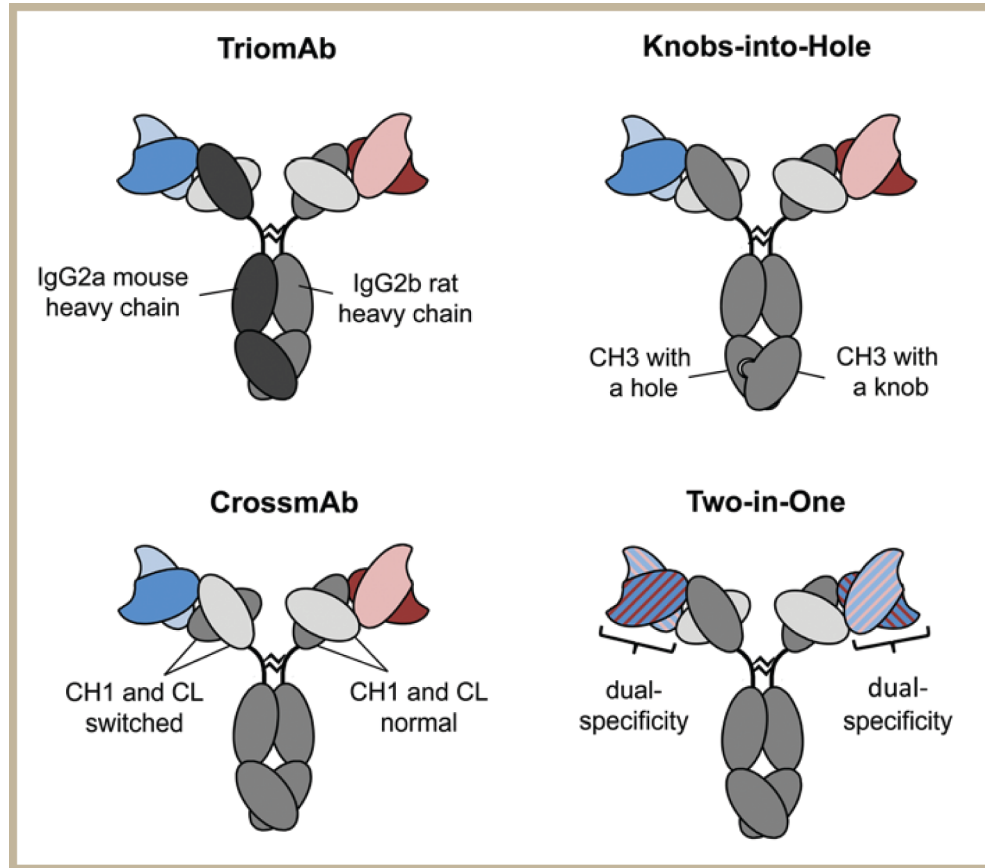


Figure 4 Different strategies for the generation of IgG-based bsAbs. Figure adapted from (Hess et al., 2014)

The second class of bsAbs mentioned above is scFv-based bsAbs. Here one molecule, the BiTE, in particular caused excitement in the scientific community. A BiTE (bispecific T cell engager) consists of one scFv against CD3 and one scFv against a tumor antigen connected via a small flexible linker (Mack et al., 1995). They potently activate T cells by forming a lytic immunological synapse only upon binding of several molecules to the tumor antigen and CD3 expressed on T cells (Wolf et al., 2005).

The FDA granted accelerated approval in December 2014 for blinatumomab (trade name Blincyto, Amgen) against acute B-cell lymphoblastic leukemia treatment, making it the first bsAb approved in the US (Sanford, 2015). Blinatumomab targets the surface antigen CD19, which is expressed on both healthy and malignant B cells, but it could be shown that the

INTRODUCTION

elimination of normal CD19 positive B cells is tolerable. Active at very low concentrations, it has been shown to be highly effective in the treatment of patients with non-Hodgkin's lymphoma (NHL) and in patients with relapsed or refractory B-precursor acute lymphoblastic leukemia (Bargou et al., 2008). This groundbreaking success raised hope that BiTEs could be used for the treatment of other hematological cancers, such as acute myeloid leukemia (AML), or even solid tumors. To date, Amgen has two more BiTEs against the epithelial cell adhesion molecule (EpCAM) and the carcinoembryonic antigen (CEA), respectively in phase 1 clinical trials (Spasevska et al., 2015).

Although BiTEs are the only scFv-based bsAbs that have so far made it into the clinics, there are certainly more formats to be considered in the future, for example diabodies, triplebodies or tetravalent tandem diabodies, which exhibit a superior cytotoxicity and potency relative to diabodies (Holliger et al., 1993; Reusch et al., 2014; Schubert et al., 2011).

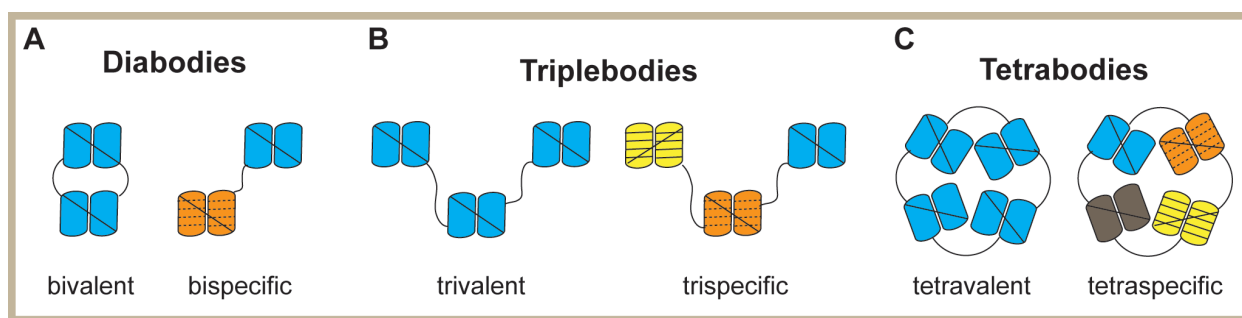


Figure 5 Illustration of various scFv-based bsAbs. (A) Diabodies consisting of two scFvs connected via a flexible linker having either one specificity (bivalent) or two different specificities (bispecific), as in a BiTE molecule. **(B)** Triplebodies have three scFvs connected via flexible linkers and **(C)** tetrabodies have four scFvs connected.

A new class of scFv-based bsAb was generated by the company Immunocore and is called Immune mobilising monoclonal TCRs Against Cancer (ImmTACs). ImmTACs target the major histocompatibility complex (MHC)-peptide complex and offer for the first time the possibility to target not only membrane antigens but also intracellular proteins of cancer cells (Oates and Jakobsen, 2013). It has to be pointed out that although small bsAbs are more effective in tissue penetration compared with larger IgG-based bsAbs, they exhibit shorter

INTRODUCTION

half-lives and thus require continuous infusion. This suggests further improvements are required to increase their serum half-life (Chames et al., 2009).

Surprisingly, no bsAb format that combines checkpoint inhibition together with tumor cell targeting within a single molecule has so far been brought into the clinic. There are, however, promising approaches under development. For example, there are attempts to redirect T cells to tumor cells with scFv-based modular systems fused to T cell stimulatory ligands (Arndt et al., 2014; Hornig et al., 2012). Furthermore, the Majeti group showed impressively in 2010 that the targeting of cancer cells via one mAb against a tumor antigen and the additional blockading of an immune checkpoint using a second mAb has a synergistic effect in tumor cell elimination. Chao *et al* demonstrated in this study that in a NHL mouse model only administration of rituximab (an anti-CD20 mAb) together with an anti-CD47 mAb yielded in complete remission in five out of eight mice. In contrast, treatment of mice with either antibody alone led to death within 30 days. They concluded that the therapeutic effect of anti-CD47 antibody in combination with rituximab is mediated primarily through macrophage phagocytosis and not through ADCC, CDC or apoptosis (Chao et al., 2010). The same group then developed an IgG-based bsAb co-targeting CD47 and CD20, which in pre-clinical NHL model experiments also showed reduced lymphoma burden and extended survival, thereby recapitulating the synergistic efficacy of anti-CD47 and anti-CD20 combination therapy (Piccione et al., 2015). The company NovImmune also realized the potential of blocking CD47 as a powerful strategy to increase immunotherapy. They developed an IgG-based bsAb against CD47 and CD19 for the treatment of B cell disease, which is currently in the pre-clinical testing phase and anticipated to enter a clinical phase I trial in 2016 (NovImmune, 2015).

1.3. Leukocyte surface antigen CD47

Leukocyte surface antigen CD47 was first purified from placenta and identified in the early 1990s as a Rhesus factor related antigen on erythrocytes, but it was soon realized to be expressed on virtually all hematopoietic cells as well as other tissues. Furthermore, it was found to be the same as the integrin-associated protein (IAP), the ovarian tumor marker OA3 and the protein Mer6 (Lindberg et al., 1994; Mawby et al., 1994).

INTRODUCTION

CD47 is a 50 kDa cell surface glycoprotein of the immunoglobulin superfamily and has six potential glycosylation sites. Comparison of the human, mouse, rat and bovine CD47 protein shows a sequence identity of 60-70% in the amino acid sequence among these species. It has an extracellular N-terminal Ig-like V-type domain, a transmembrane-spanning domain with five transmembrane helices and a short alternatively spliced cytoplasmic tail. Four different splice isoforms, ranging from 4-36 amino acids, can be found in human as well as mice, each with different tissue expression patterns (Oldenberg, 2013). The main isoform that is expressed on all hematopoietic cells, as well as endothelial and epithelial cells is the 16 amino acid form 2, while isoform 4 (36 amino acids) and 3 (23 amino acids) are expressed primarily in neurons, intestine and testes. Expression of the 4 amino acid form 1 is found in epithelial and endothelial cells (Reinhold et al., 1995). Even though tissue expression is well described, little is known regarding the functionality of the protein carrying different splice variants.

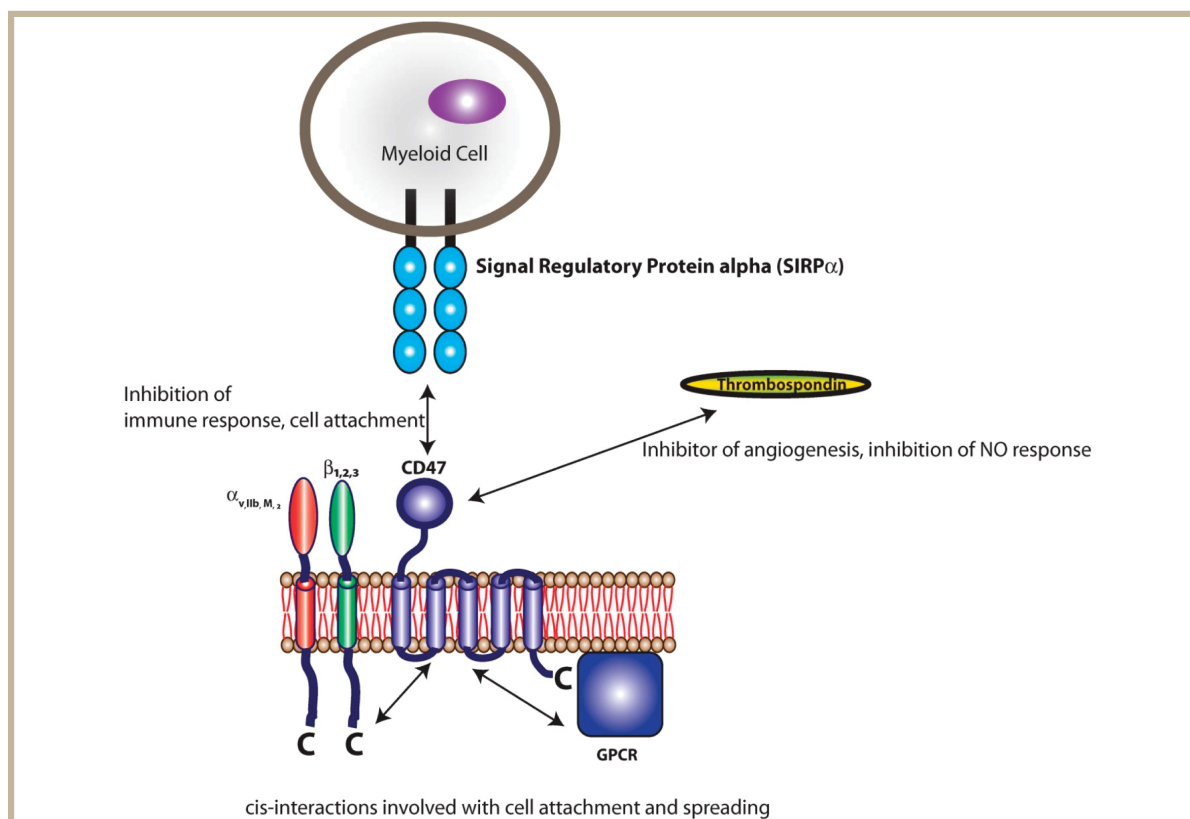


Figure 6 CD47 binding partners. CD47 is a transmembrane glycoprotein with five transmembrane helices that is expressed ubiquitously throughout the body. It interacts in *cis* with integrins regulating cell movement and in

INTRODUCTION

trans with thrombospondin, inhibiting angiogenesis, as well as with Sirp α , constituting a myeloid-specific immune checkpoint. Figure taken from (Slee et al., 2014).

So far there are three main interaction partners known: integrins, thrombospondin-1 and signal regulatory (Sirp) proteins (depicted in Figure 6). In neutrophils CD47 was shown to act in *cis* on integrins, thereby regulating neutrophil migration across endothelial and epithelial cells during inflammatory response (Liu et al., 2001). Generation of CD47-deficient mice further confirmed the importance of this protein in regulating neutrophil inflammatory responses, by showing an increased sensitivity to bacterial infection due to impaired neutrophil accumulation, which is caused by decreased neutrophil adhesion, phagocytosis and respiratory burst potential (Lindberg et al., 1996).

The second interaction partner known is thrombospondin-1 (TSP-1). It belongs to the thrombospondin superfamily, a conserved family of extra cellular, oligomeric, multidomain, calcein-binding glycoproteins. They have many complex tissue-specific roles, including activities in wound healing and angiogenesis, vessel wall biology, connective tissue organization, and synaptogenesis (Adams, 2001). In platelets, TSP-1 activates the platelet integrin and induces platelet spreading as well as aggregation, and increased focal adhesion kinase (FAK) tyrosine phosphorylation, all of which are dependent on the CD47-integrin interaction (Chung et al., 1997).

The third interaction partner mentioned here are the Sirp proteins. There are three Sirp proteins (α, β, γ) and they have similar extracellular regions but differ in their signaling potential. Sirp α has two immunoreceptor tyrosine-based inhibitory motifs (ITIMs), whose function will be explained in more detail in the following chapter. Sirp β has a very short cytoplasmic tail with no signaling motifs but its transmembrane region contains a positively-charged lysine residue, which can bind the adaptor protein DNAX activation protein 12 (DAP12/KARAP), which has an immunoreceptor-tyrosine-based-activating-motif (ITAM) (Tomasello et al., 2000). The third of the Sirp proteins, SIRP γ , has no recognizable signaling motif or ability to interact with cytoplasmic signaling molecules and is thus unlikely to generate intracellular signals (Barclay and Brown, 2006). CD47 was shown to be an interaction partner of Sirp α and Sirp γ (Brooke et al., 2004; Jiang et al., 1999) but not Sirp β

INTRODUCTION

(Seiffert et al., 2001). The interaction between CD47 and Sirp α has been shown to be multifunctional in many body systems and will be discussed in the following sections.

1.4. Signal regulatory protein α

Sirp α was the first member of the Sirp family to be identified and is also known as protein tyrosine phosphatase, non-receptor type substrate 1 (PTPNS1), SHPS-1, CD172A and P84. It is primarily expressed on cells of myeloid origin, like macrophages, granulocytes or DCs, but also neurons and down-regulates immune response through phospho-tyrosine signaling mechanisms (van Beek et al., 2005).

The extracellular region consists of three immunoglobulin superfamily domains: a distal IgV-like domain, which interacts with the IgV-like domain of CD47, and two membrane proximal IgC-like domains (Fujioka et al., 1996; Kharitononkov et al., 1997). An alternatively spliced form, which has only a single IgV-like domain, has also been identified (Veillette et al., 1998). The intracellular region of Sirp α is highly conserved between rats, mice and humans and contains two ITIMs as mentioned above. Upon phosphorylation of the tyrosine residues within this motif, the Scr homology 2 (SH2) domain containing protein-tyrosine phosphatases SHP-1 and SHP-2 can bind, leading to the deactivation of myosin 2a and the initiation of actin depolymerization within the immune cell (Slee et al., 2014). In addition, two tyrosine phosphorylated adaptor proteins, SRC-family-associated phosphoprotein 2 (SCAP2) and FYN-binding protein (FYB) (Timms et al., 1999), and the adaptor protein growth-factor-receptor-bound protein 2 (GRB2) (Kharitononkov et al., 1997) can bind the ITIMs, however their downstream signaling functions remain to be identified. The interaction between CD47 and Sirp α was suggested to function as a “marker of self” and is highly species specific, with sequence identity between mice and humans in this region differing by only 38% (Subramanian et al., 2006).

Functional studies have shown that the binding of Sirp α leads to an inhibition of cell activity, resulting in, for example, reduced phagocytosis by macrophages (Yamao et al., 2002). Furthermore it could be shown in mouse knock-out studies that red blood cells (RBCs) isolated from CD47 knock-out mice and transferred to wild-type mice were rapidly cleared from the blood by macrophages (Oldenburg et al., 2000). Consistent with this, mice

INTRODUCTION

expressing a cytoplasmic functionally inactive mutant of Sirp α also had an increased clearance of RBC (Ishikawa-Sekigami et al., 2006), which suggests that the CD47-Sirp α interaction acts as a “Don’t eat me signal” in macrophages.

As mentioned above, the amino-terminal domain of Sirp α interacts with the amino-terminal domain of CD47. The spanning distance is therefore four IgSF domains, which corresponds to a distance of 14 nm, and is approximately the same as the distance between the interacting molecules in an immunological synapse between T cells and antigen presenting cells.

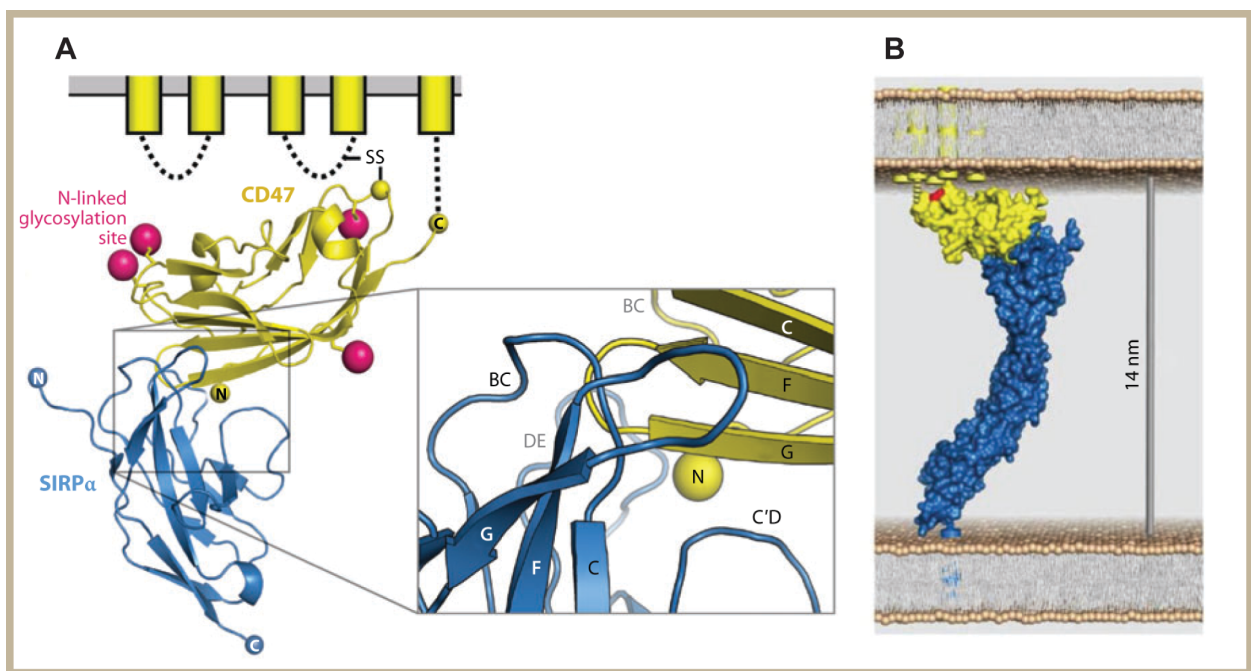


Figure 7 Structure of Sirp α IgV-like domain (blue) bound to CD47. (A) A schematic representation of the 5-transmembrane helix C-terminal domain of CD47 is shown. The interaction with SIRP α is mediated predominantly by loops at the NH₂-terminal ends of the two molecules. The NH₂ termini of CD47 and Sirp α are designated with an ‘N’. (B) The overall distance between opposing cells is estimated to be around 14 nm from analysis of the CD47-SIRP α domain 1 structure and the SIRP α domain 1–3 structure. This distance is similar to that found in immunological synapses. Figure adapted from (Barclay and Van den Berg, 2014).

It is very likely that CD47 does not constantly bind Sirp α because large abundant membrane proteins need to be redistributed for short-range interactions (Barclay and Brown, 2006). In terms of binding affinity of CD47 to Sirp α there are certainly various factors that can influence binding, such as the protein density on the cell surface and glycosylation. The

INTRODUCTION

question of whether the dynamic range of an *in vitro* assay can reflect the *in vivo* situation also needs to be addressed. It has been reported that CD47 binds to Sirp α with a higher affinity (dissociation constant $K_D \approx 2 \mu\text{M}$) than to Sirp γ ($K_D \approx 23 \mu\text{M}$) (Brooke et al., 2004). These binding affinities are typical for many proteins containing IgSF domains, such as CD80 and CD86 binding to CD28 and CTLA-4 ($0.2\text{--}20 \mu\text{M}$) (Collins et al., 2002). It is important to bear in mind, however, that these values were determined with recombinant proteins in solution and may not represent the actual situation *in vivo*.

As outlined above, Sirp α is primarily expressed on phagocytes, such as macrophages, but also DCs. Upon ligation of Sirp α with CD47, macrophages transmit a “Don’t eat me” signal that protects healthy cells from phagocytosis. Therefore the physiological role of this immune checkpoint is the orderly elimination of aged or apoptotic cells. Indeed it has been shown that CD47 expression is diminished or redistributed in apoptotic cells (Gardai et al., 2005). Erythrocytes also lose CD47 from their cell surface as they age, leading to impaired Sirp α signaling and clearance of the cells by splenic macrophages (Oldenborg, 2004). However, it has been realized that macrophages also play a crucial role in cancer and even an more important role in mAb therapy for cancer, since they express all classes of Fc γ receptors (in contrast to NK cells expressing primarily Fc γ RIIIa) (Nimmerjahn and Ravetch, 2008) and are thus capable of killing tumor cells via ADCP.

1.5. The “Don’t eat me” checkpoint in acute myeloid leukemia

The role of CD47 in cancer was first identified through studies of hematopoietic stem cells (HSCs) and leukemia. The authors found that HSCs upregulate CD47 in order to avoid phagocytosis by macrophages when they leave their niche and enter the blood stream (Jaiswal et al., 2009). They further screened various mouse as well as human leukemia cell lines and patient samples and repeatedly found that CD47 was upregulated. They particularly focused on acute myeloid leukemia (AML) stem cells and showed that the upregulation of CD47 protected those cells from macrophage uptake (Majeti et al., 2009). To test whether blockade of the Sirp α -CD47 checkpoint has an effect on AML stem cell engraftment and progression, they used mAbs against CD47 and impressively showed that engraftment was severely disturbed and AML was therefore depleted *in vivo*. They consequently hypothesized

INTRODUCTION

that blockade of the CD47-Sirp α interaction could not only increase phagocytosis of tumor cells, but also that antigens from phagocytosed tumor cells may be presented to T cells and thus activate the adaptive immune response (Figure 8).

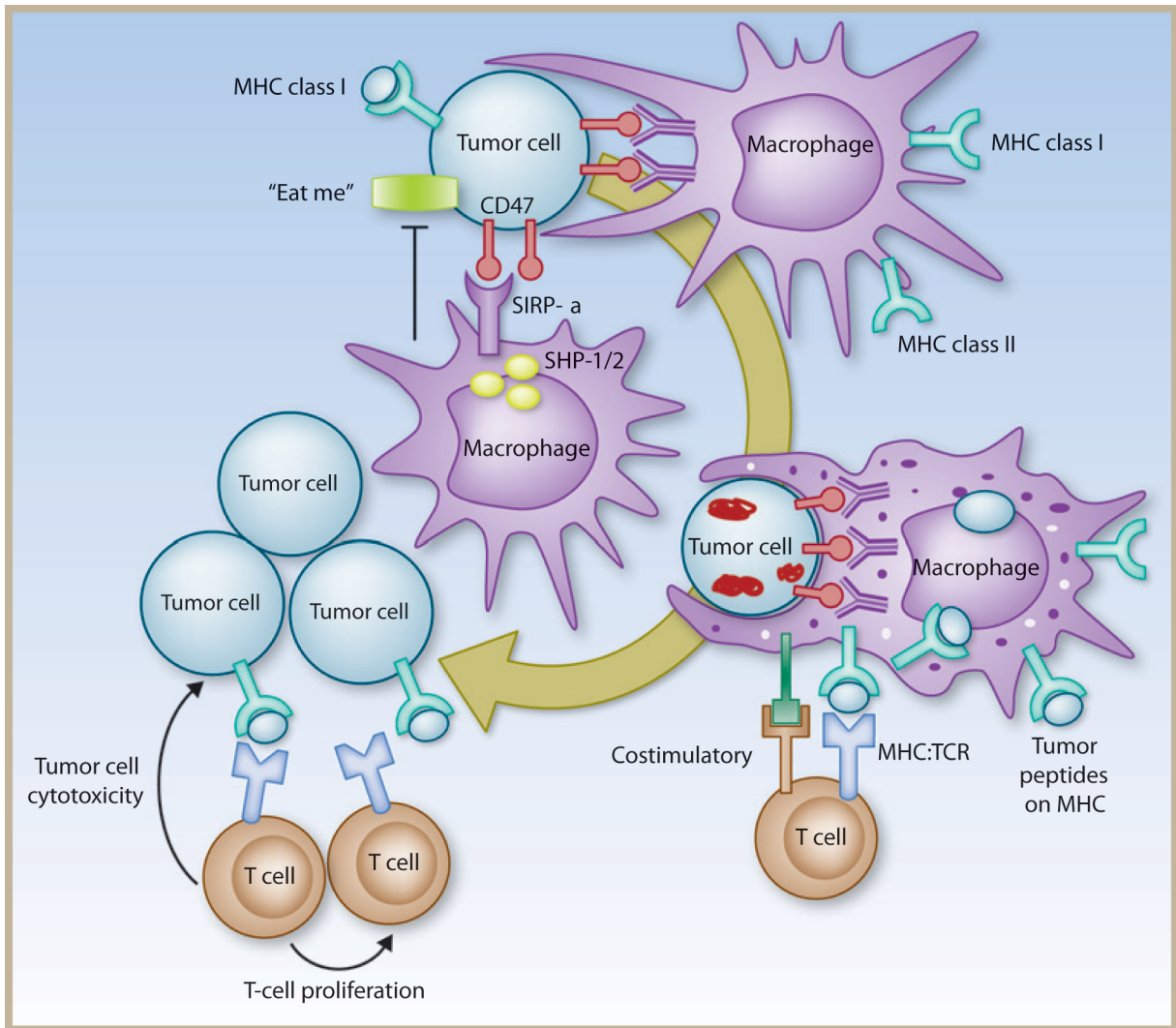


Figure 8 Mechanism of action of CD47 blocking mAbs in AML. AML cells display MHC class I molecules as well as the CD47 surface markers of ‘self’. Engagement of tumor cells CD47 (“don’t eat me” signal) with macrophages SIRP α causes activation and phosphorylation of SIRP α ITIM motifs and the recruitment of SHP-1 and SHP-2 phosphatases. This prevents myosin-IIA accumulation at the phagocytic synapse from inhibiting tumor cell phagocytosis. By blocking the CD47-SIRP α interaction with antibodies (or alternate strategies) an increase in tumor cell phagocytosis by APCs is observed. Phagocytosed tumor cells are subsequently processed and tumor-associated antigens are presented by these APCs on their MHC. Naive tumor reactive T cells can then interact with MHC on APCs and these tumor-specific T cells are further activated,

INTRODUCTION

expand, and are able to cause antigen-specific tumor cell cytotoxicity on remaining malignant cells. Figure adapted from (McCracken et al., 2015).

Furthermore it has been shown that increased expression of CD47 on human AML is associated with poor clinical outcome, which makes it an interesting target in AML therapy.

Acute myeloid leukemia is the most common myeloid disorder in adults and was 50 years ago incurable. Nowadays, AML is cured in 35-40% of patients who are 60 years old or younger, but only in 5-15% of patients who are older than 60 years old (Estey and Döhner, 2006). The chances for a cure decrease drastically with increasing age, especially since older patients are often ineligible for intensive chemotherapy due to unacceptable side effects, which reduces the median survival to 5 to 10 months (Dohner et al., 2015).

Prognostic factors can be subdivided into patient-related factors (like increasing age, coexisting conditions and poor performance status) and disease-related factors (e.g. white-cell count, prior myelodysplastic syndrome or cytotoxic therapy for another disorder and leukemic cell genetic changes). Patient-associated factors commonly predict treatment-assigned early death, whereas disease-associated factors predict resistance to current standard therapy (Dohner et al., 2015). Additionally, the identification of molecular markers (*NPM1* and *CEBPA* mutations and *FLT3* internal tandem mutations) (Estey and Döhner, 2006) as well as the use of multiparameter flow cytometry to identify aberrant cell phenotypes are being used as predictive markers to assess therapy outcome (Grimwade and Freeman, 2014).

The enormous heterogeneity of the disease, which makes it tremendously difficult to treat, has been realized over the last 15 years. AML is characterized by the clonal expansion of myeloid blasts in the peripheral blood, bone marrow or other tissues (O'Donnell et al., 2012) with the presence of both a founding clone and at least one subclone (The Cancer Genome Atlas Research, 2013). Due to the high incidence of relapse in AML there is the growing opinion that remaining malignant cells have stem cell-like properties and these have therefore been termed leukemia stem cells (LSCs) or pre-leukemic hematopoietic stem cells (Corces-Zimmerman et al., 2014). Data from clonal evolution studies showed that genes involved in epigenetic regulation (like *DNMT3A*, *ASXL1*, *IDH1* and *TET2*) are often mutated in these LSCs and occur early in the progression of AML (Shlush et al., 2014). Aside from being

INTRODUCTION

capable of multilineage differentiation, they can survive chemotherapy and expand during remission, leading to relapse of disease. Furthermore they may share properties with normal HSCs or progenitor cells, which makes them difficult to target with conventional cancer treatments (Goardon et al., 2011).

1.6. Conventional AML therapy

After an initial assessment of the patient's prognostic factors the method of choice in the treatment of AML is still chemotherapy. If the patient is eligible for intensive induction chemotherapy treatment starts with continuous-infusions of cytarabine with an anthracycline. A complete response is obtained in 60-85% of adults younger than 60 years old but the response rates are lower in older patients (40-60%). The reason for this is that older patients more frequently have a higher mutation load and other clinically relevant coexisting conditions. Such patients are thus less likely to benefit from induction chemotherapy and are instead candidates for investigational therapy (Dohner et al., 2015).

In the case of positive response to induction chemotherapy, consolidation therapy is added in the event tumor cells are remaining. There are several options available, which again depend on the individual patient's status. The preferred procedure consists of two to four cycles of intermediate-dose cytarabine (Lowenberg, 2013), however autologous as well as allogeneic hematopoietic-cell transplantation (HCT) may also be reasonable options (Koreth et al., 2009; Vellenga et al., 2011). The curative effect of allogeneic HCT in patients with AML is contributed by the immunologic graft-versus-leukemia (GVL) effect. In order to avoid major side effects, such as graft-versus-host disease (GVHD), a human leukocyte antigen (HLA)-matched donor is preferred but this still does not exclude GVHD. To prevent GVHD excessive immunosuppression is needed, which in turn can lead to fatal infections and recurrence of leukemia (Pasquini et al., 2012). Indeed the major complication appearing in transplantation therapy is the relapse of AML. New approaches under investigation include post-transplantation maintenance therapy, specific mutation inhibitors as well as targeted therapy immunotoxins, such as gemtuzumab ozogamicin (Dohner et al., 2015).

Recurrence of AML occurs in most patients within the first three years after diagnosis. The disease outcome is determined again by various patient-related and disease-related factors

INTRODUCTION

that define the salvage regimen. The intention is again to achieve a complete remission so that the patient can subsequently undergo allogeneic hematopoietic-cell transplantation. Patients who are unable to receive intensive salvage therapy can only receive low-intensity therapy, supportive care or, if they wish, new investigational therapies (Thol et al., 2015).

1.7. Antibody therapy for AML

Novel therapies with higher efficacy and lower toxicity are strongly needed for the treatment of AML. The selection of an appropriate antigen target is essential for the development of a successful antibody drug. The observation that ablation of the surface antigen CD33 cells could restore normal hematopoiesis *in vitro* in some leukemias with clonal dominance limited to granulocytes/monocytes suggested the myeloid differentiation antigen expressed on leukemic blast from 85-90 % of patients could be a valid target (Bernstein, 2000). The first trial with a mAb in AML therapy was performed 20 years ago with a mouse mAb against CD33 (Scheinberg et al., 1991). Further improvements resulted in the generation of lintuzumab, a humanized IgG1 version of the mouse mAb (Caron et al., 1992). Unfortunately lintuzumab showed no benefit in a phase 3 trial in patients with relapsed AML (Feldman et al., 2005).

The first CD33-directed therapy approved by the FDA was the immunoconjugate drug gemtuzumab ozogamicin (trade name Mylotarg; Pfizer), which was approved in the year 2000 on the basis of data from a non-randomized, phase 2 trial of 142 patients with relapsed disease (Bross et al., 2001; Larson et al., 2002). Gemtuzumab ozogamicin was withdrawn from the market in 2010, however, due to concerns about toxicity and lack of efficacy in a randomized phase 3 S0106 trial (Petersdorf et al., 2009). It has been shown in various studies, however, that lower doses of the drug (3-6 mg/m² instead of 9 mg/m²) as well as different administration strategies (either single dose or fractionated) are safe and also effective. Meta-analysis of these studies evaluated that the addition of gemtuzumab ozogamicin to induction therapy significantly reduced the risk of relapse and improved overall survival rate at 5 years, especially in patients with favorable cytogenetic characteristics but also in those with intermediate characteristics (Hills et al., 2014).

INTRODUCTION

Gemtuzumab ozogamicin is a recombinant, humanized (CDR-grafted) anti-CD33 monoclonal antibody of the IgG4 isotype (clone hP67.6) covalently attached to the cytotoxic antitumor antibiotic calicheamicin (N-acetyl- γ -calicheamicin) via a bifunctional linker. Upon binding of CD33 the drug is internalized and calicheamicin is released by hydrolysis into the leukemic cell. Once released intracellularly, single- and double-stranded DNA breaks are induced, resulting in a strong cellular response with cell-cycle arrest and subsequent DNA repair or, if the amount of damage is overwhelming, apoptosis and cell death, predominantly via mitochondrial membrane permeabilization and caspase activation (Linenberger, 2005).

Not only gemtuzumab ozogamicin has shown promising results in CD33-directed AML therapy, however, as other groups have also developed bsAbs against CD33. Just as the CD19/CD3 BiTE blinatumomab has been shown to be very effective in lymphoblastic leukemias, a CD33/CD3 BiTE exhibited T cell recruitment and effective AML blast lysis *in vitro* as well as inhibition of tumor growth in preclinical *in vivo* models (Aigner et al., 2013; Arndt et al., 2013). Krupka *et al* evaluated the effect of AMG 330, a CD33/CD3 BiTE on primary AML patient material. They screened more than 600 patient samples for CD33 expression on HSCs, LSCs as well as blasts, and showed that kinetics of T cell-mediated target cell killing were correlated with expression levels. Since LSCs have higher levels of CD33 expression than HSCs they suggested that AMG 330 will preferentially kill LSCs. Furthermore, the CD33 negative fraction of HSCs will be spared from AMG 330-mediated T cell killing and allow for restoration of normal hematopoiesis (Krupka et al., 2014).

Another bsAb targeting CD16 and CD33 showed enhanced ADCC *in vitro* against AML cell lines as well as primary patient samples (Singer et al., 2010). Interestingly, a trispecific scFv triplebody (sctb) with the ability to dually target two different antigens (CD123 and CD33) on AML cell lines showed an even more increased efficacy compared with the bispecific format (Kugler et al., 2010). Since the surface antigen expression of CD123 was shown to be increased on the LSC compartment but not the HSCs (Jordan et al., 2000), CAR T cells against CD123 have also been generated as an effective treatment for AML therapy (Mardiros et al., 2013). The preclinical data from a CD123 mAb (clone 7G3) showed efficacy in AML therapy, however, as part of consolidation therapy, as 7G3 was much less

INTRODUCTION

effective when given to mice 28 days after transplantation, when the leukemia burden was higher (Jin et al., 2009).

As outlined previously CD47 was also reported to be a possible tumor target in AML. It has been shown that there is higher expression of CD47 in the LSC compartment than in normal HSC, and that increased expression of CD47 is a poor prognostic factor in patients with AML (Majeti et al., 2009). Many other surface markers have so far also been tested in preclinical experiments as well as clinical trials, such as TIM-3, WT1, CD96, CD44, CD52, VEGF or KIR, however the challenge will be to identify the best combinations for future AML therapy (Gasiorowski et al., 2014).

2. AIM OF THE THESIS

Acute myeloid leukemia is a severe hematologic malignancy in which the prognosis remains poor despite advances in its treatment during the last three decades. Most patients, especially those of increased age, will relapse and approximately 60% of patients will eventually succumb to their disease. Novel therapies with increased efficacy and decreased toxicity are thus desperately needed. Immunotherapy has been realized as a very potent tool in cancer treatment, with its unique possibility to specifically target tumor cells via expressed tumor markers. The success of gemtuzumab ozogamicin has proven that firstly, CD33 is a valid target in AML and secondly, that antibody therapy is a useful supplement to induction therapy. A more recent discovery of considerable interest is that blocking immune checkpoints via mAbs utilizes the effector cells of the immune system to more efficiently kill tumor cells. In AML it was shown that the blockade of the CD47-Sirp α immune checkpoint by a mAb against CD47 increased the phagocytosis of tumor cells. In fact it could be demonstrated that the simultaneous blocking of the checkpoint and targeting of tumor cells via a mAb even increased tumor cell eradication.

So far there is no antibody format available that combines immune checkpoint inhibition and tumor cell targeting. Therefore the aim of this thesis was to develop a novel antibody derivative that is able to specifically target AML cells via a high affinity anti-CD33 scFv, that is derived from gemtuzumab ozogamicin, and to locally block the CD47-Sirp α immune checkpoint via the naturally occurring extracellular Sirp α receptor domain. Use of the natural receptor domain should avoid systemic binding of the CD47 surface antigen that is expressed ubiquitously on human cells. Recruitment of CD16 expressing effector cells such as NK cells or macrophages is accomplished via another high affinity anti-CD16 scFv derived from the 3G8 mAb. The use of an scFv allows for stronger binding compared with the Fc stem of a mAb and more importantly, only binds to CD16 or Fc γ RIII, circumventing activation of all immune cells expressing various Fc γ receptors. Due to the rather weak interaction of the extracellular domain of Sirp α in the molecule to CD47 on the cells we call it a liCAD, which stands for local inhibitory checkpoint antibody derivative.

AIM OF THE THESIS

The main focus of this work was to first express and purify these molecules from human cells as well as insect cell culture, and second, to test their *in vitro* binding ability and biological activity on different AML cell lines. In collaboration with Prof. Marion Subklewe these molecules were then also tested for their biological activity on blast samples from AML patients.

3. MATERIALS AND METHODS

3.1. Materials

3.1.1. Technical equipment

Table 1 List of technical equipment used throughout this study

Innova 44 Shaker	New Brunswick Scientific
T personal thermocycler	Biometra
Aekta Purifier 10, Explorer, Basic, FPLC	GE Healthcare
Cell culture laminar-flow	BDK Luft- und Reinraumtechnik GmbH
HeraCell CO ₂ incubator	Thermo Scientific
Multitron Cell incubator	Infors HT
Guava easy cyte HT	Merck Millipore
BD FACS Calibur	BD Biosciences
LSR II	BD Biosciences
Microplate reader Infinite M1000 Pro	Tecan
Inverted laboratory microscope Leica DM IL LED	Leica
Vi-Cell™ XR cell viability analyzer	Beckman Coulter
Countess, automated cell counter	Thermo Fischer Scientific
Hemocytometer Neubauer improved	Brand GmbH + Co KG
Nanodrop ND-1000	Peqlab Biotechnologies GmbH
Realtime system CFX96	BioRad
Rotanta 460 RT centrifuge	Hettich
Tabletop centrifuges	Eppendorf
Sorval RC6+ centrifuge	Thermo Scientific
Novex® NuPAGE® SDS-PAGE Gel System	Thermo Fischer Scientific

MATERIALS AND METHODS

Agarose gel electrophoresis system	BioRad
Model 200 / 2.0 power supply	BioRad
Mini-Trans Blot® electrophoretic transfer cell	BioRad
Minimate™ TFF Capsule	Pall Life Sciences
pH-meter 766	Knick
Sartorius scale LE 22025	Sartorius AG
Thermomixer comfort	Eppendorf

3.1.2. Software

Table 2 List of software used to process data

Graph Pad Prism	GraphPad Software Inc.
InCyte Software	Merck Millipore
Diva Software	BD Biosciences
Cell Quest Pro	BD Biosciences
Adobe Illustrator	Adobe

3.1.3. Oligonucleotides

Table 3 List of oligonucleotides used to clone and sequence expression constructs

Name	Sequence
CD33scFv_KasI Fw	AGATAGGCGCCGACATTCAGCTCACTCAG
CD33scFv_STOP_EcoRV Rv	AGATAGATATCTTAGCTAGACACTGTCACCAG
CD16scFv_NotI Fw	AGATAGCGGCCGCACAAGTGACACTGAAAGAGAG
CD16scFv_XhoI Rv	AGATACTCGAGGCTTGATTTCCAGCTTGGTG
SirpIg BamHI Fw	AGATGGATCCGAGGAGGAGCTGCAGGTGATTC
SirpIg_GGGGS_ClaI Rv	AGATAATCGATCCGCTCCACCCCCCCCAGCAGAGGGTTT

MATERIALS AND METHODS

	GGCGCGCACAGAC
GGGGS_ClaI Rv_SirpIg	GGGGGGGGTGGGAGCGGATCGATTATGGCGGAGGAGGA
Fw (overlap)	GCTGCAG
SirpIg (G ₄ S) ₄ _NotI Rv	CTTGTGCGGCCGCACTGCCGCCACCACC
GGGGS_ClaI Rv_SirpIg	GGGGGGGGTGGGAGCGGATCGATTGAGGAGGAGCTGCAG
Fw (overlap)_no 2 nd ATG	
Epcam1.1_KasI Fw	AGATAGGCGCCGATATTCAGATGACCCAGAGCCC
Epcam1.1_STOP_EcoRV	GCGGAGATATCTTATGAGCTAACGGTCAGCAGGGTTC
Rv	
C15G mutation exCD47 Fw	GTAGAATTCACGTTTGGTAATGACACTGTCTG
C15G mutation exCD47 Rv	CGACAGTGTTCATTACCAAACGTGAATTCTAC
exCD47-Fctag_NdeI Fw	AGACATATGTGGCCCCTGGTAGCGGCGCTG
exCD47 FcTag_NotI Rv	AGAGCGGCCGCTAATGATGGTGATGATGGTGTTTACCC
	GGAGACAGGGAGAGGC
exCD47_BamHI Fw	GCGCGGATCCCAGCTACTATTTAATAAAAC
exCD47_NotI Rv	ATATGCGGCCGCGTGAAACAACACGATATTTTAG
CD33 FL_AgeI Fw	ATAACCGGTATGCCGCTGCTGCTACTGC
CD33 FL_EcoRI Rv	ATAGAATTCTCACTGGGTCCTGACCTCTG
S2-1 Fw_sequencing	GAACAAGCTAAACAATCTGC
S2-1 Rv_sequencing	GTATTAAAACATGACAATAC
CD33scFv Rv_sequencing	CCTGATACCATAGTTATCGAGAG
CD33 FL Rv_sequencing	CCCAGCAGTCTGAACCGGCCCTG

MATERIALS AND METHODS

3.1.4. Amino acid sequences

Table 4 Protein sequences of scFvs and extracellular domains

Name	Sequence
N-terminal Ig domain of Sirp α (Sirp Ig)	EEELQVIQPDKSVLVAAGETATLRCTATSLIPVGPIQWFR GAGPGRELIYNQKEGHFPRVTTVSDLTKRNNMDFSIRIGN ITPADAGTYCYVKFRKGSPDDVEFKSGAGTELSVRAKPS
Sirp α high affinity (Sirp Ig_CV1)	EEELQIIQPDKSVLVAAGETATLRCTITSLFPVGPIQWFRG AGPGRVLIYNQRQGPFRVTTVSDTTKRNNMDFSIRIGNI TPADAGTYCYIKFRKGSPDDVEFKSGAGTELSVRAKPS
Extracellular Sirp (Sirp ex)	EEELQVIQPDKSVLVAAGETATLRCTATSLIPVGPIQWFR GAGPGRELIYNQKEGHFPRVTTVSDLTKRNNMDFSIRIGN ITPADAGTYCYVKFRKGSPDDVEFKSGAGTELSVRAKPSA PVVSGPAARATPQHTVSFTCESHGFSPRDITLKWFKNGNE LSDFQTNVDPVGESVSYSIHSTAKVVLTREDVHSQVICEV AHVTLQGDPLRGTANLSETIRVPPTLEVTQQPVRAENQVN VTCQVRKFYPQRLQLTWLENGNVSRTEASTVTENKDGTY NWMSWLLVNVS AHRDDVKLTCQVEHDGQPAVSKSHDLKV SAHPKEQGSNT
CD16 scFv (VL)	DTVLTQSPASLAVSLGQRATISCKASQSVDFDGDSEFMNWWYQ QKPGQPPKLLIYTTSNLESGIPARFSASGSGTDFTLNIHPVEEE DTATYYCQQSNEDPYTFGGGKLEIK
CD16 scFv (VH)	QVTLKESGPGILQPSQTLSTCSFSGFSLRTSGMGVGVWIRQPS GKGLEWLAHIWWDDDKRYNPALKSRLTISKDTSSNQVFLKI ASVDTADTATYYCAQINPAWFAYWGQGLTVTVSA
CD33 scFv (VL)	DIQLTQSPSTLSASVGDRVTTITCRASESLDNYGIRFLTWFFQQK

MATERIALS AND METHODS

	PGKAPKLLMYAASNQGSGVPSRFSGSGSGTEFTLTISLQPD DFATYYCQQTKEVPWSFGQGTKVEVK
CD33 scFv (VH)	EVQLVQSGAEVKKPGSSVKVSCKASGYTITDSNIHWVRQAP GQSLEWIGYIYPYNGGTDYNQKFKNRATLTVDNPTNTAYM ELSSLRSEDFAFYVCVNGNPWLAYWGQGTLLTVSS
CD47 scFv (VL)	DIVMTQSPLSLPVTPGEPASISCRSSQSLVHSNGKTYLHWYL QKPGQSPRLLIYKVSNRFSGVPDRFSGSGSGTDFTLKISRVE ADDVGIYYCSQSTHVPYTFGQGTKLEIK
CD47 scFv (VH)	QVQLVQSGAEVKKPGASVQVSCKASGYTFTNHVIHWLRQA PGQGLEWMGYIYPYNDGTKYNEKFKDRVTMTSDTSISTAY MELSSLRSDDTAVYYCARGGYTYDDWGQATLTVSS

3.1.5. Buffers

Table 5 List of buffers used for biochemical and cell culture methods

	Buffer composition
10 x PBS (1 l)	80 g NaCl, 2 g KCl, 14.4 g Na ₂ HPO ₄ x 2 H ₂ O, 2 g KH ₂ PO ₄ , pH 7.4
1 x PBS-T (1 l)	100 ml 10 x PBS, 0.1% Tween-20
10 x transfer buffer (1 l)	30.3 g tris base, 144 g glycine
1 x transfer buffer (1 l)	100 ml 10 x transfer buffer, 20 % ethanol
4 x Laemmli buffer	0.11 M Tris (pH 6.8), 16% (v/v), 4% (w/v) SDS, 5% (v/v) β-mercaptoethanol, 0.05% (w/v) bromophenol blue
1 x MES SDS running	MES pH 7.2 50 mM, Tris base 50 mM, SDS 0.1%, EDTA 1 mM, pH

MATERIALS AND METHODS

buffer (1 l)	7.3
Coomassie stain	50% (v/v) ethanol, 7% (v/v) acetic acid, 0.2% (w/v), Coomassie Brilliant Blue R250
20 x ECL solution	2 M tris base, pH 8.5
1 x ECL staining solution (10 ml)	10 ml 20 x ECL solution, 3 μ l H ₂ O ₂ , 25 μ l cumaric acid, 50 μ l luminol
FACS buffer	1 % BSA, 1 mM EDTA, in PBS

3.1.6. Antibodies

Table 6 List of FACS and western blot antibodies

Description	Reactivity	Isotype	Clone	Company
CD47-PE	Human	Mouse IgG1 kappa	CC2C6	BioLegend
CD56-APC	Human	Mouse IgG1 kappa	AF12-7H3	BioLegend
CD16-PE	Human	Mouse IgM	VEP13	BioLegend
CD16-Alexa 647	Human	Mouse IgG1 kappa	B73.1	BioLegend
CD33-FITC	Human	Mouse IgG1 kappa	HIM3-4	BD Pharmingen
CD3-FITC	Human	Mouse IgG2	HIT3	BioLegend
penta HIS-Alexa 488	HIS tag	Mouse IgG1		Quiagen
HIS-HRP	HIS tag	Mouse IgG2b	GG11-6F4.3.2	Miltenyi Biotec

3.2. Molecular biology methods

3.2.1. Molecular cloning

For bacterial expression of scFvs and SirpIg domains, all used scFvs as well as extracellular SirpIg domains were ordered at Geneart and cloned into the pAK400 vector behind the pELB leader sequence using SfiI restriction sites. Therefore, 1 µg of vector and insert DNA were incubated with 10 U of restriction enzyme and 1 x corresponding reaction buffer (all Thermo Fischer Scientific) and filled up with MilliQ H₂O. Reactions were incubated for 1 to 2 hours at appropriate temperatures (according to manufacturer's instructions) and then analyzed on a 1 % agarose gel. Relevant DNA bands were cut out and a gel clean up was performed using a Nucleospin gel and PCR purification kit (Macherey-Nagel) according to the protocol.

For ligation reactions, vector and insert DNA were mixed in a ratio of 1:2 and incubated with 1 µl T4 DNA ligase, 1 x T4 DNA ligase buffer (both Thermo Fischer Scientific) and MilliQ H₂O to a volume of 10 µl for 10 minutes to 1 hour at room temperature. The total ligation mix was then used for transformation reactions.

Transformation of plasmid DNA was performed using chemically competent *E.coli* XL1 Blue cells (Stratagene). Briefly, 100 µl of bacterial cells were mixed with 10 µl of plasmid DNA and incubated for 30 minutes on ice. Cells were then heat shocked for 45 seconds at 42 °C and put on ice for 2 minutes again. After addition of 100 µl LB medium, cells were incubated for 1 hour at 37 °C and plated on an LB agar plate supplemented with chloramphenicol (34 µg/ml). The next day, single colonies were picked and cultured in LB medium containing antibiotics over night at 37 °C / 200 rpm, and plasmid DNA was isolated using an isolation kit (NucleoSpin Plasmid Easy Pure, Macherey Nagel). All sequences were verified by sequencing at Eurofins MWG Operon.

For expression of liCAD proteins in human FreeStyle™ 293-F cells (Thermo Fischer Scientific), genes were cloned into the pSecTag vector after an Ig kappa leader sequence and a 6 x histidin tag. The front building block of the liCAD was always inserted using SfiI restriction sites, the middle one using NotI / XhoI, and the last one using KasI / EcoRV

MATERIALS AND METHODS

restriction sites. Restriction digest, ligation reactions and transformations were performed as described above. *E. coli* cells were plated on LB agar plates supplemented with ampicillin (100 µg/ml).

For expression of liCAD proteins in *Drosophila melanogaster* Schneider S2 cells (ExpreS²ion Biotechnologies), a BIP secretion signal followed by a 6 x histidin tag was cloned into the pExpreS2-1 vector or pExpreS2-2 vector (both ExpreS²ion Biotechnologies) using EcoRI / BamHI. Afterwards the liCAD was introduced via BamHI / EcoRV restriction sites after PCR amplification. The front module was then exchanged using SfiI restriction sites. Again restriction digest, ligation reactions and transformations were performed as described above. *E.coli* cells were grown on LB agar plates containing zeocin (50 µg/ml) or kanamycin (100 µg/ml).

3.2.2. Polymerase chain reaction (PCR)

Some scFvs were amplified by PCR from plasmid DNA using Phusion Flash Master Mix (Finnzymes, Espoo, Finland) using primers as shown in Table 3. A typical PCR reaction contained 10-100 ng template DNA and 10 µM of each primer in 20 µl of 1 x PCR mix.

The following PCR program was used:

Cycle	Temperature	Time
1	98 °C	30 sec.
2	98 °C	10 sec.
3	50 – 72 °C (depending on melting temp. of used primer)	20 sec.
4	72 °C	20 sec. / 1 kb
	Repeat 2 - 4	30 x
5	72 °C	120 sec.
6	4 °C	pause

MATERIALS AND METHODS

3.2.3. Site-directed mutagenesis

To introduce an additional SirpIg domain on the N-terminal site of the liCAD, site-directed mutagenesis PCR was performed using Phusion Flash Master Mix. Therefore, 200 ng of plasmid DNA were mixed with 2 μ M of each primer and 3 % DMSO in 20 μ l of 1 x PCR mix.

The following PCR program was used:

Cycle	Temperature	Time
1	98 °C	30 sec.
2	98 °C	10 sec.
3	50 – 72 °C (depending on melting temp. of used primer)	20 sec.
4	72 °C	30 sec. / 1 kb
	Repeat 2 - 4	20 x
5	72 °C	120 sec.
6	4 °C	pause

After the PCR amplification, 1 μ l of DpnI restriction enzyme (Thermo Fischer Scientific) was added to the reaction tube and incubated for 3 hours at 37 °C to digest maternal plasmid DNA. Afterwards, 10 μ l of the sample were transformed into chemically competent XL-1 *E.coli* cells as described before. Colonies were screened, and positive clones were verified by sequencing.

3.3. Protein biochemistry methods

3.3.1. Periplasmic protein expression in *E.coli*

To overexpress a scFv or extracellular SirpIg domains, pAK400 plasmids containing the corresponding open reading frames (ORFs) were transformed into competent *E.coli* BL21 (DE) cells (NEB). Transformations were carried out as mentioned above, and cells were plated on LB agar plates supplemented with chloramphenicol (34 µg/ml). Several colonies were inoculated in a 50 ml pre-culture and grown over night at 37 °C in a shaking incubator at 200 rpm. The following day, 3 l LB cultures were inoculated 1:100 with the pre-culture and grown at 37 °C to an OD600 of ~ 0.7. The *E.coli* culture was then cooled down on ice to 18 °C and protein production was induced by addition of 0.5 mM IPTG. Expression was held over night at 18 °C in a shaking incubator at 200 rpm and cells were collected the next morning at 5000 rpm for 10 minutes using a SLC 6000 rotor (Sorvall). Cell pellets were put on ice and protein purification was performed immediately.

3.3.2. Purification of polyhistidine-tagged periplasmic proteins

Bacterial cell pellets were resuspended in 100 ml of cold periplasmic lysis buffer (100 mM Tris pH=8, 1 mM EDTA, 500 mM saccharose) and incubated on ice for 30 minutes. After 30 minutes of centrifugation at 4000 rpm, the supernatant was transferred to SS-34 tubes (Sarstedt) and centrifuged again for 15 minutes at 15000 rpm using a SS-34 rotor (Thermo Scientific). The supernatant was transferred to a fresh tube and dialysed over night against a 100 x volume of PBS. In order to perform affinity chromatography as a first purification step, Ni²⁺-NTA agarose beads (Quiagen) were added, followed by rotation over night at 4 °C.

The subsequent day, beads were collected at 4000 rpm for 5 minutes and loaded into a Bio-Spin® chromatography column (Bio Rad). Beads were rinsed 3 times with washing buffer (20 mM Tris-HCl pH=9, 300 mM NaCl, 10 mM imidazol) and rinsed 6 times with elution buffer (20 mM Tris-HCl pH=9, 300 mM NaCl, 200 mM imidazol). All wash and elution steps were collected in eppendorf tubes and samples were analyzed by discontinuous

MATERIALS AND METHODS

polyacrylamide gel electrophoresis (SDS-PAGE). Fractions containing the protein of interest were pooled and, depending on the purity, either subsequent size exclusion chromatography on a S75 10/300 GL column (GE Healthcare) was performed or the protein was immediately concentrated (Amicon spin concentrators, Millipore), aliquoted and shock frozen in liquid nitrogen.

3.3.3. Expression of liCADs in human FreeStyle™ 293-F cells

For expression of liCAD proteins, pSecTag vectors containing the desired ORFs were transfected into human FreeStyle™ 293-F cells using TransIT®-LT1 transfection reagent (Mirus Bio LLC) according to the manufacturer's protocol. In brief, cells were sown at a density of 0.5×10^6 / ml the day before transfection. For a 20 ml culture, 20 μ g of plasmid were mixed with 40 μ l of TransIT-LT1 transfection reagent as well as 2 ml of OptiMEM® reduced serum medium (Thermo Fischer Scientific) and incubated for 20 minutes at room temperature. Afterwards, the mixture was added to the cells dropwise, and cells were incubated at 37 °C, 5 % CO₂ in a shaking incubator for 5 to 7 days. In order to avoid clumping of the cells, between 6 and 12 hours after transfection anti-clumping factor (Thermo Fischer Scientific) was added to the medium at a dilution of 1:750. Cells were centrifuged at 1200 rpm for 5 minutes using a Rotanta 460 RF centrifuge (Hettich) and the supernatant was collected. Supernatants were either stored at -20 °C or used immediately for subsequent protein purification.

3.3.4. Purification of polyhistidine-tagged liCADs from FreeStyle™ 293-F cell supernatant

All liCAD proteins were designed containing an N-terminal polyhistidine tag. Therefore, cell culture supernatants were incubated with Ni²⁺-NTA agarose beads rotating over night at 4 °C and subsequently affinity chromatography was performed as described in 3.3.2. Fractions were analyzed by SDS-PAGE and those containing the protein of interest were pooled and dialyzed over night at 4 °C into a low salt buffer (20 mM Tris-HCl pH=9, 50 mM NaCl) in order to perform anion-exchange chromatography on a MonoQ 5/50 GL column (GE Healthcare) the following day. To separate the protein of interest from impurities, a 4-step

MATERIALS AND METHODS

gradient of buffer A (20 mM Tris-HCl pH=9, 50 mM NaCl) and buffer B (20 mM Tris-HCl pH=9, 1 M NaCl) was performed as shown in Table 7. Peak fractions were again analyzed by SDS-PAGE and, according to purity, overexpressed proteins were either immediately concentrated and shock frozen or fractions were pooled and subjected to size exclusion chromatography on a Superdex 200 10/300 GL column (GE Healthcare) in a gel filtration buffer (20 mM Tris-HCl pH=9, 300 mM NaCl). SDS-PAGE of peak fractions was performed to confirm purity of the protein of interest and the fractions containing the protein were pooled, concentrated, shock frozen and stored at -80°C .

Table 7 Protocol of 4-step gradient purification

Number of column volumes (CV) / % buffer A and B	
1. step	5 CV 100 % buffer A, 0 % buffer B
2. step	1 CV 10 % buffer B
3. step	20 CVs linear gradient 10 % to 30 % buffer B
4. step	16 CVs 100 % buffer B

3.3.5. Expression of liCAD proteins in Schneider 2 cells

In order to overexpress liCADs in insect cells, pS2-1 or pS2-2 vectors expressing the corresponding proteins were transfected into *Drosophila melanogaster* Schneider 2 (S2) cells using Lipofectamin® 2000 (Thermo Fischer Scientific) according to the manufacturer's protocol. Briefly, Lipofectamin® 2000 was mixed with OptiMEM® in a 1 : 1 ratio and incubated for 5 minutes at room temperature. In parallel, 500 ng plasmid DNA per 1×10^6 cells / ml were mixed with OptiMEM® in a proportionate ratio and later mixed with the Lipofectamin® 2000 / OptiMEM® solution in a 1 : 9 DNA : Lipofectamin® 2000 ratio. After 20 minutes of incubation at room temperature, the transfection mixture was applied dropwise to the cells.

For the generation of a stably expressing S2 cell line, transfected cells were selected using either 2 mg/ml zeocin (Thermo Fischer Scientific) or 4 mg/ml G418 (InvivoGen) for 26 days according to the manufacturer's protocol. In brief, cells were sown at a density of 2×10^6 / ml

MATERIALS AND METHODS

in 5 ml EX-CELL® 420 medium (Sigma Aldrich) lacking fetal bovine serum (FBS) (Thermo Fischer Scientific), transfected as mentioned above and incubated at 27 °C in a T25 flask (Sarstedt). After 4 to 6 hours, 1 ml of FBS was added and 24 hours afterwards the medium was supplemented with the corresponding selection agent. Cells were monitored daily, splitted thus if required (mostly every other day) and kept at a volume of 6 ml. After 14 days of selection, the total cell suspension was transferred to a T75 flask (Sarstedt) and kept at a volume of 15 ml until day 26, when the cells were finally transferred into a 125ml Corning® flask (Corning®) in EX-CELL® 420 medium with 10 % FBS without selection agent incubating in a shaking incubator at 27 °C / 95 rpm.

For expression of the desired protein of interest, cells were counted and sown at a density of 8×10^6 / ml in EX-CELL® 420 medium without FBS. Expression was held over 4 to 5 days at 27 °C in a shaking incubator at 95 rpm. Cells were centrifuged at 3000 rpm for 5 minutes in a Rotanta 460 RF centrifuge (Hettich) and the supernatant was collected. Supernatants were either stored at - 20 °C or used immediately for further purification of the overexpressed protein of interest.

3.3.6. Purification of polyhistidine-tagged liCAD proteins from S2 cell supernatant

Collected supernatants were centrifuged in a SS-34 tube for 5 minutes at 15000 rpm in a SS-34 rotor to ensure a cell- or debris-free protein solution. Afterwards, buffer exchange into 20 mM Tris-HCl pH 8, 300 mM NaCl buffer was performed using a Minimate™ TFF Capsule (Pall Life Sciences) with an Omega™ 30 K membrane. As a first purification step, affinity chromatography was again performed as described in 3.3.2. Due to a higher amount of drosophila cell impurities, a further anion-exchange purification followed by an optional size exclusion chromatography was performed as outlined in detail in 3.3.4.

3.3.7. Discontinuous Polyacrylamide Gel Electrophoresis (SDS-PAGE)

Protein samples were analyzed by discontinuous polyacrylamide gel electrophoresis (SDS-PAGE) (Laemmli 1970) using the Novex® NuPAGE® SDS-PAGE Gel System (Life

MATERIALS AND METHODS

Thermo Fischer Scientific). Protein samples were mixed with Laemmli buffer, denatured for 5 minutes at 95 °C and then separated on a NuPAGE® 4 – 12 % Bis-Tris gel (Thermo Fischer Scientific). Gels were run at 200 V in 1 x MES SDS running buffer, stained afterwards with Coomassie staining solution and destained in water. Table 5 summarizes buffer composition of buffers.

3.3.8. Western blot analysis

Protein samples were first separated according to size by SDS-PAGE as mentioned above and then transferred to a PVDF blotting membrane (BioRad) using a Mini-Trans Blot® electrophoretic transfer cell (BioRad). Therefore, three layers of Whatman paper, followed by the PVDF membrane, the SDS-PAGE gel and another three layers of Whatman paper, all presoaked in 1 x transfer buffer, were assembled in the blotting machine and the transfer of proteins to the membrane was carried out at 100 V for 60 min. The membrane was incubated in PBS-T / 3 % milk powder + 1 : 10000 anti-HIS antibody (Quiagen) for 60 minutes at room temperature and afterwards washed 3 times for 20 minutes with PBS-T.

For detection of the proteins, the membrane was incubated for 1 minute with 1 x ECL staining solution, pat dried with a paper towel and immediately put into an exposure cassette. Exposure was carried out with a light sensitive Hyperfilm™ ECL™ (GE Healthcare). The films were developed in a Kodak X-Omat M35 developing machine. Used buffer compositions are summarized in Table 5.

3.3.9. Small angle x-ray scattering (SAXS)

Small-angle X-ray scattering (SAXS) data were collected at EMBL/DESY Hamburg beamline PETRA-3 P12. Protein samples after size-exclusion chromatography and centrifugation were measured at different concentrations between 0.7 and 2.6 mg/ml. Before and after each sample, the corresponding buffer was measured and used for buffer correction. No sample showed signs of aggregation or radiation damage, and scattering data were processed and analysed using programs of the ATSAS package (Konarev et al., 2006).

3.4. Cell culture methods

3.4.1. Cell lines and media

All human and hamster cell lines were either bought at the Deutsche Sammlung von Mikroorganismen und Zellkulturen (DSMZ) or Thermo Fischer Scientific. *Drosophila melanogaster* Schneider 2 (S2) cells were bought at ExpreS2ion Biotechnologies.

MOLM-13

MOLM-13 cells are human cells established from the peripheral blood of a 20-year old patient suffering from acute myeloid leukemia. They grow in suspension and were maintained in RPMI 1640 + GlutaMAX (Thermo Fischer Scientific), 20 % FBS at a density of $0.5 - 2 \times 10^6$ cells / ml. The day before an experiment, cells were split to 0.5×10^6 cells / ml into fresh medium.

OCI-AML3

OCI-AML3 cells were kindly provided by Prof. Marion Subklewe. OCI-AML3 cells are a human cell line established from the peripheral blood of a 57-year old patient suffering from acute myeloid leukemia. Cells grow in suspension and were maintained in RPMI 1640 + GlutaMAX, 10 % FBS at a density of $0.5 - 2 \times 10^6$ cells / ml. The day before an experiment cells were split to 0.5×10^6 cells / ml into fresh medium.

Jurkat

Jurkat cells are human cells established from the peripheral blood of a 14-year old patient with acute lymphoblastic leukemia (ALL). They grow in suspension and were maintained in RPMI 1640 + GlutaMAX, 10 % FBS at a density of $0.5 - 2 \times 10^6$ cells / ml.

THP-1

THP-1 cells were established from the peripheral blood of a 1-year old boy suffering from acute monocytic leukemia. Cells grow in suspension and were maintained in RPMI 1640 + GlutaMAX, 10 % FBS at a density of $0.1 - 1 \times 10^6$ cells / ml.

MATERIALS AND METHODS

FreeStyle™ 293-F HEK cells

The FreeStyle™ 293-F cell line is derived from 293 HEK cells and is adapted to suspension cell culture in FreeStyle™ 293 expression medium (Thermo Fischer Scientific) without FBS. Cells were kept shaking at 125 rpm in 125 ml Erlenmeyer flasks (Corning) at a density of $0.5 - 2 \times 10^6$ cells / ml. The day before transfection, cells were split to 0.5×10^6 cells / ml into fresh medium.

Flp-IN™-293 cell line

Flp-IN™-293 cells are 293 HEK cells with a stably integrated FRT site at a transcriptionally active genomic locus. Cells grow in adherent culture and were maintained in DMEM + GlutaMAX (Thermo Fischer Scientific), 10 % FBS, 50 µg / ml zeocin to a confluence of 80 % - 90 %.

CD33-Flp-IN™-293 cells

CD33-Flp-IN™-293 cells were kindly provided by Monika Herrmann and are transfected with the eukaryotic expression vector pcDNA™ / FRT containing full-length human CD33. Cells grow in adherent culture and were maintained in DMEM + GlutaMAX, 10 % FBS, 100 µg / ml hygromycin B gold (InvivoGen) to a confluence of 80 % - 90 %.

Flp-IN™-CHO cell line

Flp-IN™-CHO cells are Chinese hamster ovary cells with a stably integrated FRT site at a transcriptionally active genomic locus. Cells grow in adherent culture and were kept in Ham's F-12 medium (Biochrom), 10 % FBS, 100 µg / ml zeocin to a confluence of 80 % - 90 %.

CD33-Flp-IN™-CHO cells

CD33-Flp-IN™-CHO cells were created by transfecting the eukaryotic expression vector pcDNA™ / FRT containing full-length human CD33 into the parental Flp-IN™-CHO cell line. Cells grow in adherent culture and were maintained in Ham's F-12 medium, 10 % FBS, 550 µg / ml hygromycin B gold to a confluence of 80 % - 90 %.

MATERIALS AND METHODS

CD47-Flp- INTM-CHO cells

CD47-Flp-INTM-CHO cells were transfected with the eukaryotic expression vector pcDNATM / FRT containing full-length human CD47. Cells grow in adherent culture and were maintained in Ham's F-12 medium, 10 % FBS, 550 µg / ml hygromycin B gold to a confluence of 80 % - 90 %.

CD16-CHO cells

CD16-CHO cells were kindly provided by Claudia Roskopf. Cells stably express full-length human CD16, grow in adherent culture and were maintained in Ham's F-12 medium, 10 % FBS, 400 µg / ml G418 to a confluence of 80 % - 90 %.

Schneider 2 (S2) cells

Schneider cells are derived from a primary culture of late stage *Drosophila melanogaster* embryos. They grow both in a semi-adherent monolayer as well as in suspension and were maintained shaking at 95 rpm in EX-CELL® 420 medium with L-glutamine , 10 % FBS with a density of 5 – 50 x 10⁶ cells / ml.

3.4.2. Maintenance of cells

All human cell lines were maintained at 37 °C, 5 % CO₂. Cells were checked every day and passaged 2 times a week. In order to passage suspension cells, they were first resuspended, then mixed with trypan blue stain (0.4 %) in a 1:1 ratio and subsequently counted using a Countess automated cell counter (Thermo Fischer Scientific). For passaging adherent cells, medium was aspirated, cells were carefully washed with PBS (Thermo Fischer Scientific) and incubated with 1 ml of 0.05 % trypsin-EDTA (1 x) (Thermo Fischer Scientific) for 2 – 3 minutes at 37 °C in the incubator. Cells were loosened by carefully tipping the plate, and the enzymatic reaction was stopped by the addition of FBS containing media. Cells were counted as mentioned above and the respective amount was put back on the plate.

Drosophila melanogaster Schneider 2 (S2) cells were maintained at 27 °C without CO₂ shaking at 95 rpm in an Innova 44 shaker (New Brunswick Scientific). A 1:3 dilution of cells

MATERIALS AND METHODS

was counted using the Vi-Cell™ XR cell viability analyzer (Beckman Coulter) and the respective amount of cells was put back into a 125 ml Erlenmeyer Corning® flasks to a total volume of 25 ml.

3.4.3. siRNA mediated transient knock down of CD47 in FreeStyle™ 293-F HEK cells and transfection of control proteins

20 ml of FreeStyle™ 293-F HEK cells were cultured in Erlenmeyer flasks at a density of 0.5×10^6 cells / ml and transfected the next day with siRNAs as well as the expression plasmid as follows: First, 400 μ l OptiMEM were mixed with 20 μ l Lipofectamin RNAiMAX reagent (Thermo Fischer Scientific) and incubated for 5 minutes at room temperature. In the mean time, 400 μ l OptiMEM were mixed with 10 nM ON-TARGET plus Human CD47 siRNA-SMARTpool (Thermo Scientific), afterwards combined with the transfection reagent solution and dropped to the cells. Additionally, 2 ml OptiMEM, 20 μ l expression plasmid and 40 μ l TransIT were mixed, incubated for 20 minutes at room temperature and also dropped to the cells. After 4 days, the cells were centrifuged and incubated with anti-CD47 antibody as described below for flow cytometric analysis. Supernatant was collected and incubated over night with Ni^{2+} -NTA agarose beads and the protein was purified as described in 3.3.4.

3.4.4. Generation of CD47 and CD33 Flp-In™ CHO cell lines

As mentioned above, CD47 and CD33 Flp-In™ CHO cells were generated by transfection of the eukaryotic expression vector pcDNA™ / FRT containing human full-length CD47 or CD33, respectively. Cells were transfected with Lipofectamin 2000® according to the manufacturer's protocol. Briefly, 1×10^5 cells were plated in a well of a 24-well plate in 500 μ l Ham's F-12 Medium, 10 % FBS without antibiotics. The next day, cells were transfected with a DNA:Lipofectamin 2000® ratio of 1:2 at 80 % - 90 % confluence. Therefore, first 2 μ l Lipofectamin 2000® were mixed with 48 μ l OptiMEM and incubated for 5 minutes at room temperature. In the mean time 100 ng of pcDNA™ / FRT vector were mixed with 900 ng pOG44 vector (1 : 9 ratio) and filled up to a total volume of 50 μ l with OptiMEM. Afterwards Lipofectamin 2000® and DNA solutions were mixed, incubated for 20 minutes at room temperature and added dropwise to the cells. After 6 hours, medium was exchanged

MATERIALS AND METHODS

and 48 hours after transfection positive clones were selected by adding 550 μg / ml hygromycin B gold to the medium. Selection medium was changed every other day and polyclonal cell lines were grown. After approximately 4 weeks, cells were passaged to a 10 cm cell culture dish and subsequently analyzed for surface expression of CD47 or CD33, respectively. Positive clones were selected and aliquots were frozen in Ham's F – 12 medium + 10 % FBS + 10 % DMSO (Sigma) using a freezing container (Nalgene Mr. Frosty). After 3 days, cells were transferred to a liquid nitrogen tank.

3.4.5. Isolation of peripheral blood mononuclear cells (PBMCs) from whole human blood

For PBMC isolation, 100 ml of donor blood were split up to 20 ml and filled up with PBS to 50 ml. Further, 25 ml of blood-PBS mixture were carefully pipetted onto 12 ml of a Biocoll separating solution (Biocrom AG) and spun with 818 g for 30 min. at room temperature without acceleration and deceleration. Afterwards, the PBMCs were carefully removed using a disposable Pasteur pipette, washed twice with RPMI 1640 + GlutaMAX, 10 % FBS, 1 % HEPES buffer (Biocrom AG) and kept at 37 °C, 5 % CO₂ for further experiments.

3.4.6. Expansion of human NK cells from whole human blood

PBMCs were isolated from 40 ml of human whole blood using a Biocoll gradient as described previously. PBMCs were washed twice in RPMI 1640 + GlutaMAX supplemented with 1 % HEPES buffer and 10 % FBS and furthermore plated at a cell density of 5×10^6 cells / ml in RPMI 1640 + GlutaMAX supplemented with 5 % human serum (Thermo Fischer Scientific), 0.25 $\mu\text{g}/\text{ml}$ IL-2 (Thermo Fischer Scientific) and 10 $\mu\text{g}/\text{ml}$ OKT-3 monoclonal anti-CD3 antibody (Biolegend). After 5 days cells were collected at 1200 rpm / 5 minutes, washed with PBS and again plated in RPMI 1640 + GlutaMAX, 5 % human serum, 0.5 % Pen/Strep and 0.25 $\mu\text{g}/\text{ml}$ IL-2. The following 16 days the cells were split every other day to a cell density of 0.5×10^6 cells / ml and NK cell number as well as killing potential was assessed on day 1 (d1), d5, d9, d14, d21, respectively. In order to assess NK cell numbers, a CD3, CD16, CD56 surface marker staining was performed. On d21, cells were furthermore

MATERIALS AND METHODS

pelletted at a cell density of 20×10^6 cells / ml and subsequently frozen down in human serum + 10 % DMSO using a freezing container. After 3 days, cells were then transferred to a liquid nitrogen tank.

3.4.7. Cell staining and analysis of surface marker

In general, all cells were counted as mentioned above and 1×10^5 cells were distributed to a v-bottom 96-well plate (Costar). Cells were centrifuged for 4 minutes at 1400 rpm, pellets were resuspended in 50 μ l FACS buffer containing the antibody mixture of choice and incubated for 30 minutes on ice in the dark. For compensation, single stain controls of each antibody present in the mixture was performed. After the incubation, cells were washed with 200 μ l FACS buffer and finally taken up in fresh 200 μ l FACS buffer before they were either analyzed on a Guava easyCyte 6HT (Merck, Millipore) or transferred to a polystyrene round-bottom tube (BD) and measured on a FACS Calibur™ (BD).

3.4.8. Binding studies

To check binding abilities of generated liCADs, 1×10^5 cells expressing the respective surface antigen were centrifuged as outlined in 3.4.7, taken up in 30 μ l FACS buffer containing 15 μ g / ml liCAD and incubated for 30 minutes on ice. After washing with 200 μ l FACS buffer they were incubated with 50 μ l FACS buffer containing 1:200 anti-HIS antibody and incubated again for 30 minutes on ice in the dark. Cells resuspended only in FACS buffer containing 1:200 anti-HIS antibody served as a background control. After washing again, cells were taken up in 200 μ l FACS buffer and analyzed on a Guava easyCyte 6HT.

3.4.9. K_D determination of liCADs

To determine K_D values of liCADs, 1×10^5 cells expressing the respective surface antigen were centrifuged, incubated with protein and stained with an anti-HIS antibody as outlined above, but cells were taken up in a dilution series from 0.01 μ g / ml to 15 μ g / ml liCAD. Again, cells resuspended only in FACS buffer containing 1:200 anti-HIS antibody served as

MATERIALS AND METHODS

a background control and fluorescence intensity of the secondary anti-HIS antibody was measured on a Guava easyCyte 6HT. One drop of rainbow calibration particles (8 peaks, 3.0 – 3.4 μm (BioLegend)) was diluted in 200 μl FACS buffer and served as a standard for fluorescence intensities. Obtained median fluorescence intensities of the different dilutions and particles were exported and converted to channel numbers using the respective rainbow calibration data sheet. Converted values were then further normalized and plotted as a dose-response curve in Prism software (Graph Pad Software Inc.). The obtained dose-response curves were analyzed using a non-linear regression, one-site specific binding model, and K_D values were determined.

3.4.10. Cytotoxicity assay

The cytotoxic bioactivity of liCADs was analyzed by determining the ability to induce cell lysis of target cells. Specific lysis was plotted against the logarithm of liCAD concentration using Prism software (Graph Pad Software Inc.). The obtained dose-response curves were analyzed using the integrated four parameter non-linear fit model. Calculated concentrations of half-maximal kill values (EC_{50}) were used as indicators for bioactivity.

For liCAD mediated killing of $\text{CD47}^+\text{CD33}^+$ MOLM-13 tumor cells, cryopreserved IL-2 expanded NK cells were thawed in RPMI 1640 + GlutaMAX medium complemented with 5 % human serum. MOLM-13 cells were split to a density of 0.5×10^6 cells / ml in RPMI 1640 + GlutaMAX supplemented with 20 % FBS 24 hours prior to the assay setup. The following day 1×10^6 MOLM-13 cells were labeled with 16.6 μg / ml calcein AM (Thermo Fischer Scientific) for 30 minutes at 37 °C and subsequently washed 3 times with RPMI 1640 + GlutaMAX supplemented with 10% FBS.

To induce liCAD mediated killing of NK cells, IL-2 expanded NK cells and MOLM-13 cells were co-incubated at an effector-to-target ratio of 2:1 in RPMI 1640 + GlutaMAX + 10 % FBS in the presence of 10 nM to 0.1 pM liCAD (conc.(protein)) at 37 °C, 5 % CO_2 . Background was determined in samples containing only target cells (background MOLM), spontaneous lysis was determined in samples containing only target cells and effector cells (background NK) and maximal lysis was determined adding 50 μl of RPMI 1640 +

MATERIALS AND METHODS

GlutaMAX + 10 % + Triton - 100 (Roth) to labeled target cells (max lysis). Values were determined in duplicates. After 4 hours, cells were spun down at 1200 rpm / 5 minutes, 100 μ l of medium were transferred to a 96-well black polystyrene plate (Nunc) and absorption at 485 nm was measured using a TECAN plate reader.

The specific lysis was calculated according to following mathematical equation:

$$\text{specific lysis (\%)} = 100 \times \left[\frac{\text{conc. (protein)} - \text{background Nk}}{\text{max lysis} - \text{background MOLM}} \right]$$

3.4.11. Preferential lysis of CD47⁺ CD33⁺ target cells

Since CD47 is a ubiquitously expressed surface marker on human cells, we wanted to demonstrate that the low affinity Sirp α domain within the liCAD indeed favors a preferential lysis of CD47⁺ CD33⁺ tumor target cells. In order to do so, a cytotoxicity assay was performed with mixed single positive and double positive cell populations. In more detail, 1×10^6 Flp-INTM 293 HEK cells and CD33 Flp-INTM 293 HEK cells were calcein labeled as described above. Since HEK cells are human embryonic kidney cells, they express CD47 on their cell surface. Therefore, the unmanipulated Flp-INTM 293 HEK cells are single positive for CD47 and the transfected CD33 Flp-INTM 293 HEK cells are double positive for CD47 and CD33. Both have consistent levels of CD47 since it is expressed naturally. Two reactions were set up side by side: One reaction containing calcein labeled CD47⁺ cells and unlabeled CD47⁺ CD33⁺ cells, and the second reaction containing unlabeled CD47⁺ cells and calcein labeled CD47⁺ CD33⁺ cells. In both reactions the ratio of single positive and double positive cells was 1:1. Target cells were co-incubated with PBMCs in an effector-to-target ratio of 2:1 in RPMI 1640 + GlutaMAX + 10 % FBS in the presence of either maximal determined protein amount or evaluated half maximal kill values (conc. (protein)). Background was determined in samples containing only corresponding labeled and unlabeled HEK cells (background HEK), spontaneous lysis was determined in samples containing only corresponding labeled and unlabeled HEK cells and effector cells (background PBMC) and maximal lysis was determined by adding 50 μ l of RPMI 1640 + GlutaMAX + 10 % + Triton-X 100 to corresponding labeled and unlabeled HEK cells (max lysis). Values were determined

MATERIALS AND METHODS

in triplicates. Both reactions were incubated for 4 hours at 37 °C, 5 % CO₂. Afterwards, cells were spun down at 1200 rpm for 5 minutes, 100 µl of medium were transferred to a 96-well black polystyrene plate (Nunc) and absorption at 485 nm was measured using a TECAN plate reader.

The specific lysis was calculated again according to the following mathematical equation:

$$\text{specific lysis (\%)} = 100 \times \left[\frac{\text{conc. (protein)} - \text{background Nk}}{\text{max lysis} - \text{background HEK}} \right]$$

Calculated values were illustrated in Prism software as a bar graph and p-values were determined using an unpaired t-test (p < 0.05).

3.4.12. CD14-positive selection of monocytes

In order to generate human M2 macrophages, monocytes were isolated from PBMCs using CD14 MicroBeads (Miltenyi Biotech) according to the manufacturer's protocol. In short, 1 x 10⁷ PBMCs were pelleted and resuspended in 100 µl MACS buffer (Miltenyi Biotech). 20 µl of CD14 MicroBeads were mixed to the cell suspension and incubated for 15 minutes on ice. Afterwards, cells were washed with 2 ml of MACS buffer and centrifuged for 5 minutes at 1200 rpm. After an MS-column (Miltenyi Biotech) was washed with 500 µl MACS buffer, the cell suspension was put onto the column in a magnetic separator (Miltenyi Biotech). CD14 cells are thereby bound to the magnet and will not flow through the column. Cells were washed 3 times with MACS buffer. Subsequently the column was removed from the magnetic separator and CD14⁺ monocytes were eluted into a fresh tube with 1 ml MACS buffer. For higher starting PBMC numbers, volumes of buffers used were adjusted accordingly. Finally, monocytes were washed with PBS, centrifuged, counted and either PKH67 stained or plated into 24-well plates at a density of 0.1 x 10⁶ cells / well in X-Vivo medium (Lonza) containing 10 % autologous serum.

MATERIALS AND METHODS

3.4.13. PKH67 staining of monocytes and THP-1 cells

For staining of 2×10^7 monocytes or THP-1 cells, cells were resuspended in 1 ml DiIc solution (Sigma Aldrich) in a glass tube. 2 μ l PKH67 dye (Sigma Aldrich) were mixed with 1 ml DiIc solution and rapidly added to the cell suspension. Cells were incubated for 90 seconds at room temperature and staining was stopped by addition of 2 ml autologous serum. After 1 minute, cells were washed with medium once and counted for further experiments.

3.4.14. PKH26 staining of MOLM - 13 and THP-1 cells

For staining of 2×10^7 MOLM-13 or THP-1 targets, cells were first carefully washed in serum free medium and further resuspended in 1 ml DiIc solution. 4 μ l PKH26 dye (Sigma Aldrich) were mixed with 1 ml DiIc solution and rapidly added to the cell suspension. Cells were incubated for 5 minutes at room temperature by periodically inverting the tube. Incubation was stopped by addition of 2 ml FBS and incubated for 1 minute. Afterwards 4 ml of medium was added, cells were spun down and transferred to a fresh tube. Cells were washed twice and finally counted for subsequent experiments.

3.4.15. Generation of THP-1 macrophages

THP-1 macrophages were generated by plating 0.1×10^6 THP-1 cells / well into 24-well plates and differentiating them for 2.5 days in RPMI 1640 + GlutaMAX medium complemented with 10 % FBS and 10 nM PMA (Sigma Aldrich). Afterwards, medium was exchanged and THP-1 macrophages were used for subsequent phagocytosis assays

3.4.16. Generation of M2 macrophages

M2 macrophages were generated by differentiating monocytes for 5 days in M-CSF containing medium. Therefore 0.1×10^6 monocytes were plated into 24-well plates in 400 μ l X-Vivo medium + 10 % autologous medium + 1 % P/S containing 20 ng / ml M-CSF (R&D Systems) and cultured at 37 °C, 5 % CO₂. After 3 days, medium was exchanged and on day 5 macrophages were used for subsequent phagocytosis assays.

MATERIALS AND METHODS

3.4.17. Phagocytosis assay

PKH67 stained M2 macrophages or THP-1 macrophages were generated as described above and incubated with PKH26 stained MOLM-13 or THP-1 target cells, respectively, in an effector-to-target ratio of 2:1 in serum free X-Vivo medium. A 4-fold dilution series of liCADs was prepared and incubated at a concentration ranging from 100 μ M to 0.1 μ M with the cells for 2 hours at 37 °C, 5 % CO₂. Macrophages with target cells only but no protein served as a background control. Polybead® Carboxylate Red Dye Microspheres 6 μ m (Polysciences) incubated with macrophages instead of target cells were used as positive control. In order to exclude adhesion of target cells to the macrophages instead of engulfment, a control reaction with macrophages, target cells and protein was set up and kept for 2 hours at 4 °C. As an additional adhesion control, macrophages were pre-treated with 10 μ M cytochalasin D (Sigma Aldrich) and further incubated with target cells and protein. Treatment of macrophages with cytochalasin D inhibits actin polymerization and therefore prevents phagocytic activity. Assays were performed in triplicates or quadruplicates.

After 2 hours incubation, cells were collected into 1 ml FACS tubes (BD) as follows: First supernatant was transferred, then wells were washed with 200 μ l PBS. Macrophages were detached from plates by incubation with 100 μ l 1x TrypLE Express Enzyme (Thermo Fischer Scientific) for 5 minutes at 37 °C, 5 % CO₂. Reaction was stopped by addition of 100 μ l FBS and cells were transferred to the corresponding FACS tubes after careful resuspension. Tubes were centrifuged for 5 minutes at 1200 rpm, the supernatant removed, pellets resuspended in 100 μ l FACS buffer and transferred to a v-bottom 96-well plate. Cells were centrifuged again and stained for CD16 as described in 3.4.7. Afterwards, cells were washed again, taken up in 100 μ l FACS buffer, transferred to fresh FACS tubes and analyzed on a LSR II flow cytometer (BD) using Diva Software (BD).

Obtained data were exported into Excel and increase in phagocytosis was calculated by subtraction of the background control. Increase of phagocytosis was plotted against increasing concentration in a dose-response curve using Prism Software.

3.4.18. NK cell mediated cytotoxicity of *ex vivo* expanded AML cells

Primary AML patient samples were *ex vivo* expanded on feeder cells in the AML long term culture system as described in (Krupka et al., 2014) for 7 days. Cytotoxicity assays were performed with healthy donor NK cells at effector-to-target cell ratios of 5:1 and 2:1. Cells were incubated on MS-5 feeder cells (Krupka et al., 2014) in a-MEM (PAN Biotech) (supplemented with 12.5% fetal calf serum (FCS), 12.5% horse serum, 1% penicillin/streptomycin/glutamine recombinant human granulocyte-colony stimulating factor (rhG-CSF), rhu interleukin (IL)-3 and rhu thrombopoietin (TPO) (Peprotech, Hamburg, Germany) and 57.4 mM 2-mercaptoethanol (Sigma-Aldrich, Munich, Germany)) for 24 hours with 50nM of liCAD protein or no protein as a control condition. Subsequently cells were harvested and stained for CD16, CD56 and CD33 and analysed by flow cytometry. Lysis of AML cells was assessed flow cytometrically and analysed using Graph Pad Prism 6.

4. RESULTS

4.1. Cloning and expression of liCADs in FreeStyle™ 293-F cells

The coding genes for the extracellular domains of Sirp α (Sirp ex), Sirp α N-terminal Ig domain (SirpIg) and high affinity Sirp α (SirpIg_CV1) as well as for the scFvs of anti-CD47 (α CD47), anti-CD16 (α CD16) and anti-CD33 (α CD33) were PCR amplified and cloned into the eukaryotic expression vector pSecTag 2 Hygro B according to 3.2.1 and transfected into FreeStyle™ 293-F cells. Figure 9 illustrates a schematic representation of different liCADs used throughout this study.

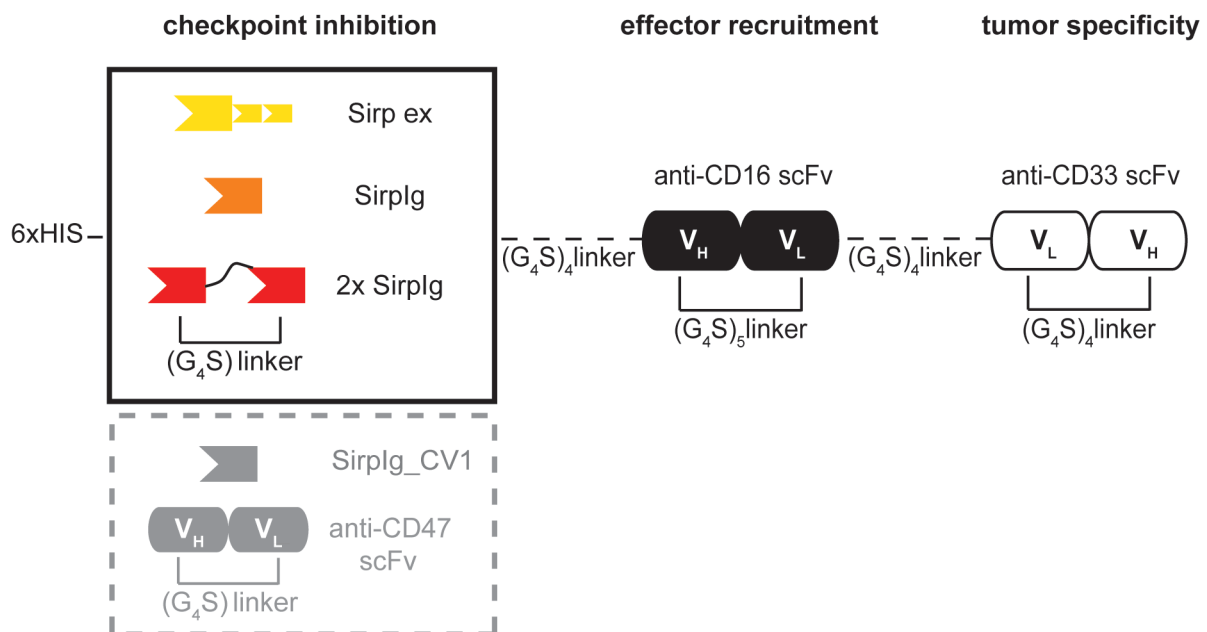


Figure 9 Construct design of liCADs. Checkpoint inhibition domains were cloned N-terminally, followed by a central anti-CD16 scFv serving as effector recruiting domain and the C-terminal anti-CD33 scFv tumor specific domain. In yellow the extracellular domain Sirp ex is shown, in orange and red constructs containing one or two extracellular SirpIg domains are shown, whereas in grey control constructs are illustrated.

As N-terminal checkpoint inhibition elements either the extracellular domain Sirp ex consisting of one Ig-like V type domain followed by an Ig-like C1 type 1 domain and an Ig-like C1 type 2 domain or the Ig-like V type domain SirpIg was used. In order to increase

RESULTS

avidity for CD47 a double SirpIg construct was generated, connecting two SirpIg domains with a five amino acid linker (GGGGS linker). As control constructs for CD47 blockade the published high affinity mutant SirpIg_CV1 was used as well as an anti-CD47 scFv, consisting of a variable heavy (V_H) and variable light (V_L) chain connected by one GGGGS linker. All liCADs contain a central anti-CD16 scFv, consisting of a V_H chain connected by a (GGGGS)₅-linker to the V_L chain and performing effector cell recruitment. The C-terminal anti-CD33 scFv is composed of a V_L chain connected to the V_H chain by a (GGGGS)₄-linker. Individual domains are connected by (GGGGS)₄-linker. Due to the Ig κ leader sequence within the expression vector, proteins were secreted into the cell culture medium. A N-terminal hexa-Histidine tag (6xHIS) served as first capture step for protein purification.

4.1.1. Expression of Sirp ex. α CD16. α CD33, SirpIg. α CD16. α CD33 and SirpIg.SirpIg. α CD16. α CD33

Sirp ex. α CD16. α CD33 (95 kDa) as well as SirpIg. α CD16. α CD33 (72 kDa) and SirpIg.SirpIg. α CD16. α CD33 (85 kDa) were well expressed in FreeStyle™ 293-F cells as shown in Figure 10. Affinity chromatography using Ni²⁺-NTA beads was used as a first capture step. Figure 10 illustrates the course of purification on a denaturing SDS-PAGE gel. The protein was well bound to the Ni²⁺-NTA agarose beads and washed for three times to get rid of unspecifically bound protein. Negligible amounts of desired protein came off the beads during washing steps. However, intensive effort to recover the complete protein amount did not improve the binding capacity of the protein to the beads.

RESULTS

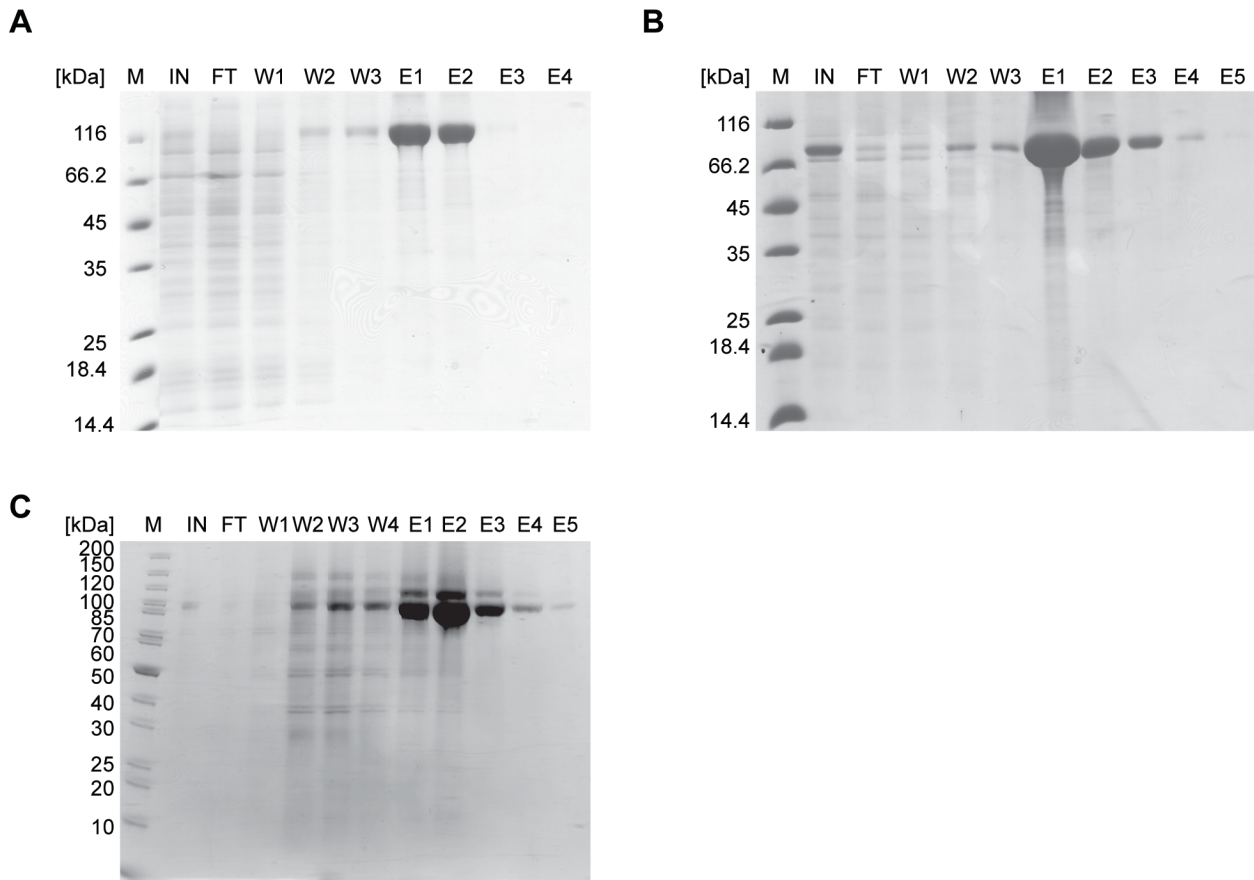
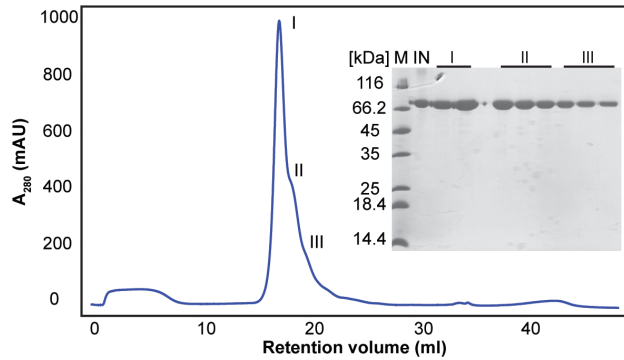


Figure 10 Affinity chromatography of proteins expressed in FreeStyle 293-F cells. Ni²⁺-NTA purification of (A) Sirp ex.αCD16.αCD33, (B) SirpIg.αCD16.αCD33 and (C) SirpIg.SirpIg.αCD16.αCD33 shows already pure protein within elution fractions E1-E3. Marker (M), input of protein (IN), flow through (FT), wash fractions (W1-W4), and elution fractions (E1-E5).

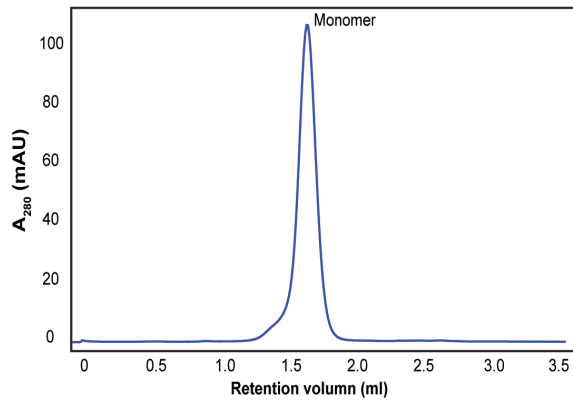
Elutions fractions 1-3 were pooled and a subsequent anionic exchange chromatography on a HiTrap Q column was performed. As shown exemplary for SirpIg.αCD16.αCD33 in Figure 11B, the protein eluted in one main peak (I), followed by 2 shoulders (II and III). When analyzed on a denaturing SDS-PAGE gel, all peak fractions contained the protein of interest. Analytical size exclusion chromatography on a Superdex 200 5/150 GL column revealed, that the main peak fraction I ran only in one peak, suggesting mainly monomer (Figure 11B), whereas fractions II and III contained a second peak, potentially indicating increasing amounts of aggregates (Figure 11C). Therefore, collecting the main peak after anionic exchange yielded in mainly monomer protein. Peak II and III were further pooled and monomer was separated from aggregate on a Superdex 200 10/300 GL.

RESULTS

A



B



C

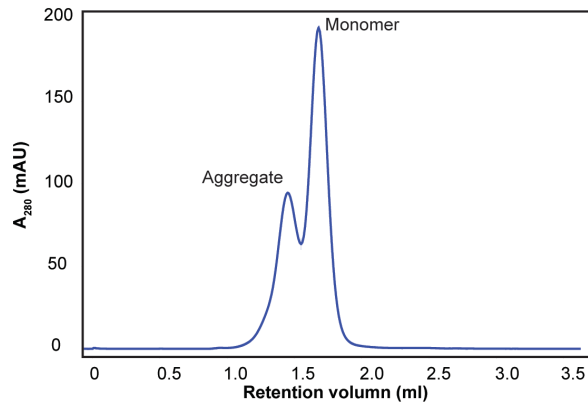


Figure 11 Anionic exchange chromatography and size exclusion chromatography of SirpIg.αCD16.αCD33. (A) Anionic exchange chromatography with a HiTrapQ column showed a main peak (I) with 2 shoulders (II and III) that also contained the protein of interest. (B) When subjected to analytical size exclusion chromatography on a Superdex 200 5/150 GL column a monomer could only be obtained in the main peak fraction I. (C) Within fraction II and III potential aggregation peaks were detected on size exclusion chromatography and monomer peaks could be separated again. Marker (M), input of protein (IN).

The extracellular domain of Sirp α (37.5 kDa) as well as the N-terminal Ig-like V type domain only (14.2 kDa) was also expressed periplasmatically in *E.coli* BL21 cells. Denaturing SDS-PAGE analysis of Sirp ex revealed a degradation band at the size of the N-terminal Ig-like V type domain only (Figure 12A), which suggested a higher instability of this protein compared to the SirpIg only.

RESULTS

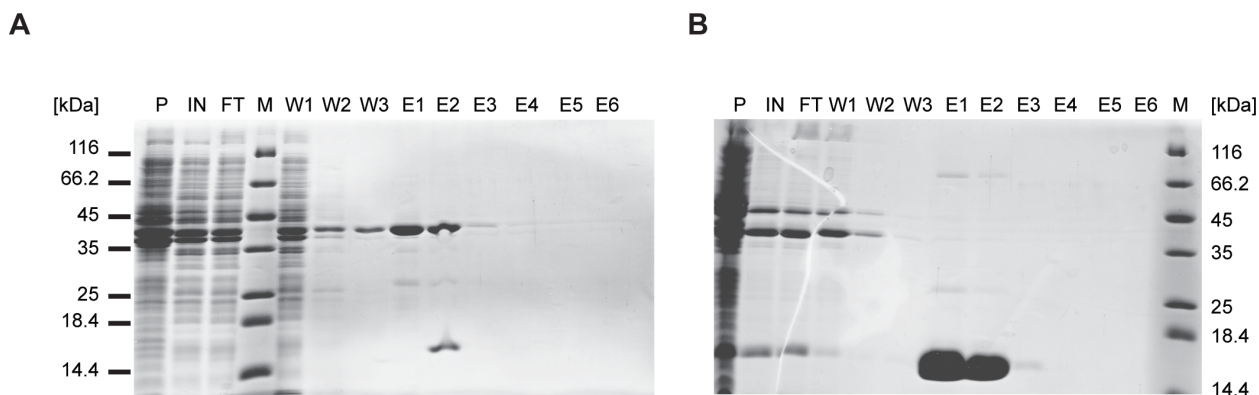


Figure 12 Affinity chromatography of Sirp ex and SirpIg expressed periplasmatically in *E.coli* BL21 cells. (A) Sirp ex (37.5 kDa) elutes mainly in elution fractions E1 and E2, however a degradation band at around 15 kDa is clearly visible. (B) SirpIg (14.2 kDa) elutes in elution fraction E1 and E2. Marker (M), pellet (P), input of protein (IN), flow through (FT), wash fractions (W1-W3), and elution fractions (E1-E6).

As crystallization data have revealed that the N-terminal Ig V type domain of Sirp α is sufficient for binding to CD47 and separate expression of the extracellular Sirp α showed degradation bands when expressed in *E. coli*, we decided to carry out all subsequent studies with the SirpIg. α CD16. α CD33 protein only.

4.1.2. Expression of SirpIg_CV1. α CD16. α CD33 and α CD47. α CD16. α CD33

To purify control molecules that bind to CD47 (SirpIg_CV1. α CD16. α CD33, 72 kDa and α CD47. α CD16. α CD33, 85 kDa) the transfection and expression procedure was carried out in FreeStyle™ 293-F cells the same as described before. After incubation of the cell supernatant with Ni²⁺-NTA agarose beads, purification fractions were analyzed on a denaturizing SDS-PAGE gel. No protein could be detected in the input fraction as well as the wash and elution fractions (Figure 13A). However, flow cytometric analysis of transfected FreeStyle™ 293-F cells with fluorescently labeled anti-HIS antibody showed that protein was indeed well expressed but immediately bound to the FreeStyle™ 293-F cells due to high affinity for CD47 as illustrated in Figure 13B.

RESULTS

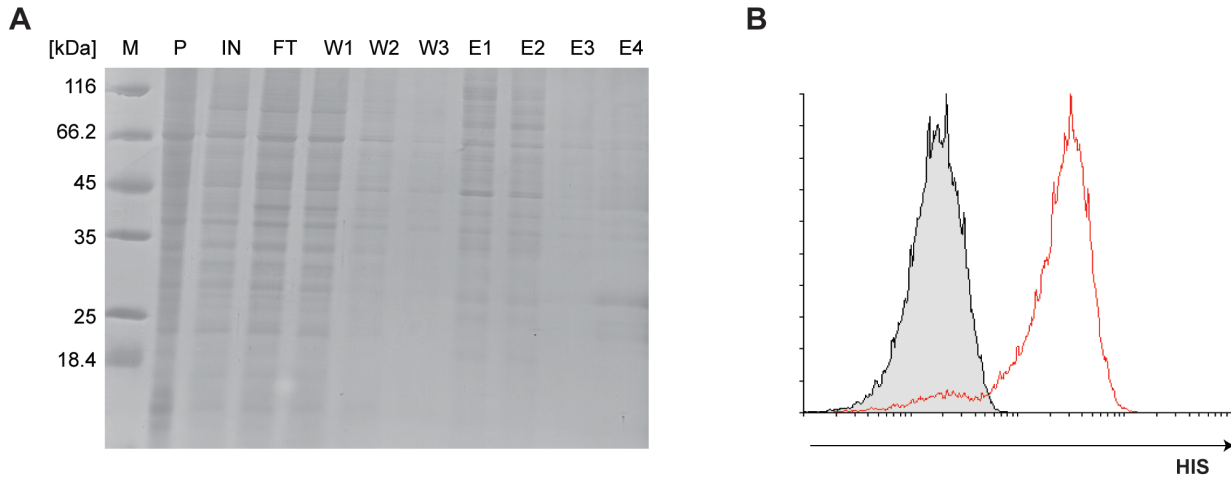


Figure 13 Expression of control constructs. (A) SDS-PAGE analysis of α CD47. α CD16. α CD33 did not show any eluted protein at a size of 85 kDa. Marker (M), pellet (P), input of protein (IN), flow through (FT), wash fractions (W1-W3) and elution fractions (E1-E4). (B) Flow cytometric analysis with anti-HIS antibody of FreeStyle™ 293-F cells 5 days after transfection revealed that protein was bound to the cells (red chromatogram). Untransfected cells incubated with anti-HIS antibody served as a background control and are represented in grey.

4.2. siRNA mediated transient knock down of CD47 in FreeStyle™ 293-F cells

In order to avoid immediate binding of control molecules, CD47 was transiently knocked down using an ON-TARGET plus siRNA SMARTpool directed against CD47. As depicted in Figure 14A a partial knock down of CD47 could be obtained as can be seen by the decrease in fluorescence intensity of the CD47-PE signal. Comparison of untransduced FreeStyle™ 293-F cells stained for CD47 (red chromatogram) as well as the isotype control (grey chromatogram) with the transduced FreeStyle 293-F cells (blue chromatogram) shows that a full knock down of CD47 could by far not be obtained, but still parallel knock down of CD47 and expression of control proteins lead to lower binding probability to the FreeStyle™ 293-F cells. Figure 14B shows a denaturing SDS-PAGE analysis of a Ni^{2+} -NTA purification of α CD47. α CD16. α CD33 without (left) and with (right) CD47 transient knock down. Elution fraction E1 and E2 contain protein only in case of the CD47 knocked down FreeStyle 293-F cells (marked with a red star). In case of SirpIg_CV1. α CD16. α CD33 even more protein could be obtained from affinity chromatography as shown in Figure 14C. Furthermore, these findings were confirmed by western blot analysis against anti-HIS tag

RESULTS

(Figure 14D). As shown, again only the elution fractions of the CD47 knocked down FreeStyle™ 293-F cells contained protein.

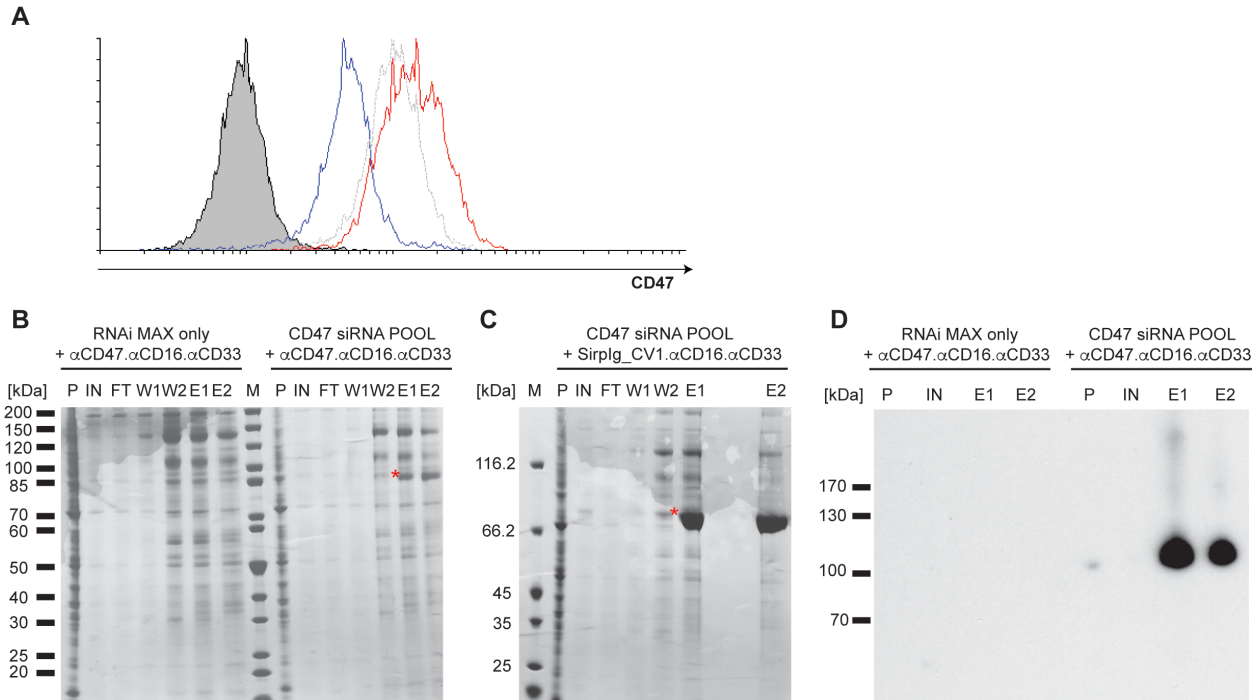


Figure 14 Transient CD47 knock down of FreeStyle 293-F cells. (A) Flow cytometry reveals a partial knock down of CD47 when analyzing untransfected (red line), Lipofectamin RNAiMAX transfection reagents only treated (light grey dashed line) and ON-TARGET PLUS human CD47 SMARTpool treated (blue line) cells with anti-CD47-PE. Untransduced cells stained with an anti-CD47 isotype control are illustrated in dark grey and represent CD47 negative cells. (B) SDS-PAGE analysis of α CD47. α CD16. α CD33. Marker (M), Pellet (P), input (IN), flow through (FT), wash fractions (W1, W2), elution fractions (E1, E2). (C) SirpIg_CV1. α CD16. α CD33 after affinity chromatography clearly shows protein in elution fractions E1 and E2 (red star) only in the CD47 siRNA treated Freestyle 293-F cells compared to control cells. Marker (M), Pellet (P), input (IN), flow through (FT), wash fractions (W1, W2), elution fractions (E1, E2). (D) Western blot analysis against the HIS-tag further confirmed protein expression in E1 and E2 of CD47 knocked down cells. Pellet (P), input (IN), elution fractions (E1, E2).

4.3. Cloning and expression of liCADs in *Drosophila melanogaster* Schneider 2 cells

Schneider's embryonic *Drosophila* cell line 2 (S2) can be used for stable expression of a variety of recombinant proteins using vectors specifically engineered for protein expression

RESULTS

in *Drosophila* cells. As described for the eukaryotic expression system, also for the *Drosophila* expression system the coding genes for the extracellular Ig-like V type domain Sirp α (SirpIg) and high affinity Sirp α (SirpIg_CV1) as well as for the scFvs of anti-CD47 (α CD47), anti-CD16 (α CD16) and anti-CD33 (α CD33) were PCR amplified and cloned into the *Drosophila* expression vector pS2-1 or pS2-2 and transfected into S2 cells. The signal sequence from the insect BiP gene was exploited to direct the recombinant protein through the secretory pathway of S2 cells into the culture medium. After buffer exchange using a Minimate Tangential Flow Filtration (TFF) system, soluble protein could easily be purified by Ni^{2+} -NTA affinity chromatography as a first capture step. Figure 15A shows exemplary for SirpIg. α CD16. α CD33 the enrichment of protein of interest in elution fractions E1 to E3. Quite substantial amount of protein could also be seen in the wash fraction already, which is most likely due to the low affinity of the 6xHIS tag to Ni^{2+} -NTA agarose beads. Therefore, only one washing step was performed. In addition to the protein of interest also some unspecific higher molecular weight proteins (above 200 kDa) were obtained, that could be removed by anionic exchange. To this end, elution fractions E1-E3 were pooled and subjected to a MonoQ 5/50 GL column using a 4-step gradient elution profile. As shown in Figure 15B, peak I contained only liCAD protein whereas unspecific S2 proteins could be separated and eluted in a later second peak (II). Elution fractions within the first peak were then further collected and subjected to size exclusion chromatography in order to separate aggregate from monomeric protein. Consequently, protein was loaded onto a Superdex 200 increase 10/300 GL column and peak fractions were additionally analyzed on a denaturing SDS-PAGE gel. As illustrated in Figure 15C, a smaller first peak eluted shortly before a main second peak, which represent a small aggregation peak and a main monomer peak of protein of interest. As a result, pure liCAD protein could be obtained in a 3-step purification procedure.

RESULTS

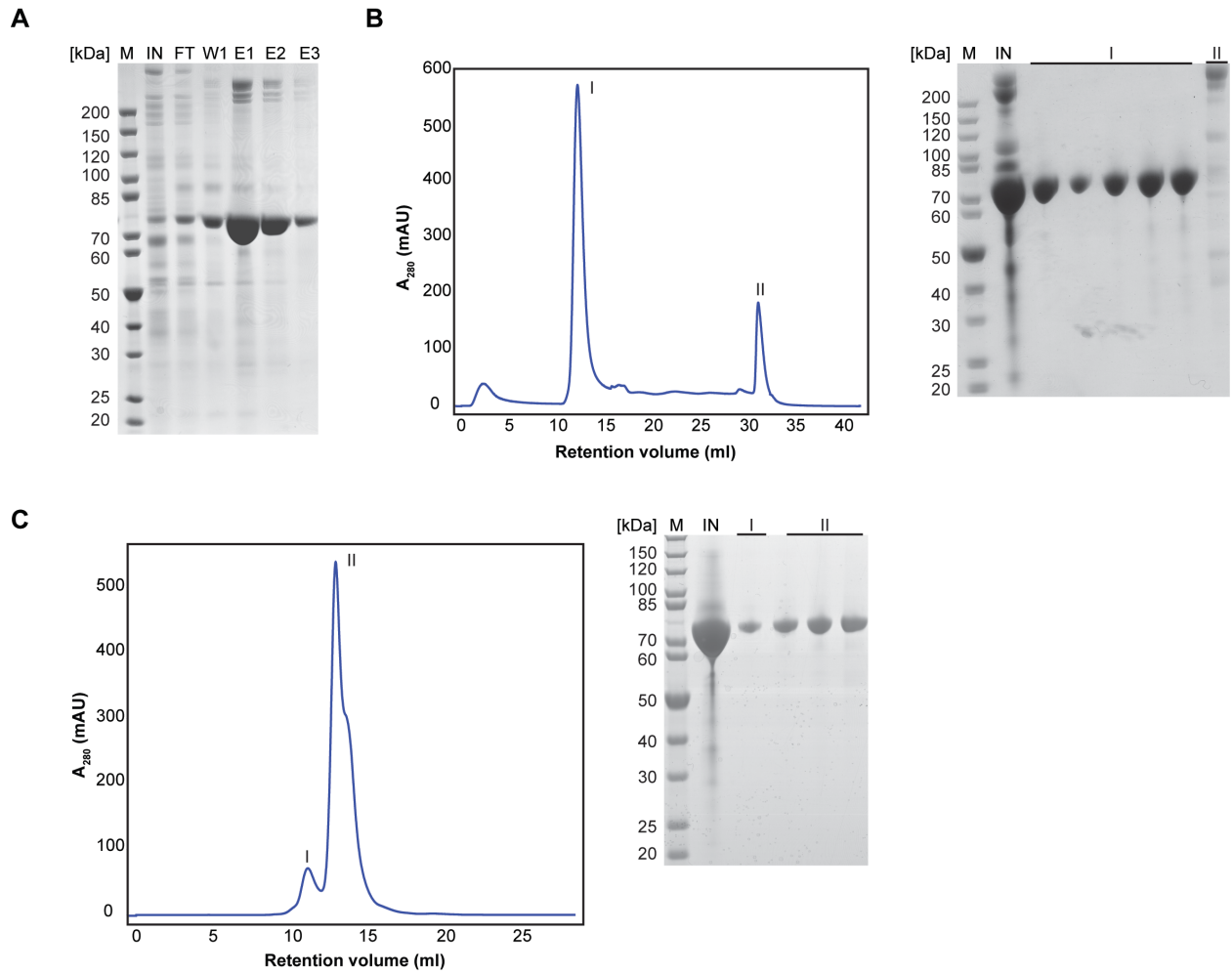


Figure 15 Protein purification of liCADs expressed in S2 cells. (A) Exemplary Ni^{2+} -NTA chromatography shows a clear protein band at a size of 75 kDa in case of SirpIg. α CD16. α CD33. Marker (M), input (IN), flow through (FT), wash fraction (W1), elution fractions (E1-E3). (B) Anionic exchange chromatography using a MonoQ 5/50 GL column separates liCAD protein (peak I) from unspecific S2 cell proteins (peak II) Marker (M), input (IN). (C) Concluding size exclusion chromatography on a Superdex 200 increase 10/300 GL further separated aggregate (peak I) from monomeric protein (peak II). Marker (M), input (IN).

RESULTS

4.4. Small-angle X-ray scattering of SirpIg.αCD16.αCD33 and SirpIg.SirpIg.αCD16.αCD33

The two main liCAD proteins, SirpIg.αCD16.αCD33 and SirpIg.SirpIg.αCD16.αCD33, were analysed by small angle X-ray scattering (SAXS), to verify that the protein in solution is indeed monodisperse and of multi-domain structure. For this purpose, three different concentrations (2.6 mg/ml, 1.5 mg/ml and 1 mg/ml) were measured in case of SirpIg.αCD16.αCD33 and two different concentrations (1.4 mg/ml and 0.7 mg/ml) were measured for SirpIg.SirpIg.αCD16.αCD33.

As shown in Figure 16A, scatter blots of raw data already revealed a monomeric protein in solution. Further data transformation to a Kratky plot (Figure 16B) and a Guinier plot (Figure 16C) strengthened the evidence of no present aggregates but properly folded protein in solution. Additionally the $P(r)$ distribution (Figure 16D) clearly indicated a multi-domain protein being measured.

RESULTS

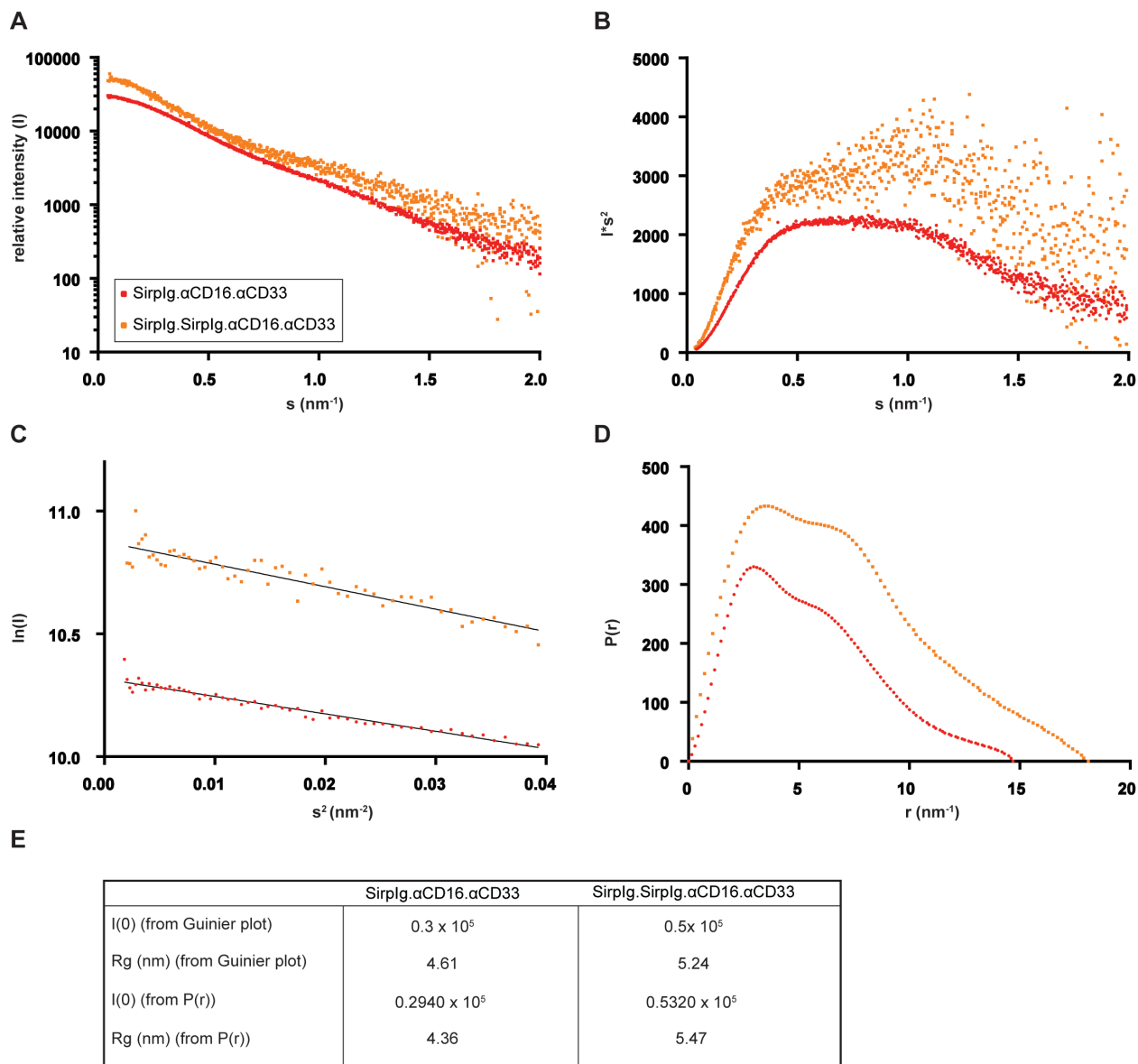


Figure 16 Data analysis of SAXS. (A) Scattering intensity plot of Sirplg.αCD16.αCD33 (red) and Sirplg.Sirplg.αCD16.αCD33 (orange). (B) Kratky plot as well as (C) Guinier transformation reveal properly folded and monomeric protein in solution. (D) $P(r)$ distribution shows characteristic plots for multi-domain proteins. (E) Summary of $I(0)$ and R_g values obtained from Guinier transformations and distance distributions.

A low-resolution model of the structure could be obtained by calculating 10 models and averaging the best ones. The crystal structure of two scFv as well as of the N-terminal Ig-like V type domain of Sirp α could be fitted into it using Pymol, as shown for separate proteins in Figure 17A and in an overlay of both molecules in Figure 17B.

RESULTS

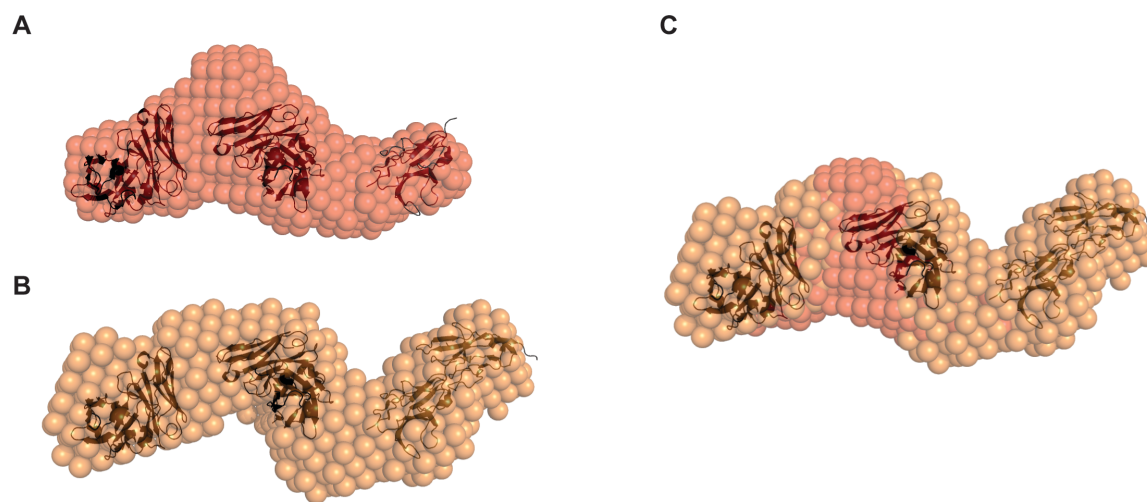


Figure 17 Structure modeling and fitting of liCADS. (A) Theroretical models of SirpIg.αCD16.αCD33 (red) and (B) SirpIg.SirpIg.αCD16.αCD33 (orange) could be calculated and crystal structures of scFvs as well as the N-terminal Ig-like V type domain of Sirp α were fitted to the liCAD density. (C) Overlay of both models.

In summary, these data confirm that liCAD proteins are indeed monodisperse and of multi-domain structure, which theoretically enables binding capability and further biological activity.

4.5. Binding studies of liCAD proteins

In order to test binding of liCAD proteins to cell surface antigens, we did binding studies using flow cytometry. Since CD47 is expressed on every human cell and thus also on human cell lines, liCADs could not be tested for binding to CD33 or CD16 due to a constant CD47 binding. To overcome this problem, single domains of liCADs were purified and seperatly tested for binding to respective antigens.

Figure 18 summerizes flow cytometric binding studies on THP-1, Jurkat and stably transfected CHO-CD16 cells used in this study. Proteins were incubated at a saturating concentration and binding to the target cell was further analyzed by incubation with a secondary anti-HIS tag antibody. Binding of Sirp α to CD47 is reported to be in the low μM range. Therefore, owing to the low interaction strength, binding of SirpIg could not be detected on Jurkat cells (A). Several other human cell lines (eg. Freestyle 293FTM cells,

RESULTS

THP-1 cells or MOLM-13 cells) were tested for binding studies but SirpIg binding could never be demonstrated (data not shown). For higher affinity CD47 binders, like the high affinity mutant SirpIg_CV1 and the anti-CD47 scFv, binding could be shown on THP-1 cells (B and C). Since THP-1 cells are of monocytic origin, they also express CD33 on their cell surface and thus, binding of the anti-CD33 scFv could be shown (D). Additionally, the immune cell-recruiting domain was checked for binding by using CHO cells stably transfected to express CD16. Here we could demonstrate that the anti-CD16 scFv is able to bind to its target antigen on a living cell. Dashed black lines represent target cells incubated with anti-HIS tag antibody only.

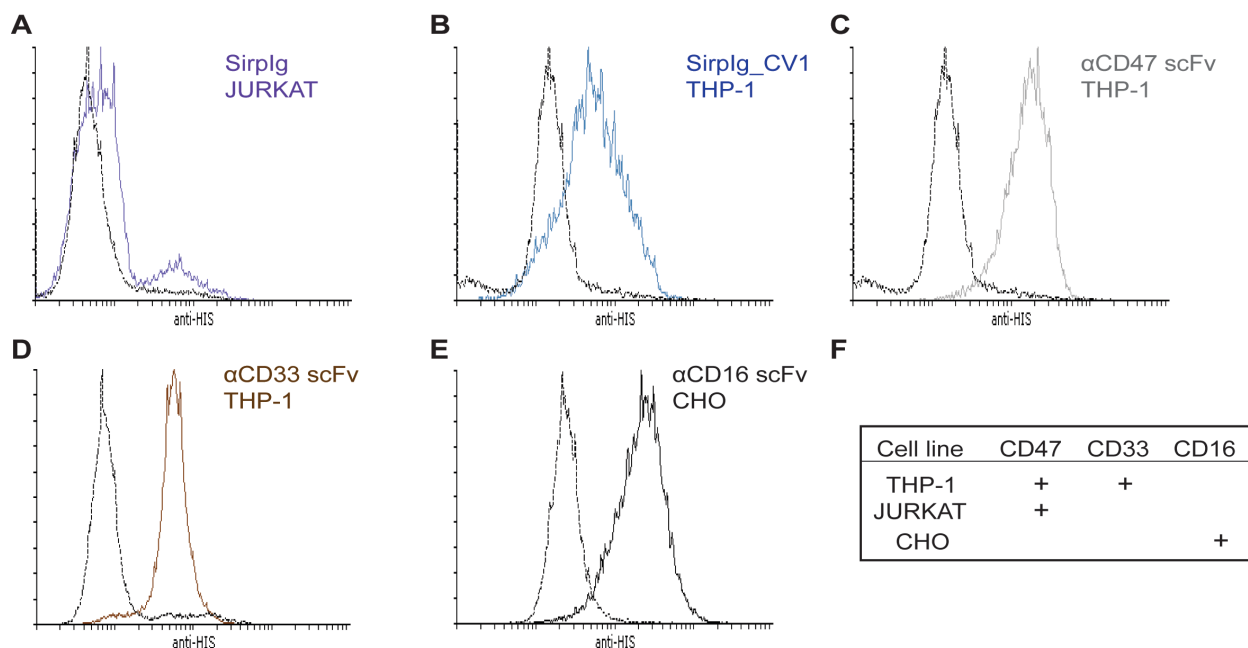


Figure 18 Binding studies of separate liCAD domains on human cell lines. (A) Binding of the naturally occurring SirpIg to human CD47 on Jurkat cells could not be detected due to low interaction strength. (B) High affinity mutant SirpIg_CV1 binds to human THP-1 cells (C) as well as anti-CD47 scFv and (D) anti-CD33 scFv. (E) Binding of anti-CD16 scFv could be detected using CD16 expressing CHO cells. Dashed black lines represent isotype controles. (F) Cell lines used for flow cytometric analysis. + indicates respective surface antigen expression.

RESULTS

4.6. Generation of CHO Flp-InTM cells stably expressing CD33 and CD47

As CD47 is expressed ubiquitously on human cells, a cell system expressing only CD47 or CD33 had to be generated in order to get valid binding data on liCAD molecules. We chose Chinese hamster ovary (CHO) Flp-InTM cells that do not express human antigens and had FRT sites integrated at a transcriptionally active genomic locus. Consequently, upon transfection of an Flp-InTM expression vector, targeted integration and high level of expression of the protein of interest is ensured. In order to generate CD47 and CD33 expressing CHO cell lines, full-length human CD47 as well as CD33 were cloned into pcDNATM/FRT expression vectors as described in 3.4.4. Stable clones were raised over several weeks and antigen expression was analyzed by flow cytometry. As shown in Figure 19A untransfected parental CHO cells were checked for human CD47 (red chromatogram), CD33 (blue chromatogram) and CD16 (green chromatogram) cell surface expression. As expected, none of the antigens could be detected on CHO cells. Individual established lines were then also checked for CD47, CD33 and CD16 expression (data not shown) however, as expected, cell lines were only positive for stably transfected antigens. Figure 19B summarizes most important surface marker expression analysis.

RESULTS

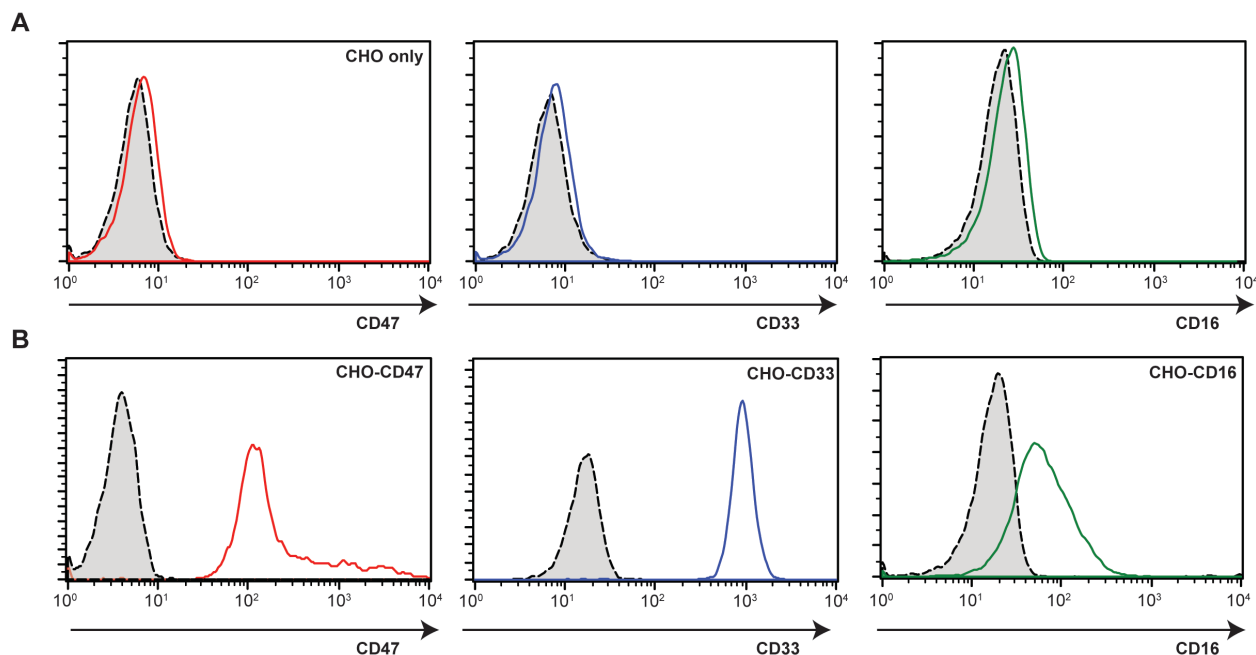


Figure 19 Characterization of CHO cell lines. (A) CHO Flp-INTM cells were first analyzed for CD47 (red), CD33 (blue) and CD16 (green) expression. Grey chromatograms with black dashed lines always represent corresponding isotype controls. (B) CD47 expression was confirmed in CHO-CD47 cells (red), CD33 in CD33 transfected CHO cells (blue) and CD16 in CHO-CD16 cell lines (green).

Flow cytometry of generated cell lines confirmed that CD47 is only expressed in CHO-CD47 cells but not on CHO-CD33 and CHO-CD16 cells. Further, CD33 expression was solely shown in CHO-CD33 cells and CHO-CD16 cells were checked positively only for CD16 expression. All cell surface stainings were compared to an isotype control of the respective antibody, which is shown in grey chromatograms with black dashed lines.

4.7. Binding studies of liCAD proteins on CHO cell lines

To test binding of individual liCAD domains within the full molecule, saturation binding assays were performed on stably transfected CHO Flp-INTM cells that only express CD47, CD33 or CD16, respectively. Bound liCAD protein was quantified by flow cytometry after staining with an α -HIS tag antibody coupled to an Alexa Fluor 488 dye.

Using the CHO-CD47 cells, SirpIg binding (Figure 20A) to CD47 could be detected, however, to a weaker extend than SirpIg.SirpIg (Figure 20B), as can be seen by the shifts in

RESULTS

mean fluorescence intensity in the histogram. Control molecules were also tested for binding to CD47 and as shown in Figure 20C and D α CD47 scFv binds less strong than the high affinity mutant of SirpIg, SirpIg_CV1. Binding of α CD33 scFv to CHO-CD33 cells as well as α CD16 scFv to CHO-CD16 cells could also be detected via flow cytometry. Both had similar shifts in mean fluorescence intensity, indicating likewise affinities. The grey chromatograms with dashed black lines represent CHO cells incubated with α -HIS tag antibody only as a background control. None of the molecules showed binding to CHO only cells (data not shown).

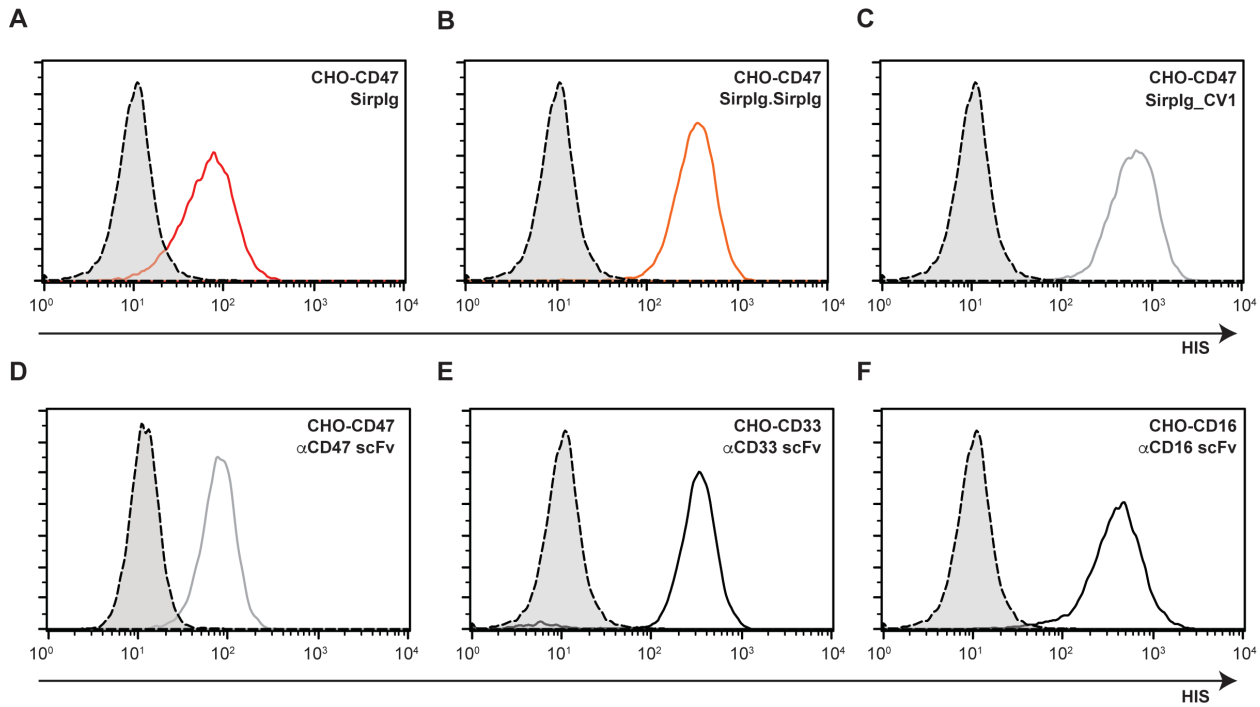


Figure 20 Binding of individual liCAD domains to target antigens. (A, B) SirpIg (red) shows weaker binding to CD47-CHO cells compared to SirpIg.SirpIg (orange). (C, D) SirpIg_CV1 binds to CD47 with a higher affinity than the α CD47 scFv, as can be seen by shifts in mean fluorescence intensity. (E) α CD33 scFv binds to CHO-CD33 cells with high affinity (F) as well as α CD16 scFv to CD16 on CHO cells. Grey chromatograms with dashed black lines represent CHO cells incubated with α -HIS tag antibody only as a background control.

RESULTS

4.7.1. K_D determination of liCAD proteins on CHO cell lines

As shown in Figure 20 all liCAD molecules were able to bind to CD47 on CD47-CHO cells and therefore, dissociation constants (K_D) could be evaluated. Bound liCAD was quantified by flow cytometry after staining with an anti-HIS tag antibody labeled with Alexa-488. K_D values were calculated by computational analysis with Graph Pad Prism 6. Curves were normalized and fitted to a nonlinear fit, one site specific binding model and normalized mean fluorescence intensities were plotted against various liCAD concentrations. All measurements were performed in technical duplicates and repeated three times.

The binding affinity for Sirp α to CD47 is reported to be in the low μ M range as previously discussed. The measured K_D -value for SirpIg. α CD16. α CD33 is 588 nM \pm 240 nM (Figure 21A). Considering the huge deviations within measurements it is obvious that a low affinity interaction is measured in this case. Duplication of SirpIg dramatically increases binding affinities since a K_D -value of 21 nM \pm 3.8 nM was determined, as shown in Figure 21B. Therefore, SirpIg.SirpIg. α CD16. α CD33 binds around 30-times stronger compared to SirpIg. α CD16. α CD33 and almost as strong as the high affinity mutant. SirpIg_CV1. α CD16. α CD33 binds with a K_D -value of 16.9 nM \pm 3 nM (Figure 21C) the strongest to CD47, which was expected since it is reported to be a high affinity mutant of wild type SirpIg. The K_D -value of the second control molecule, α CD47. α CD16. α CD33, is 147 nM \pm 38 nM (Figure 21D), which is more than 8-times weaker than the high affinity mutant and is compared to the wild type SirpIg and double SirpIg in between binding affinities.

RESULTS

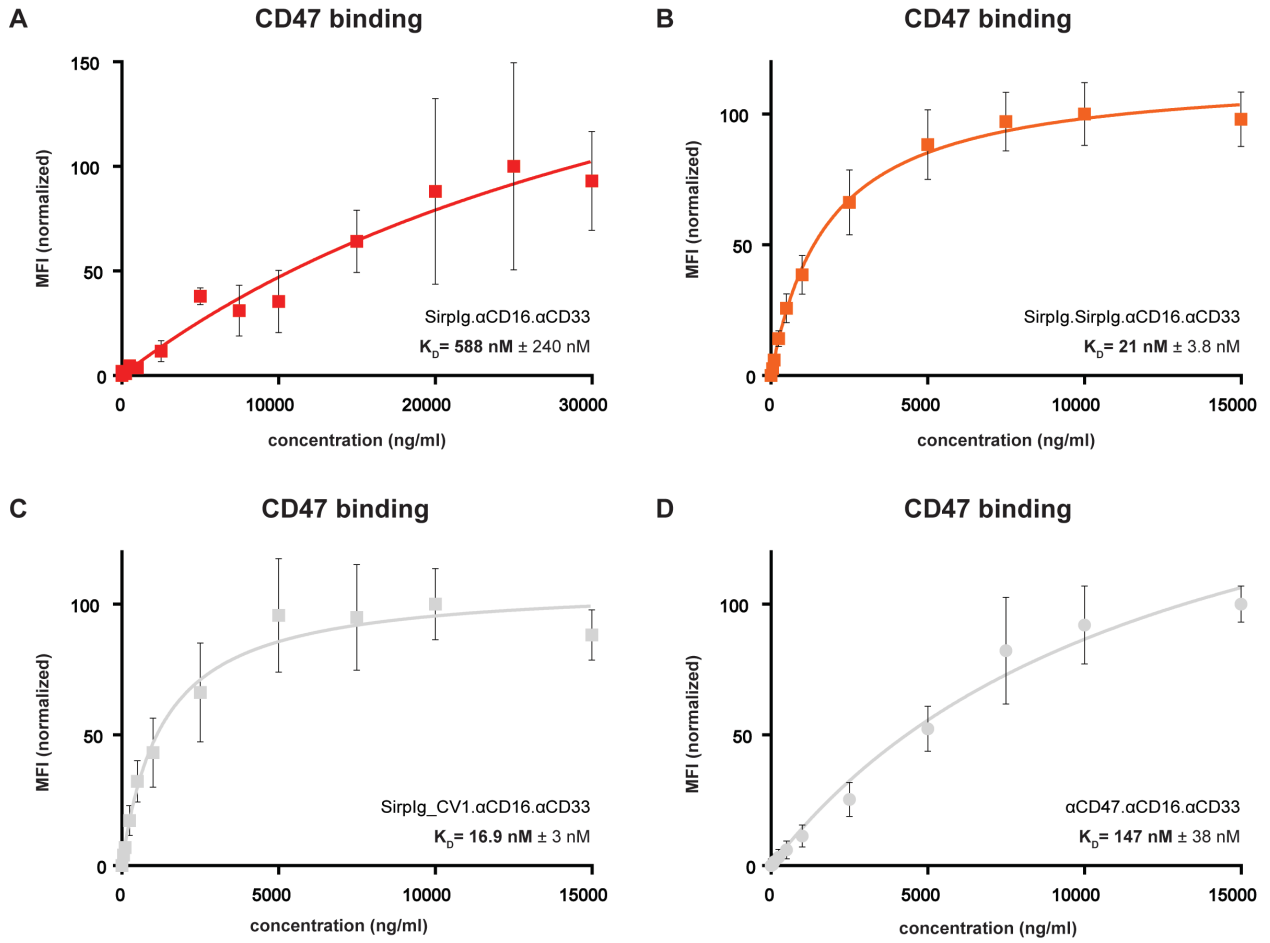


Figure 21 K_D determination of liCAD molecules for CD47 binding on CD47-CHO cells was determined by flow cytometry. (A) Dissociation constant of Sirplg binding to CD47 is $588 \text{ nM} \pm 240 \text{ nM}$. (B) Sirplg.Sirplg binds to CD47 with a K_D of $21 \text{ nM} \pm 3.8 \text{ nM}$ and showed much stronger binding when compared to single Sirplg. (C) High affinity mutant Sirplg_CV1 binds with the strongest affinity to CD47 ($16.9 \text{ nM} \pm 3 \text{ nM}$). (D) K_D determination of αCD47 scFv reveals $147 \text{ nM} \pm 38 \text{ nM}$, showing the second lowest binding affinity to CD47 compared to the other CD47 binders. Error bars represent standard error of the mean (SEM) of triplicates.

K_D values were also determined for αCD16 scFv and αCD33 scFv by incubating a serial dilution of Sirplg.αCD16.αCD33 on CD16-CHO or CD33-CHO cells, respectively. The dissociation constant for αCD16 scFv is $19.8 \text{ nM} \pm 3.4 \text{ nM}$ (Figure 22A). For the αCD33 scFv a K_D value of $9.8 \text{ nM} \pm 2.6 \text{ nM}$ was determined as shown in Figure 22B.

RESULTS

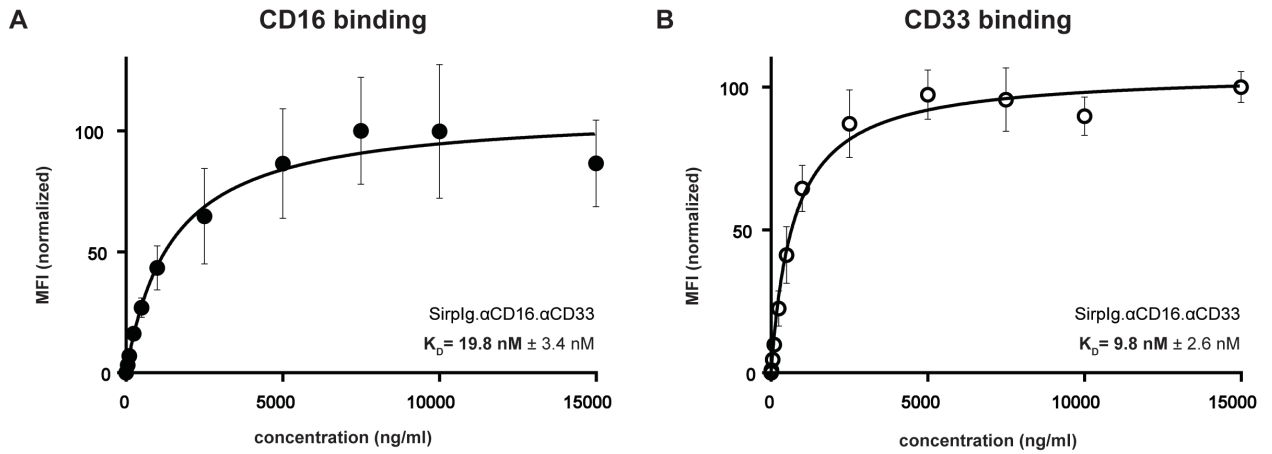


Figure 22 K_D determination of liCAD molecules for CD16 and CD33 binding. (A) Binding of SirpIg.αCD16.αCD33 revealed a K_D value of $19.8 \text{ nM} \pm 3.4 \text{ nM}$ for CD16 binding. (B) αCD33 scFv binds with an affinity of $9.8 \text{ nM} \pm 2.6 \text{ nM}$ to CD33-CHO cells. Error bars represent standard error of the mean (SEM) of triplicates.

RESULTS

4.8. Biological functionality of liCAD proteins

4.8.1. Cytotoxicity assay with *in vitro* IL-2 expanded NK cells

The potential of liCAD molecules to induce cytotoxicity on MOLM-13 cells, which is an AML cell line highly expressing CD33, was first tested with *in vitro* expanded NK cells as effector cells. Target cells were calcein labeled and incubated with effector cells at an effector-to-target ratio of 2:1 for 4 hours. Supernatants were analyzed for fluorescence intensities at 480 nm using a TECAN plate reader. The percentage of specific lysis was calculated as described in 3.4.10, data were transformed to logarithms and fitted to a sigmoidal dose-response equation in Graph Pad Prism 6. Half maximal effective concentrations (EC_{50}) were calculated as indicator for specific bioactivity. All experiments were performed in technical duplicates and were repeated three times.

As illustrated in Figure 23, SirpIg. α CD16. α CD33 (red curve) has a calculated EC_{50} value of 341 pM (95% CI = 146 pM - 794 pM), which is almost 10-times higher than SirpIg.SirpIg. α CD16. α CD33 (39 pM (95% CI = 6 pM - 244 pM, orange curve). Compared to the bispecific control α CD33. α CD16 (black curve), that has an EC_{50} value of 1 060 pM (95% CI = 558 pM - 2 300 pM), one can appreciate that indeed dual targeting leads to an increased cytotoxicity on MOLM-13 cells. Control molecule SirpIg_CV1. α CD16. α CD33 (grey curve, filled circle) has a calculated EC_{50} value of 3.2 pM (95% CI = 2 pM - 16 pM) and the half maximal effective concentration for α CD47. α CD16. α CD33 (grey curve, clear circle) is 101 pM (95% CI = 60 pM - 203 pM). These findings correlate with determined binding affinities, since molecules having a higher affinity for CD47 induce killing at a lower concentration than weaker binder. The control molecule (α HER2. α CD16. α HER2) did not induce cytotoxicity of HER 2 negative target cells, which excludes unspecific activation of NK cells by CD16 binding only.

RESULTS

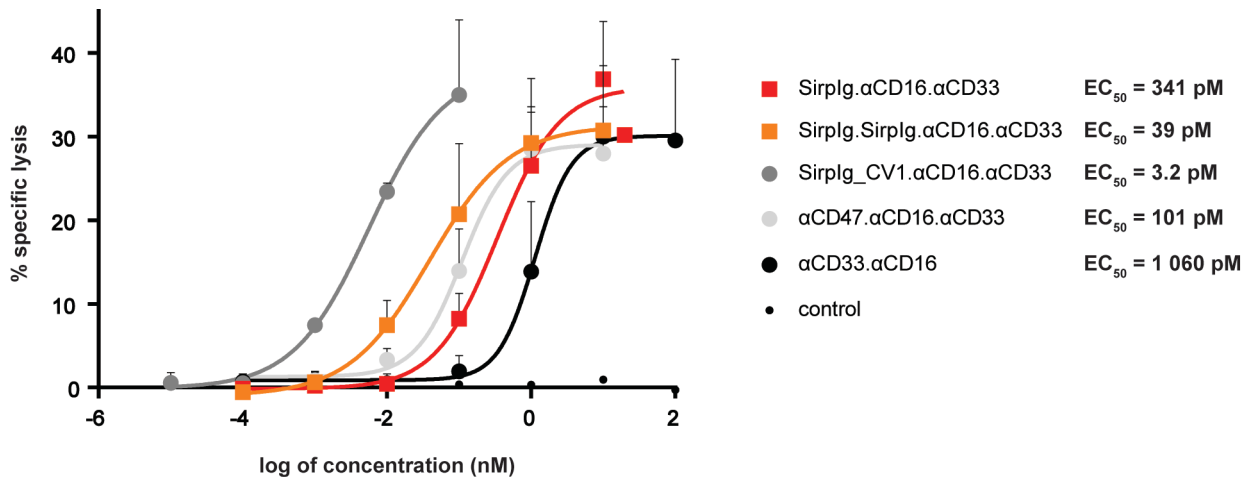


Figure 23 LiCAD dependent cytotoxicity assay on MOLM-13 cells. Sirplg.αCD16.αCD33 (red) and Sirplg.Sirplg.αCD16.αCD33 (orange) show lower half maximal effective concentrations compared to the αCD33.αCD16 bispecific control. This suggests an increased cytotoxic potential of liCAD molecules possibly due to dual targeting of MOLM-13 cells. EC₅₀ values of control liCADs Sirplg_CV1.αCD16.αCD33 (dark grey) and αCD47.αCD16.αCD33 (light grey) correspond to determined binding affinities to CD47. Error bars represent standard error of the mean (SEM) of triplicates. αHER2.αCD16.αHER2 (control) did not induce cytotoxicity.

4.8.2. Cytotoxicity assay with primary NK cells

In order to rule out, that liCAD induced cytotoxicity observed in assays with IL-2 expanded NK cells was not only due to pre-stimulation and activation of NK cells, we wanted to test if liCAD molecules also show biological functionality in unstimulated, none IL-2 expanded primary NK cells. To do so, MACS sorted NK cells from healthy donors were kindly provided by Prof. Marion Subklewe.

Assays were carried out as described above. Due to different healthy donor NK cell samples, killing capacity of effector cells varied, which effected percentage of specific lysis of tumor cells. Therefore, one representative out of three performed experiments is shown.

Figure 24A illustrates killing curves of NK cells incubated with CD33 high expressing MOLM-13 tumor target cells. The EC₅₀ value of Sirplg.αCD16.αCD33 (red curve) is 22 pM (95% CI = 11.8 pM - 416 pM). Again the EC₅₀ value was drastically lowered by duplication

RESULTS

of SirpIg (orange curve), yielding in an EC_{50} of 1.5 pM (95% CI = 0.02 pM - 114 pM). SirpIg_CV1. α CD16. α CD33 (dark grey curve) shows in turn the strongest killing capacity with an EC_{50} value of 0.6 pM (95% CI = 0.05 - 6.4 pM) and the half maximal effective concentration of α CD47. α CD16. α CD33 (light grey curve) was determined as 10.2 pM (95% CI = 1.5 pM - 69 pM). Comparing all liCADs to the bispecific controls, it is obvious that addition of a second tumor targeting domain increases cytotoxic activity, as can be seen by EC_{50} values of α CD33. α CD16 with 71.6 pM (95% CI = 10.4 pM - 492 pM) or 4800 pM (95% CI = 87.7 pM - 261 pM) in case of SirpIg. α CD16 (both black). Generally, all liCAD molecules showed equal killing potential independent of NK cell origin. Only EC_{50} values shifted to an even lower pM range, which could be explained by higher CD16 expression levels on primary NK cells compared to IL-2 expanded NK cells (data not shown). The α HER2. α CD16. α HER2 specificity control did not show any cytotoxic potential, indicating no unspecific NK cell activation upon CD16 binding also in primary material.

In order to validate biological functionality of liCAD molecules also for cells expressing lower levels of CD33 on their surface, we performed liCAD dependent cytotoxicity assays with OCI-AML3 cells that were kindly provided by Prof. Marion Subklewe. As shown in Figure 24B the EC_{50} value of SirpIg. α CD16. α CD33 (red curve) is 17.3 pM (95% CI = 21.2 pM - 141 pM) and for SirpIg. SirpIg. α CD16. α CD33 (orange curve) is 4.3 pM (95% CI = 0.38 pM - 47.7 pM). Again, dual targeting of CD47 and CD33 increases biological activity as is demonstrated by the EC_{50} value of the bispecific controls α CD33. α CD16 with 411 pM (95% CI = 118.2 pM - 1.4 nM) as well as SirpIg. α CD16 with an EC_{50} value of 16.3 nM (95% CI = 954.7 pM - 279.3 nM) (both black). CD47 control construct SirpIg_CV1. α CD16. α CD33 (dark grey curve) shows in turn the strongest killing capacity with an EC_{50} value of 0.3 pM (95% CI = 0.031 - 2.3 pM) and the EC_{50} value of the triplebody α CD47. α CD16. α CD33 (light grey curve) was determined as 9.7 pM (95% CI = 0.1 pM - 902 pM).

RESULTS

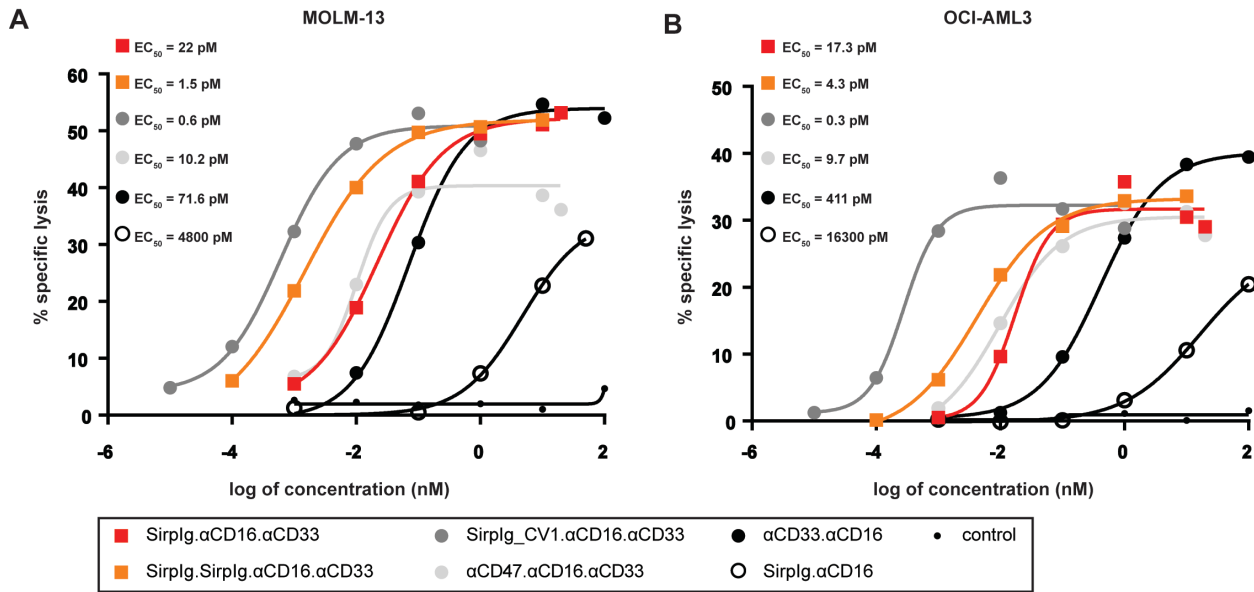


Figure 24 LiCAD dependent cytotoxicity assay using primary NK cells. (A) Redirected lysis assay of MOLM-13 cells shows that dual targeting of tumor target cells increases cytotoxic potential drastically, which can be seen by the EC₅₀ values of Sirplg.αCD16.αCD33 (red) with 22 pM and Sirplg.Sirplg. αCD16.αCD33 (orange) with 1.5 pM when compared to bispecific control αCD33.αCD16 with 9631 pM and Sirplg.αCD16 with 14940 pM (both black). CD47 control molecules are shown in grey. One representative experiment is shown out of three. **(B)** Using OCI-AML3 cells, which are CD33 low expressing target cells, same trends in specific lysis of tumor cells and similar EC₅₀ values compared to MOLM-13 cells can be seen. Only bispecific control molecules αCD33.αCD16 and Sirplg.αCD16 (both black) show drastic decrease in their half maximal effective dose. One representative experiment is shown out of three.

Comparing half maximal effective doses of molecules between CD33 high and CD33 low expressing tumor cells, merely minor differences can be seen. Most importantly, only EC₅₀ values of bispecific molecules shift to higher values, meaning lower biological activity, in case of CD33 low expressing OCI-AML3 cells but not liCADs targeting CD47 and CD33. It has been shown that OCI-AML3 and MOLM-13 cells have comparable amount of CD47 molecules on their cell surface (unpublished data). Thus, this effect cannot be due to higher CD47 levels on OCI-AML3 cells that compensate for lower CD33 levels. This suggests that simultaneous binding of CD47 and CD16 on the NK cell in combination with tumor targeting via CD33, probably leads to a costimulatory or additive activating effect in the effector cells.

RESULTS

To further evaluate the potential of liCAD molecules to induce serial lysis of tumor cells by individual NK cells we performed an effector-to-target-cell (E:T) ratio titration as shown in Figure 25. MOLM-13 cells were mixed with NK cells at an E:T ratio of 2:1, 1:1, 0.5: and 0:1. Assays were performed with half maximal effective dose of corresponding liCAD molecules the way described above. Assays were performed in technical triplicate and repeated 3 times.

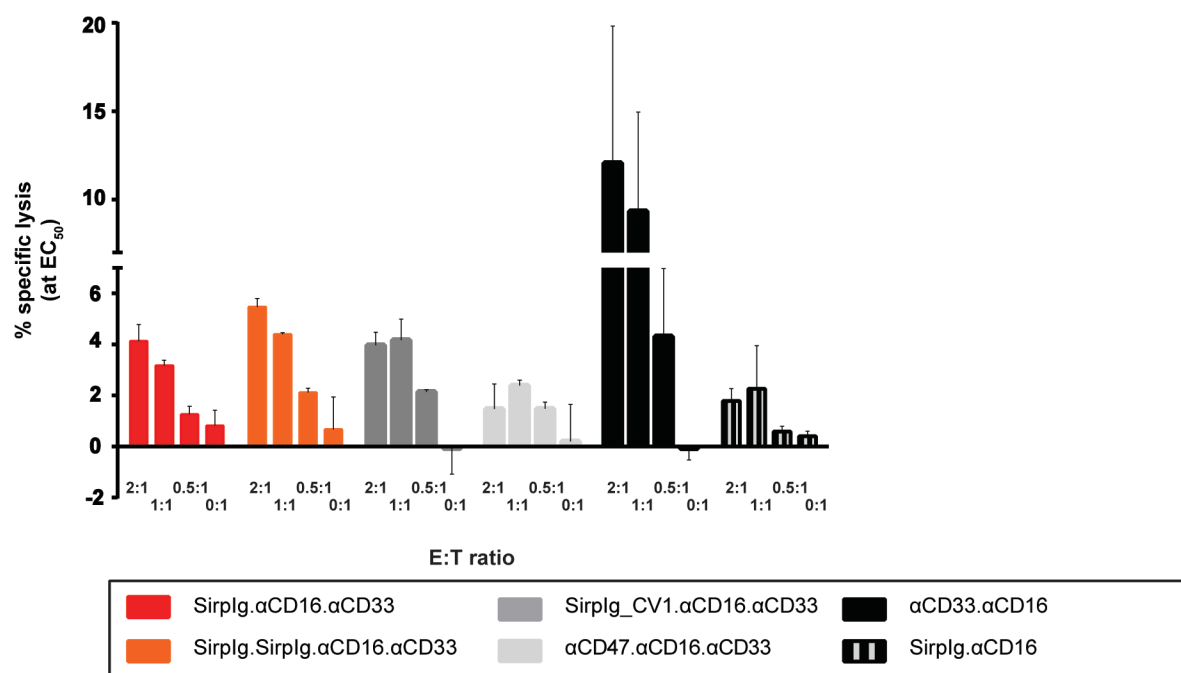


Figure 25 Effector-to-target-cell ratio titration does not indicate serial lysis of NK cells. E:T ratio titration of liCAD molecules reveals similar specific lysis of tumor cells at ratios of 2:1 and 1:1 but a drop by half at 0.5:1. Error bars represent standard error of the mean (SEM) of triplicates.

E:T ratio titrations of Sirplg.αCD16.αCD33 (red bars) and Sirplg.Sirplg.αCD16.αCD33 show similar specific lysis values in case of the ratio of 2:1 and 1:1. However, at a ratio of 0.5:1 the specific lysis of tumor cells drops to more than half. Since the control reaction without NK cells (E:T is 0:1) shows in both cases approximate specific lysis values, this suggests a non-specific tumor cell lysis for reactions at an E:T ratio of 0.5:1. Also for control liCADs Sirplg.CV1.αCD16.αCD33 (dark grey bar) and αCD47.αCD16.αCD33 (light grey bar) as well as bispecific controls αCD33.αCD16 (black bars) and Sirplg.αCD16 (black/grey striped bar) similar results are obtained.

RESULTS

4.8.3. LiCAD dependent phagocytosis

As outlined in the introduction, the Sirp α -CD47 interaction is known to constitute a “Don’t eat me signal” in macrophages, dendritic cells and neutrophils. The approach to interrupt this interaction using α CD47-mABs has been proven successful in several pre-clinical studies (Chao et al., 2010; Liu et al., 2015). In order to analyse the ability of LiCADs to indeed increase phagocytic uptake in macrophages, a phagocytosis assay was established. We first set out to establish a cell line based macrophage assay using the THP-1 monocytic cell line in order to be able to work in an autologous setting. To do so, THP-1 target cells were incubated with THP-1 macrophages as explained in detail in material and methods. Subsequently we performed assays with primary monocytes differentiated to CD16 expressing M2 macrophages.

THP-1 cell and MOLM-13 cells were stained with PKH-26 and incubated with PKH-67 stained THP-1 macrophages or M2 macrophages, respectively, for 2 hours in serum free conditions at an effector to target ratio of 2:1. Afterwards cells were analysed by flow cytometry for PKH-67/PKH-26 double positive events. Increase in phagocytosis was determined and data were transformed to logarithms and fitted to a one site—specific binding with hill slope equation in Graph Pad Prism 6. All experiments were performed in technical triplicates or quadruplicates and repeated three times.

Figure 26 illustrates the gating strategy for the evaluation of actively phagocytosed target cells by macrophages. First, cells were gated for the PKH-67 positive cell population, which represents macrophages. Furthermore, PKH-67 and PKH-26 double positive events were gated and quantified, representing macrophages that engulfed one or more cells. In case of THP-1 macrophages we additionally subgated for CD16 expression (not shown) and subsequently analyzed PKH-67 and PKH-26 double positive events. As can be seen in Figure 26, incubation of target cells with macrophages alone already induces phagocytosis of tumor cells at a background level of around 20 %. Thus, an increase in phagocytosis, as percent over the background control, was determined as depicted in Figure 27 and Figure 28A and B.

RESULTS

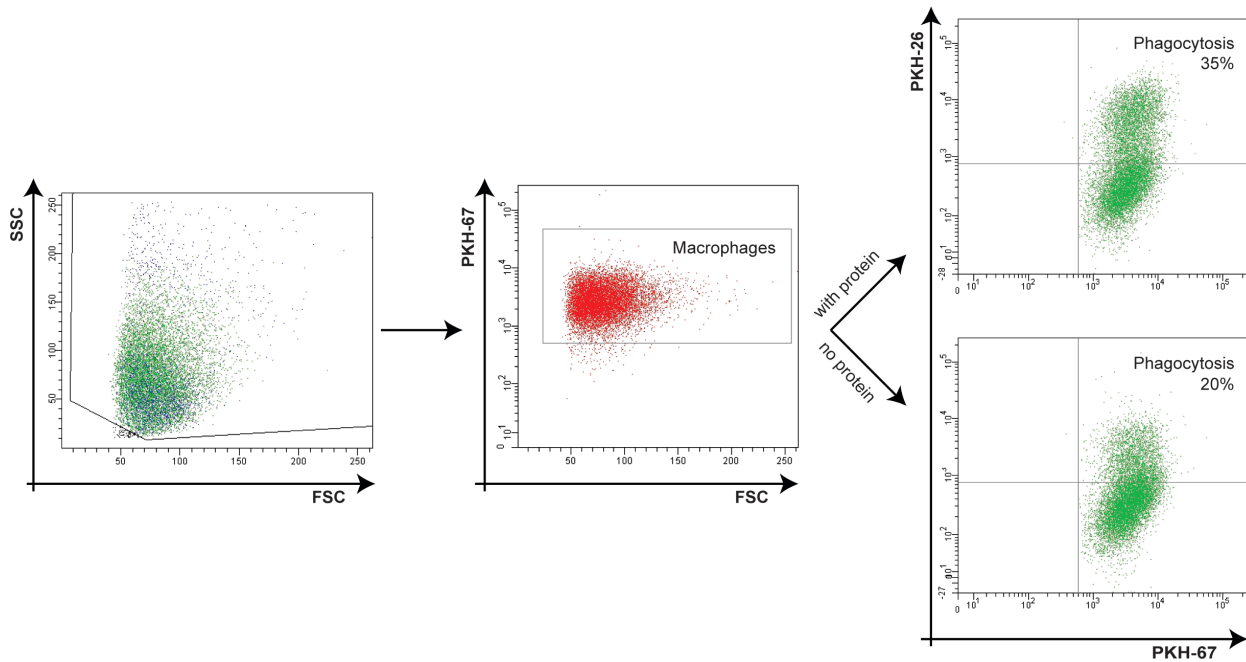


Figure 26 Gating scheme for phagocytosis assay. Cells were first gated for PKH-67⁺ macrophages and further down gated on PKH-67/PKH-26 double positive events. These events represent macrophages that have actively engulfed a PKH-26 stained target cell. As shown exemplary, incubation of target cells with macrophages but no protein already leads to a background phagocytosis of around 20 %, whereas incubation with protein leads to a phagocytosis of around 35 %.

Figure 27A shows that analysis of the total THP-1 macrophage population for phagocytosis of target cells results in highest increase in phagocytosis by incubation with SirpIg_CV1 only and SirpIg only (black dashed curves, filled and empty circles). Incubation with SirpIg_CV1.αCD16.αCD33 yields in the third highest increase in phagocytosis. However, as indicated by the dotted black line in the dose-response curve, the control molecule already induces a fairly high unspecific background phagocytosis rate, thus, we could not detect phagocytosis above the background for the rest of the liCAD molecules.

RESULTS

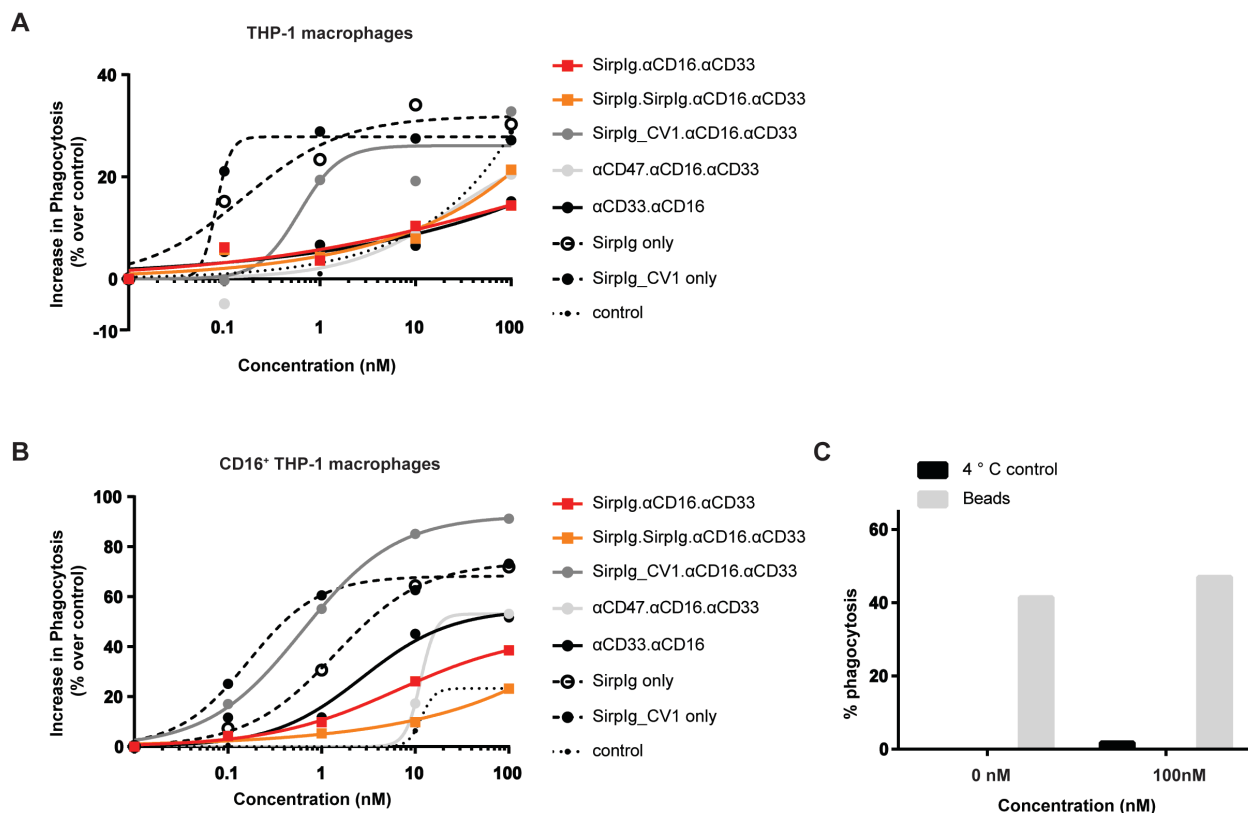


Figure 27 Phagocytosis assay of THP-1 cells with THP-1 macrophages. (A) Total THP-1 macrophages were analysed for phagocytosed target cells upon liCAD incubation. Single domain Sirplg_CV1 and Sirplg only (both black dashed curves) induce phagocytosis to a higher extend than Sirplg.αCD16.αCD33 (red curve), Sirplg.Sirplg.αCD16.αCD33 (orange curve), αCD47.αCD16.αCD33 (light grey curve) and αCD33.αCD16 (black curve). Only the high affinity liCAD Sirplg_CV1.αCD16.αCD33 (dark grey curve) shows an increase in phagocytosis that is above unspecific background phagocytosis (black dotted curve). (B) Analysis of CD16⁺ THP-1 macrophages shows a lower unspecific activation of macrophages (black dotted curve). Again Sirplg_CV1.αCD16.αCD33 (dark grey curve), Sirplg_CV1 only and Sirplg only (both black dashed lines) yield in higher increase in phagocytosis compared to Sirplg.αCD16.αCD33 (red curve), Sirplg.Sirplg.αCD16.αCD33 (orange curve), αCD47.αCD16.αCD33 (light grey curve) and αCD33.αCD16 (black curve) (C) To verify that active phagocytosis was determined, 4 °C control reactions and macrophages incubated with beads were measured without protein and maximal protein amount. Mean values out of two experiments are shown.

We determined that only around 5% of THP-1 macrophages expressed CD16 on their cell surface (data not shown). Consequently, we subgated macrophages on CD16 expression and analysed the increase of phagocytosis in CD16⁺ THP-1 macrophages. In contrast to the total THP-1 macrophage analysis, unspecific phagocytosis induced by the control molecule is clearly diminished however, still present starting at a concentration of 10 nM (Figure 27B,

RESULTS

dotted black curve). Again SirpIg_CV1 only as well as SirpIg only (black dashed curves, filled and empty circles) yield in a higher increased phagocytosis rate of target cells compared to SirpIg. α CD16. α CD33 (red curve), SirpIg.SirpIg. α CD16. α CD33 (orange curve) and α CD47. α CD16. α CD33 (light grey curve). The high affinity liCAD SirpIg_CV1. α CD16. α CD33 (dark grey curve) shows in turn best performance compared to the lower affinity liCADs and similar results to SirpIg_CV1 only. Surprisingly, the bispecific control liCAD α CD33. α CD16 (black curve) yields in an increased phagocytosis of THP-1 cells between the trispecific liCADs and the single domain SirpIg variants, which lead us to the conclusion that this cell line based phagocytosis assay might not be a proper model system to mimic the activity of primary macrophages.

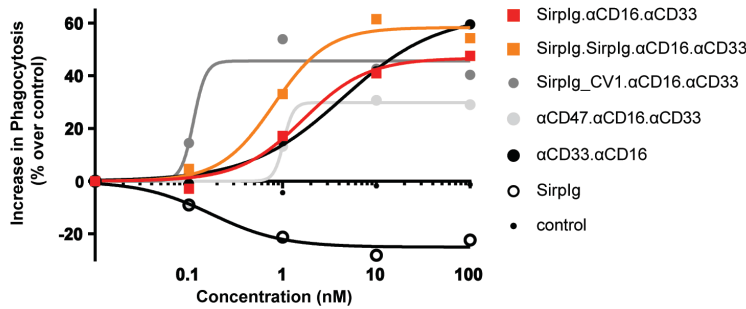
Therefore, we next established a phagocytosis assay with primary M2 macrophages that were incubated with MOLM-13 cells as targets. As shown in Figure 28A, SirpIg.SirpIg. α CD16. α CD33 is indeed able to block the Sirp α -CD47 immune checkpoint and an increase in phagocytosis can be observed compared to a bispecific control liCAD α CD33. α CD16. Though, SirpIg. α CD16. α CD33 seems not to be sufficient in inhibiting the “Don’t eat me” signaling, since both bispecific liCAD and SirpIg. α CD16. α CD33 have almost overlaying dose response curves. We further tested, whether blockade of Sirp α -CD47 interaction would be sufficient to induce phagocytosis in primary M2 macrophages, but no phagocytosis was observed in this case. Thus, we could demonstrate that on one site an activating signal via Fc gamma receptors is necessary to induce phagocytosis but on the other site, Fc gamma receptor binding only is not sufficient to induce unspecific activation of macrophages, as can be seen by the control construct α Her-2. α CD16. α Her-2. Furthermore, control molecules SirpIg_CV1. α CD16. α CD33 and α CD47. α CD16. α CD33 showed expected behaviour in phagocytosis assays, as the high affinity SirpIg_CV1. α CD16. α CD33 is the strongest inducer of phagocytosis and the rather weak binding α CD47. α CD16. α CD33 molecule shows similar induction potential to SirpIg. α CD16. α CD33.

Since most of the pre-existing studies on CD47 blockade by the Weissman group were carried out using an α CD47 mAB, we compared the liCAD molecules to the same clone called B6H12 which they used in their studies. As demonstrated in Figure 28B liCADs are

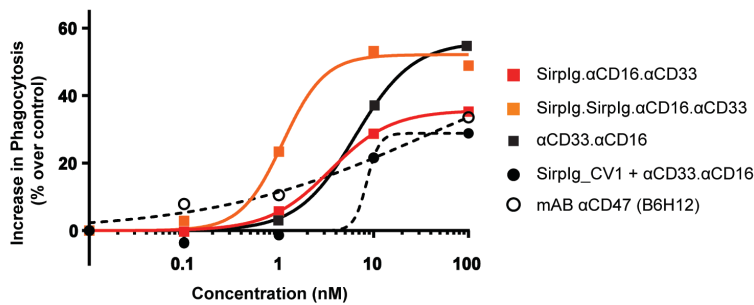
RESULTS

far better inducers of phagocytosis, however, a combination of α CD47 mAB and a second α CD33 mAB would have to be tested in order to correlated and compare biological activities.

A



B



C

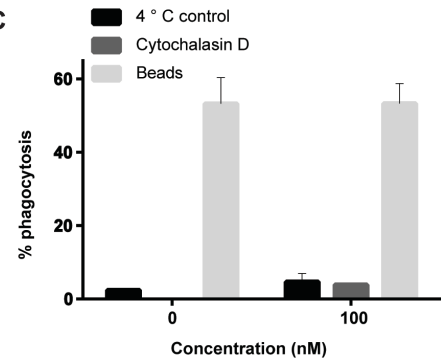


Figure 28 Phagocytosis assay of MOLM-13 target cells with primary M2 macrophages. (A) All liCAD molecules were tested for their ability to induce phagocytosis. Sirplg.αCD16.αCD33 induces similar phagocytosis rates compared to the bispecific control αCD33.αCD16, indicating that low affinity blockade of the Sirp α-CD47 interaction does not increase phagocytosis in macrophages. The Sirplg.Sirplg.αCD16.αCD33 molecule increases phagocytic uptake of target cells in macrophages. Sirplg_CV1.αCD16.αCD33 shows highest ability to induce phagocytosis and αCD47.αCD16.αCD33 exhibits similar phagocytosis rates as Sirplg.αCD16.αCD33. Sirplg only and the control molecule αHer-2.αCD16.αHer-2 do not induce phagocytosis. **(B)** The mAB αCD47 (B6H12) was compared to liCADs and showed far less phagocytosis induction potential. Incubation of macrophages and target cells with Sirplg_CV1 only together with the bispecific liCAD αCD33.αCD16 does not rescue induction of phagocytosis. **(C)** In order to verify that active phagocytosis was determined, 4 °C control reactions, Cytochalasin D pre-treated macrophages and macrophages incubated with beads were measured without protein (0 nM) and maximal protein amount (100 nM). One representative experiment is shown out of three.

RESULTS

In order to exclude measurements of adhesion artefacts, like target cells not engulfed by macrophages but just sticking to the outside of a macrophage and therefore, generating a PKH-67/PKH-26 double positive event, a 4 °C control reaction and a reaction with Cytochalasin D pre-treated macrophages were carried out in parallel. Cytochalasin D inhibits actin polymerization preventing phagocytosis ability of macrophages, which holds also true for macrophages kept at 4 °C. As shown in Figure 27C as well as Figure 28C, phagocytosis was inhibited at 4 °C and in assays with cytochalasin D pre-treated macrophages (Figure 28C only). We thus conclude that the increase in phagocytosis is not caused by an adhesion artefact. Additionally, polystyrene beads, a commonly known inducer of phagocytosis, were used as a positive control. Incubation with and without protein further demonstrates that binding of Fc gamma receptor does not unspecifically increase phagocytosis of beads (Figure 27C and Figure 28C).

4.8.4. Preferential killing of CD33 Flp-INTM 293 HEK cells

Studies on blocking CD47 have pointed out the beneficial effects in tumor cell eradication but due to the ubiquitous expression of CD47 on human cells, systemic blockade might lead to severe side effects. Thus it is of particular importance to show that liCAD molecules preferentially induce killing of CD47/CD33 double positive cells even in the presence of CD47 single positive cells. In order to address this crucial question we set out to establish an *in vitro* redirected cytotoxicity assay. A CD33 expressing, stably transfected Flp-INTM 293 HEK cell line was generated by Monika Herrmann and kindly provided for this study. Since CD47 was not manipulated, untransduced Flp-INTM 293 HEK cells could be used as single positive and CD33 Flp-INTM 293 HEK cells as double positive target cells, with both cell types having same CD47 levels.

Single and double positive cells were mixed in a 1:1 ratio and incubated with NK cells in an effector to target cell ratio of 2:1 for 4 hours. Two reactions were set up in parallel, one having single positive cells calcein labeled and the other one having the double positive cell fraction calcein labeled. Assays were set up either with increasing protein concentrations leading to dose-response curves, or determined protein concentrations, leading to maximal

RESULTS

and half maximal effective response, respectively. All experiments were performed in technical triplicates and repeated three times.

Figure 29 illustrates dose response curves of preferential killing assays showing specific lysis of CD47 single positive Flp-INTM 293 HEK cells in panel A and specific lysis of CD47/CD33 double positive cells in panel B.

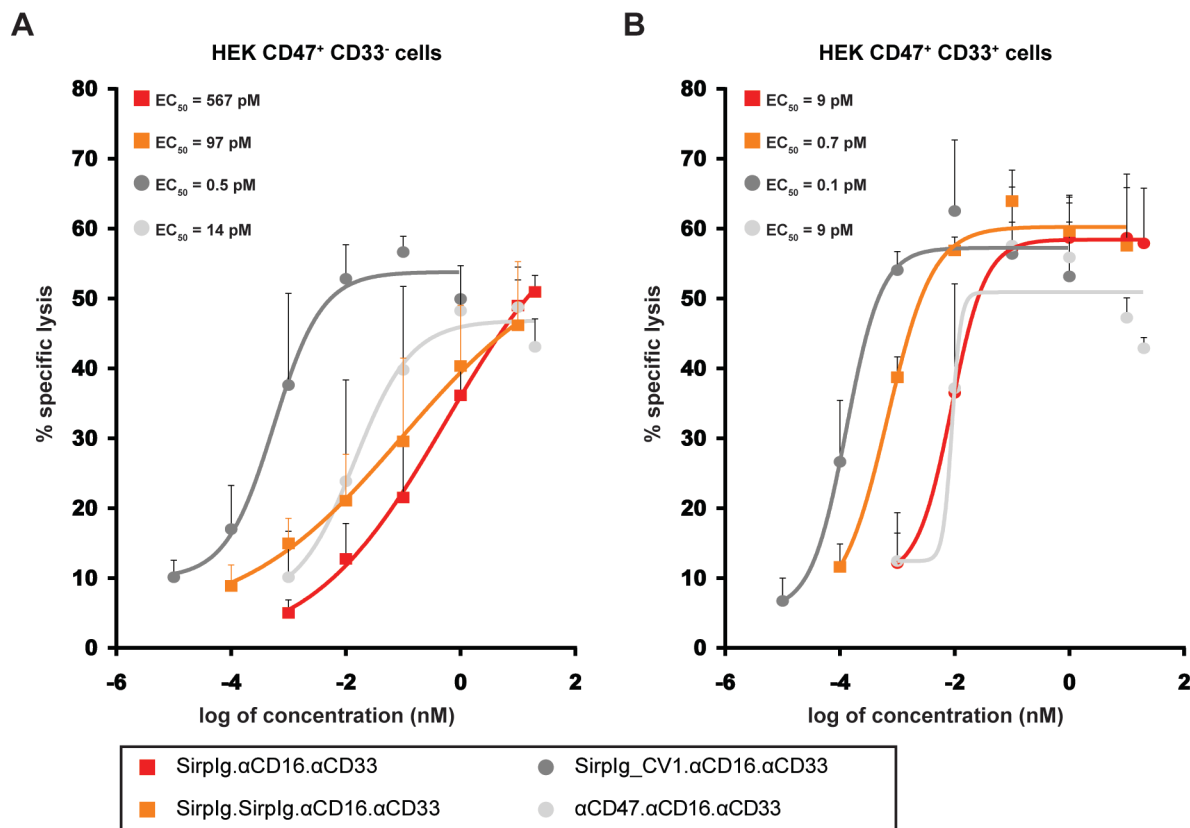


Figure 29 Dose response curves of preferential killing assays. (A) % specific lysis of CD47 single positive Flp-INTM 293 HEK cells is shown for all tested liCADs. Sirplg.αCD16.αCD33 (red curve) and Sirplg.Sirplg.αCD16.αCD33 (orange curve) have higher EC₅₀ values compared to CD47 high affinity molecules Sirplg.CV1.αCD16.αCD33 (dark grey curve) and αCD47.αCD16.αCD33 (light grey curve), indicating worse targeting and therefore the ability of avoiding systemic binding of CD47. (B) % specific lysis of CD33 Flp-INTM 293 HEK cells is shown for all tested liCADs. Error bars represent standard error of the mean of triplicates.

Sirplg.αCD16.αCD33 (red curves) has an EC₅₀ of 567 pM (95% CI = 5.1 pM-62 nM) for single positive cells compared to 9 pM (95% CI = 4.5 pM-17 pM) for double positive cells,

RESULTS

indicating that SirpIg within the liCAD does not sufficiently target cells and therefore, is likely not to bind systemically to the ubiquitously expressed CD47 surface antigen. The same holds true for SirpIg.SirpIg.αCD16.αCD33 (orange curves) that shows EC₅₀ values of 97 pM (95% CI = 0.2 pM-36.7 nM) in case of single positive cells versus 0.7 pM (95 CI = 0.17 pM-2.6 pM) for CD33 Flp-INTM 293 HEK cells. SirpIg_CV1.αCD16.αCD33 (dark grey curves) has a half maximal effective concentration at 0.5 pM (95% CI = 0.2 pM-1.4 pM) for CD47 expressing cells and at 0.1 pM (95% CI = 0.065 pM-0.25 pM) for CD47/CD33 expressing cells. The control triplebody αCD47.αCD16.αCD33 (light grey curves) also exhibits very comparable EC₅₀ values between both cell types (14 pM (95% CI = 1.8 pM-109 pM) for single positive cells versus 9 pM (95% CI not determinable) for double positive cells). These data point out the advantage of a low affinity-binding to CD47 against systemic high-affinity binding. The application of low affinity liCADs in cytotoxicity assays reveals a therapeutic window that gives reason to hope for a therapeutic response on tumor cells without causing serious damage to healthy tissue.

To strengthen the potential of liCAD molecules to preferentially kill CD47/CD33 double positive tumor cells but not CD47 single positive cells, Figure 30 shows results for obtained data with maximal protein concentrations used.

RESULTS

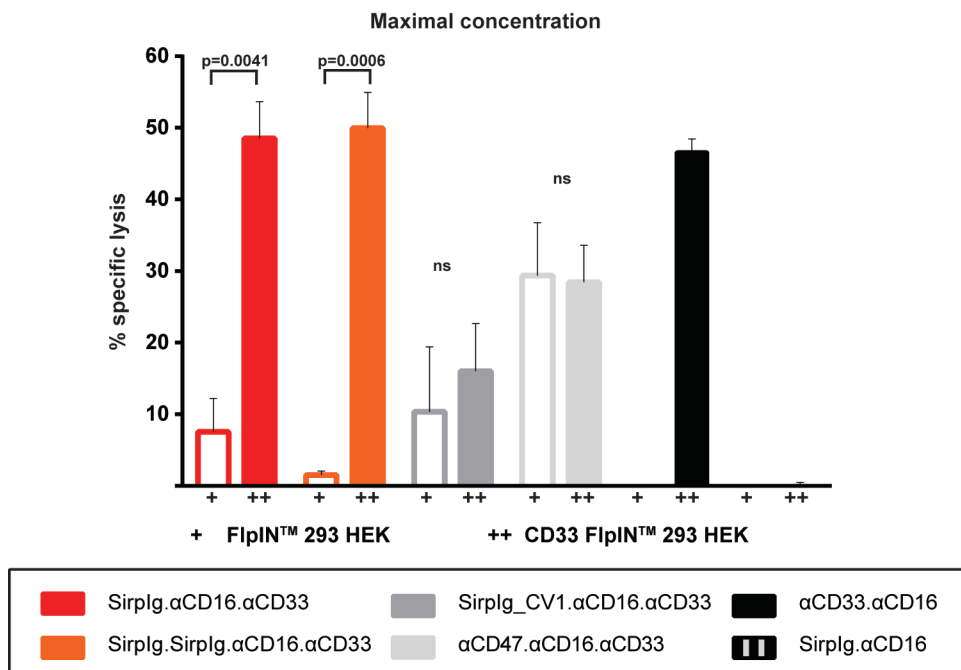


Figure 30 Maximal effective concentration of liCAD proteins analysed in preferential killing assays. SirpIg.αCD16.αCD33 (red) and SirpIg.SirpIg.αCD16.αCD33 (orange) demonstrate significant preferential lysis of CD33 Flp-IN™ 293 HEK cells over Flp-IN™ 293 HEK cells when incubated at maximal effective concentration. SirpIg.CV1.αCD16.αCD33 (dark grey) as well as αCD47.αCD16.αCD33 (light grey) induce lysis of both cell types to the same extent. Bispecific liCADs αCD33.αCD16 (black) and SirpIg.αCD16 (black/grey striped) served as controls. Error bars represent standard error of the mean of triplicates.

The results affirm impressively that SirpIg.αCD16.αCD33 (red bar, 20 nM used) as well as SirpIg.SirpIg.αCD16.αCD33 (orange bar, 10 nM used) significantly preferentially kill CD33 Flp-IN™ 293 HEK cells (SirpIg.αCD16.αCD33 $p = 0.0041$, SirpIg.SirpIg.αCD16.αCD33 $p = 0.0006$). The high affinity liCAD SirpIg.CV1.αCD16.αCD33 (dark grey bar, 1 nM used) as well as the triplebody αCD47.αCD16.αCD33 (light grey bar, 20 nM used) both kill single and double positive Flp-IN™ HEK cells to the same extent, thus, no significant differences could be detected. As expected the bispecific control molecule αCD33.αCD16 (black bar, 100 nM used) only shows killing in CD33 Flp-IN™ HEK cells. SirpIg.αCD16 (black/grey striped bar, 100 nM used), which lacks any tumor antigen-targeting domain, did not show any killing feature.

RESULTS

In order to obtain comparable specific lysis values, we decided to compare killing at half maximal effective dose concentrations of all proteins, as shown in Figure 31.

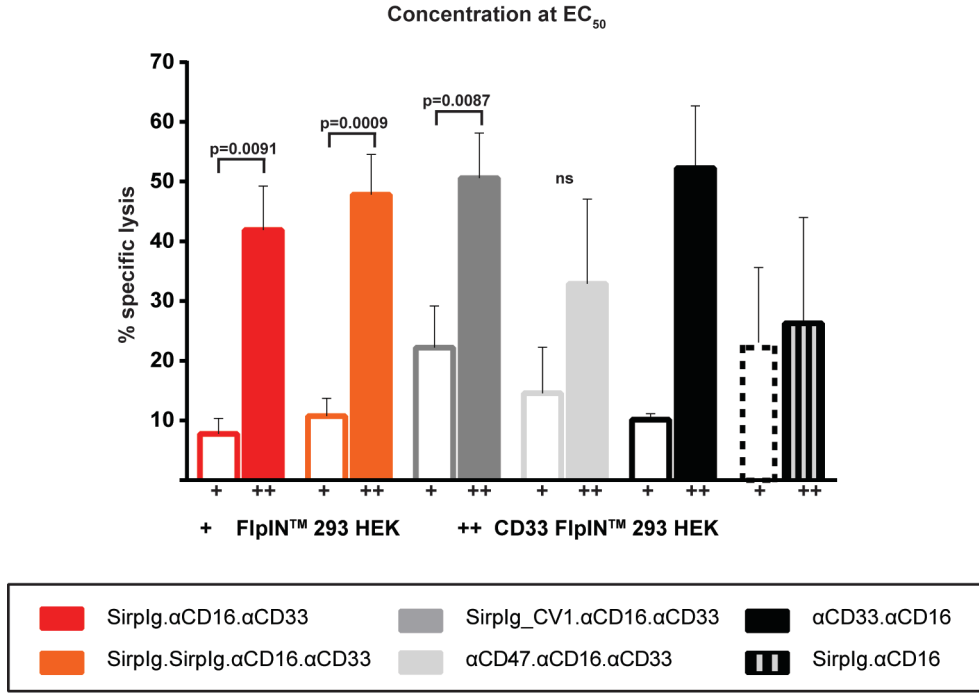


Figure 31 Half maximal effective concentration of liCAD proteins analysed in preferential killing assays. Sirplg.αCD16.αCD33 (red), Sirplg.Sirplg.αCD16.αCD33 (orange) and Sirplg.CV1.αCD16.αCD33 (dark grey) reveal significant preferential lysis of CD47/CD33 double positive cells. αCD47.αCD16.αCD33 (light grey) induce lysis of both cell types to the same extent. Bispecific liCADs αCD33.αCD16 (black) and Sirplg.αCD16 (black/grey striped) served as controls. Error bars represent standard error of the mean of triplicates

Sirplg.αCD16.αCD33 (red bar) as well as Sirplg.Sirplg.αCD16.αCD33 (orange bar) significantly preferentially kill CD33 Flp-IN™ 293 HEK cells (Sirplg.αCD16.αCD33 $p = 0.0091$, Sirplg.Sirplg.αCD16.αCD33 $p = 0.0009$), interestingly at this lower protein concentration also Sirplg.CV1.αCD16.αCD33 (dark grey bar) showed a significant killing in CD47/CD33 double positive cells ($p = 0.0087$). The control triplebody αCD47.αCD16.αCD33 (light grey bar) however, killed CD47 single positive cells to a similar extent than CD47/CD33 double positive cells. The bispecific control αCD33.αCD16 (black bar) points out an unspecific background killing of CD47 single positive Flp-IN™ 293 HEK cells of around 10 %, which has to be taken into consideration for data obtained with all

RESULTS

other liCAD molecules. SirpIg.αCD16 (black/grey stippled bar) shows, as expected, similar killing potential for both cell types.

Next, we wanted to translate gained knowledge of liCAD potential from the Flp-INTM 293 HEK cell line model system to AML tumor cell lines. Therefore we used MOLM-13 cells that express high levels of CD33 and OCI-AML3 cells, which express low levels of CD33. Both cell lines express comparable amount of CD47 on their surface. All experiments were carried out as described above for Flp-INTM 293 HEK cell lines.

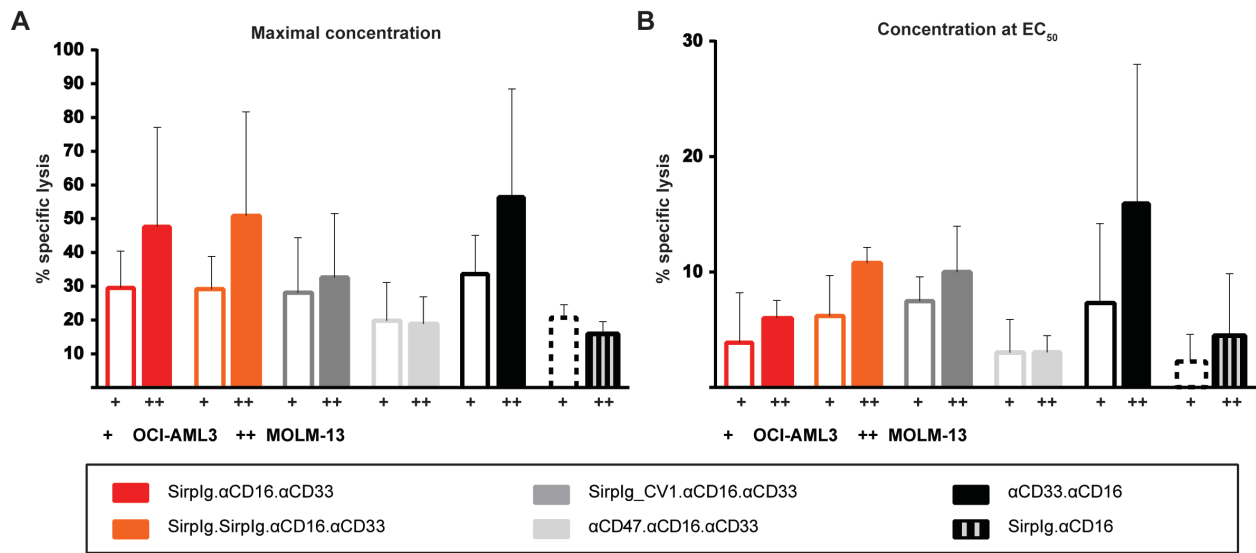


Figure 32 Preferential killing assays of MOLM-13 and OCI-AML3 cells. Same tendencies for all liCAD molecules can be seen with (A) maximal protein concentrations as well as (B) half maximal effective protein concentrations. Bispecific liCADs αCD33.αCD16 (black) and SirpIg.αCD16 (black/grey stippled) served as controls. Error bars represent standard error of the mean of triplicates.

Figure 32A and Figure 32B illustrate data obtained for maximal and half maximal effective liCAD concentrations used, respectively. In both experimental set-ups only slight differences between specific lysis of OCI-AML3 cells and MOLM-13 cells can be seen. However, SirpIg.αCD16.αCD33 (red bar) and SirpIg.SirpIg.αCD16.αCD33 (orange bar) again reveal a higher tendency to induce preferential killing of CD33 high expressing MOLM-13 cells, especially when used at maximal protein concentrations. SirpIg.CV1.αCD16.αCD33 (dark grey bar) as well as αCD47.αCD16.αCD33 (light grey bar) show in both cases same potential to kill either target cell. Bispecific control constructs αCD33.αCD16 (black bar)

RESULTS

and SirpIg.αCD16 (black/grey striped bar) demonstrate expected killing behavior. αCD33.αCD16 induces killing of MOLM-13 cells better due to higher CD33 expression levels whereas SirpIg.αCD16 induces specific lysis of both cell types to a similar extent explained by comparable CD47 expression levels.

4.8.5. NK cell mediated lysis of AML patient blast samples

All performed assays were testing the biological activity of liCADs in tumor cell lines that are easier to maintain and represent a good model to demonstrate efficacy. For the validation of these preceding results, our collaboration partner Prof. Marion Subklewe checked for liCAD-induced cytotoxicity of primary AML patient cell samples.¹

A FACS based NK cell mediated cytotoxicity assay was performed as described in detail in the section “material and methods”. Cells were analysed on day 0 and incubated subsequently for 24 hours with SirpIg.SirpIg.αCD16.αCD33 liCAD, bispecific control αCD33.αCD16 and without antibody to account for the negative control. Experiments were performed 3 times with various AML patient samples.

Figure 33A illustrates the proportion of CD33⁺ remaining cells expressed as percentage of the control condition incubated without liCAD. We show that SirpIg.SirpIg.αCD16.αCD33 (orange bar) induces stronger NK cell mediated killing of AML patient cells in contrast to the bispecific control αCD33.αCD16 (black bar). As shown in Figure 33B, analysis of the mean fluorescence intensity of CD16 expression on NK cells reveals a higher downregulation of the receptor upon liCAD binding (green histogram) compared to the αCD33.αCD16 (blue histogram) and the negative control (red histogram). Downregulation of CD16 is in concert with NK cell activation. Thus, we hypothesize that the observed increased killing potential of NK cells is due to higher activation, which might be accomplished by additional CD47 ligation. The gating of NK cells and AML cells at different effector to target ratios is illustrated exemplary in Figure 33C.

¹ All experiments were executed and analysed in the laboratory of Prof. Subklewe by Christina Krupka and data were kindly provided for this PhD study.

RESULTS

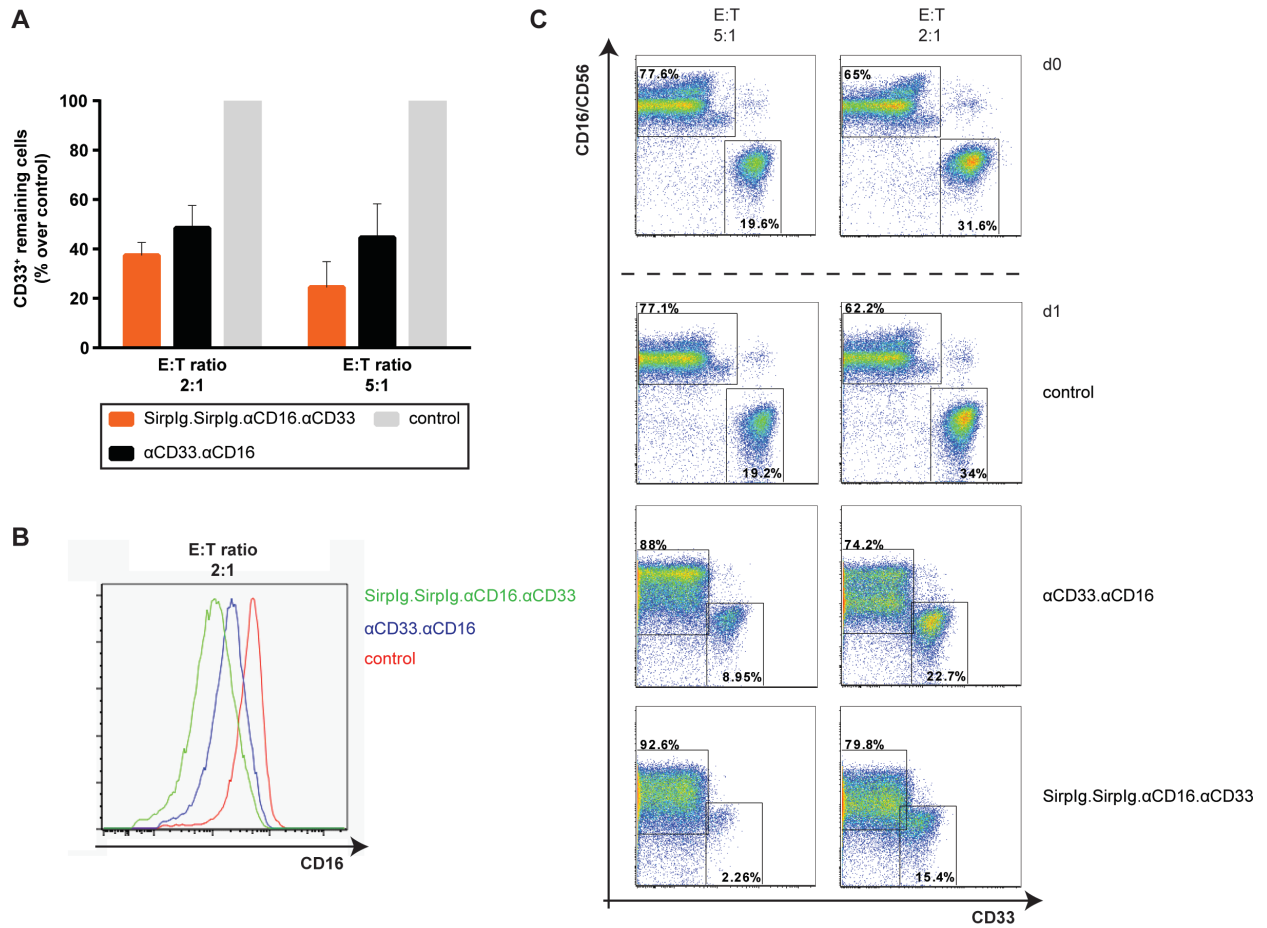


Figure 33 NK cell mediated cytotoxicity of AML patient samples. (A) Analysis of remaining CD33⁺ cells. Sirplg.Sirplg.αCD16.αCD33 (orange) shows higher killing potential compared to the bispecific control αCD33.αCD16 (black). **(B)** Exemplary illustration of the mean fluorescence intensity of CD16 expression. Upon binding to a liCAD molecule a stronger downregulation of the receptor is detected. **(C)** Gating of CD16⁺/CD56⁺ NK cells and CD33⁺ AML blasts shows higher decrease of AML cells in case of Sirplg.Sirplg.αCD16.αCD33 compared to the bispecific control αCD33.αCD16 at any E:T ratio. Incubation of NK cells and blasts with no antibody was used as a control. Error bars represent standard error of the mean of triplicates.

5. DISCUSSION

Immunotherapy has revolutionized cancer treatment. The advent of immune checkpoint inhibitors in particular caused excitement within the scientific community and provided hope to combat difficult-to-treat cancer types, such as acute myeloid leukemia (AML). The CD47-Sirp α interaction, also referred to as “Don’t eat me” signal, is a long underestimated immune checkpoint that regulates phagocytic activity of macrophages and dendritic cells. In AML it has been shown that there is higher expression of CD47 in the leukemic stem cell (LSC) compartment than in normal hematopoietic stem cells (HSCs), and that increased expression of CD47 is a poor prognostic factor (Majeti et al., 2009). Blocking of CD47 in combination with targeting a tumor antigen using mAbs has been shown to improve tumor eradication in a non-Hodgkin lymphoma (NHL) mouse model (Chao et al., 2010). Thus, this might be a promising strategy to follow up in AML, where novel therapies with higher efficacy and lower toxicity are strongly needed for treatment.

The myeloid surface antigen CD33 is a meanwhile well-established tumor target in AML therapies and there are still good prospects that it will be used in the future. The first trial with an anti-CD33 mAb in AML therapy was performed 20 years ago (Scheinberg et al., 1991). In the year 2000 the Food and Drug Administration (FDA) approved the anti-CD33 immunoconjugate drug gemtuzumab ozogamicin. Due to concerns about toxicity and lack of efficacy it was withdrawn from the market, however, it has been shown in various studies that lower doses of the drug (3-6 mg/m² instead of 9 mg/m²) as well as different administration strategies (either single dose or fractionated) are safe and also effective. Krupka et al demonstrated that AMG 330, a CD33/CD3 bispecific T-cell engager (BiTE), preferentially kills LSCs that have higher levels of CD33 expression than HSCs and therefore allows for restoration of normal hematopoiesis (Krupka et al., 2014).

The aim of this thesis was to generate a novel trispecific antibody (tsAb) format that, similar to BiTEs, recruits effector cells to CD33 expressing AML cell lines, blasts or LSCs and additionally blocks the CD47-Sirp α interaction. To this end, we used the naturally occurring

DISCUSSION

extracellular domain of Sirp α and linked it to an effector cell recruiting CD16 singel chain fragment variable (scFv) and a tumor cell recruiting CD33 scFv.

5.1. Generation and expression of liCADs, a novel trispecific antibody format

The major task of this study was to design, express and purify a novel antibody format, which we termed local inhibitory checkpoint antibody derivative (liCAD). The main advantage of this novel format is the local blockage of CD47 at the tumor side, rather than a systemic blockade of the ubiquitously expressed antigen. By using the extracellular domain of Sirp α , we hypothesize that our liCAD molecule would not bind systemically to CD47 positive cells but rather to CD33 as well as strongly overexpressing CD47 tumor cells, possibly circumventing severe side effects. We designed constructs bearing the total extracellular domain of Sirp α (referred to as Sirp ex) as well as only the N-terminal Ig-like V type domain (referred to as SirpIg), which was shown to be sufficient for binding to CD47 (Hatherley et al., 2008). Single domain expression in *E. coli* BL21 cells revealed that Sirp ex was highly unstable and was partly degraded to SirpIg. This led us to the decision to conduct further experiments and analysis solely with the N-terminal Ig-like V type domain SirpIg.

SirpIg. α CD16. α CD33 and SirpIg.SirpIg. α CD16. α CD33 were expressed in the well-established human FreeStyle™ 293-F cell system. Proteins were secreted into the cell culture supernatant due to an Ig κ leader sequence within the expression vector. A straightforward purification strategy comprising anion-exchange chromatography and size-exclusion chromatography was subsequently used and resulted in pure protein. To validate the beneficial use of the low affinity SirpIg domains we had to generate control constructs, which bind to CD47 with a higher affinity. Therefore, we designed constructs comprising a published high affinity mutant of SirpIg, called SirpIg_CV1 (Weiskopf et al., 2013) and a scFv against CD47. Extensive attempts to express and purify these control molecules in human FreeStyle™ 293-F cells failed. We realized that not the expression itself but, due to the high affinity to CD47, the proteins were immediately bound to the FreeStyle™ 293-F cell surface. Attempts to dissociate liCADs from the cell surface by using detergent or pH changes failed due to the high affinity interaction. One way to prevent the binding of the proteins to CD47 on the FreeStyle™ 293-F cells is to knockdown or ideally knockout CD47

DISCUSSION

expression. We performed a partial knockdown using an ON-TARGET plus siRNA SMARTpool directed against CD47 in parallel to transient transfection of the desired liCAD protein. By this the amount of purified protein increased, however, the yield was still too low to include further purification steps or biological studies. We could nevertheless show that partial knockdown of CD47 still results in viable FreeStyle™ 293-F cells that are capable of expressing protein. This result suggests that for future studies it might be an option to generate a stable gene knockout of CD47 in FreeStyle™ 293-F cells using, for example, the CRISPR/Cas9 genome editing technology. By doing so, the immediate binding of liCADs with higher affinity to CD47 would be solved and additionally stable cell lines could be generated that increase the protein yield.

Since the interaction of CD47 and Sirp α is species specific, another possibility to avoid protein binding to the cells is to switch to an expression system that is not of human origin. During this study we therefore used a *Drosophila melanogaster* Schneider 2 (S2) expression system (ExpreS2ion Biotechnologies). The major difference in expressed proteins between human and insect cells lies in the glycosylation pattern. S2 cells have been shown to produce paucimannose (MAN-3) N-glycosylations that are shorter compared to mammalian cells (Kim et al., 2005). With respect to the influence of glycosylation patterns on biological activity, it has been shown for mAbs that, for example, the binding characteristics for IgG1 of the same clones expressed in S2 cells or mammalian cells were indistinguishable (Johansson et al., 2007). In the case of the interaction of CD47 with Sirp α it has been reported that N-linked glycosylations of the N-terminal Ig-like V type domain of Sirp α do not influence binding behavior (Lee et al., 2007; Subramanian et al., 2006), thus we did not expect the altered glycosylation to influence its biological activity. To prove this hypothesis we analysed mammalian and insect cell expressed proteins in redirected lysis assays for their ability to induce killing of tumor cell lines and could not detect any differences in their activity. Furthermore, the Schneider 2 system was reported to be extremely well suited for bioproduction. It allows stable, non-lytic, high-level expression of a wide range of recombinant proteins, with published yields of 1 g of mAb per liter of culture (Wang et al., 2012). Stable cell lines for all of the liCADs were generated and these produced, depending on individual proteins, approximately 10 mg of liCAD per liter of culture after a four-step

DISCUSSION

purification protocol. S2 cells generally reach cell densities up to 70 million cells/ml, compared to 4 million FreeStyle™ 293-F cells/ml, which is one explanation for higher protein yields. Due to the composition of the insect cell medium, an initial buffer exchange step had to be included in the purification strategy prior to isolation of 6xHis-tagged protein with Ni²⁺-NTA agarose beads, prolonging the purification procedure by one day. To avoid this additional step, the S2 cells could be grown in an alternative insect cell media that does not interfere with the binding of the His-tag to the Ni²⁺-NTA agarose beads, although this may also alter the protein yield. Another important factor in influencing protein yield is the generation of stable cell lines itself. In this PhD thesis polyclonal stable cell lines were generated. More protein would be required, however, for the *in vivo* testing of liCAD proteins in mice. In this case, generating monoclonal stable cell lines and screening for the highest producer would certainly increase protein yield. For this particular study, however, these advantages were outweighed by the disadvantages that this procedure requires a longer generation time and additional screening time.

A crucial factor in the construct design of liCADs is the capture step to first pull down proteins from expression supernatants. In contrast to mAbs, which are purified using the Fc stem binding protein A, liCADs are not bound by protein A or any other resin frequently used in biopharmaceutical industry. Consequently, all liCADs had a N-terminally cloned 6xHis tag that exhibits a high affinity towards metal ions such as nickel (Ni) and zinc (Zn) and enables immobilised metal affinity chromatography (IMAC) to be used as a first purification step. The major drawback of using the histidine tag is the low recovery rate of protein and purity. This is because naturally occurring metal-binding proteins and the presence of histidine- as well as cysteine-rich spots within proteins are able to compete with the tagged proteins for the immobilized metal ions. However, several therapeutic candidate proteins purified using IMAC, are currently in clinical studies (Angov et al., 2003; Mack et al., 1995; Ockenhouse et al., 2006; Stoute et al., 2007).

5.2. liCADs exhibit low binding affinity to CD47

We next validated the liCADs as a novel tsAb format for their ability to locally interfere with CD47. To this end we used flow cytometry of human cell lines incubated with liCADs.

DISCUSSION

Binding was detected using an anti-His tag antibody. Due to the fact that all human cells express CD47 on their surface we could not use them to test for example binding of the anti-CD33 scFv to the antigen. To rule out additional CD47 binding we had two different strategies to follow up. First, we purified all single domains of the liCAD separately so that their binding could be characterized. We could not exclude the possibility, however, that the K_D values determined for individual domains would be representative of the values for the domain in the context of the whole liCADs. Additionally, we were unable to detect binding of SirpIg to any of the human cell lines tested. The reason for this is the binding affinity of SirpIg to CD47, which is reported to be in the high nanomolar (≈ 450 nM) (Weiskopf et al., 2013) to low micromolar (≈ 1.2 μ M) (Hatherley et al., 2008) range. This is consequently below the detection limit of the method, which depends on several washing steps to remove unspecific background signal. The big discrepancy in reported binding affinities highlights that measuring low affinity interactions *in vitro* is in general a challenging task. Furthermore, the determined binding affinities might not in any case reflect the situation *in vivo*.

The second strategy followed up implied transgenic cell line generation of non-human origin. In order to be able to use flow cytometry for binding studies, we generated Chinese Hamster Ovary (CHO) cell lines in which either human full length CD47 or human full length CD33 were highly overexpressed. Thereby we could test for binding of CD33 within the liCAD without influence from CD47 and *vice versa*. By generating these strongly overexpressing cell lines, we were also able to detect SirpIg binding to CD47 and calculate K_D values for the interaction. Even though this is certainly an artificial system with saturated amount of CD47 on the cell surface, the binding affinities determined for Sirp α are in the range of reported measurements by surface plasmon resonance. Although we could not show binding of SirpIg to CD47 on human cells, these data support the idea that the SirpIg domain used in this work would locally bind to tumor cells overexpressing CD47.

Consistent with the observation that duplication of low affinity scFvs in diabodies increases their functional affinity (= avidity) for the tumor antigen 40-fold (Adams et al., 1998), it was not surprising to see that duplication of the SirpIg domain resulted in a 30-fold tighter interaction with CD47. This is likely a result of a strong avidity effect that also results in a higher biological activity, which we could later show through redirected lysis assays and

DISCUSSION

macrophage assays. The rather low interaction determined for the control triplebody α CD47. α CD16. α CD33 might be explained by the composition of the anti-CD47 scFv, which only harbors a five amino acid linker between the variable heavy and variable light chains, compared to the 25 and 20 amino acid linkers present in the anti-CD16 and anti-CD33 scFvs, respectively. It might be that the shorter linker disturbs folding properties of the scFv and therefore influences binding affinity. The reason for why this molecule could not be purified from FreeStyleTM 293-F cells but SirpIg.SirpIg. α CD16. α CD33 could is still unclear and remains to be investigated.

5.3. liCAD molecules are able to recruit NK cells and induce tumor cell cytotoxicity

After verifying their binding capability we tested the biological activity of the generated proteins. LiCADs were designed with a central anti-CD16 scFv that binds to CD16 (also known as Fc γ RIIIa) with a high affinity. CD16 is expressed primarily on all CD56⁺ peripheral blood NK cells and is the best-characterized membrane receptor responsible for triggering of lysis (Mandelboim et al., 1999). In this study we performed *in vitro* cytotoxicity assays first using *in vitro* IL-2 expanded NK cells, which are prestimulated due to the IL-2 supplementation in the cell culture medium, and subsequently using MACS sorted NK cells. The advantage of expanded NK cells is that one can culture millions of cells from one donor, freeze them and use them for replicates. Therby less variation between the independent experiments, due to lack of donor variations of NK cells is expected. From the point of view of NK cell preparation costs it might also be profitable to make a single batch of NK cells over 21 days and use them for an ongoing study. The long-time storage of NK cells is not recommended, however, as the cell population is very fragile and tends to quickly loose its activity potential upon storage. This in turn leads to a decrease in the specific lysis of target cells. Interestingly, comparison of the half-maximal effective doses of individual molecules between expanded and sorted NK cells revealed that EC₅₀ values were between 5 to 25 times lower for MACS sorted NK cells. Consequently, the concentration of liCADs required to induce half-maximal specific lysis of the target cells was in every case lower when the experiment was performed with freshly prepared MACS sorted NK cells. This might result from differences in the CD16 expression level on the NK cells. Thus, our collaboration

DISCUSSION

partner Prof. Marion Subklewe analysed the CD16 expression on IL-2 expanded NK cells using flow cytometry and showed that CD16 expression is indeed reduced with respect to MACS sorted cells. These data certainly contribute to the observation that expanded NK cells stored in liquid nitrogen lose their activation potential over time. Therefore, we conclude that according to reliability of results concerning liCAD potential to recruit and induce effector cells, IL-2 expanded NK cells are definitely comparable to freshly prepared NK cells. It has to be kept in mind that the accuracy of half maximal effective dose estimates is affected by the long-time storage of expanded NK cells, because this results in a lower activation potential and higher EC₅₀ values compared to MACS prepared NK cells.

For assays with IL-2 expanded NK cells we could show that SirpIg.αCD16.αCD33 as well as SirpIg.SirpIg.αCD16.αCD33 had an increased potential to induce specific lysis of the AML cell line MOLM-13 compared to the bispecific control αCD33.αCD16. This would be consistent with the dual targeting effect of liCAD molecules or possibly an additive prostimulatory effect on NK cells. Tighter interaction of Sirp α to CD47 correlated with an increased potential to induce specific lysis. To rule out the possibility that the apparent activation potential of liCADs is only due to prestimulation of NK cells, we performed the same assays using primary MACS sorted NK cells. Similarly, we could demonstrate the same tendency in activation potential in primary MACS sorted NK cells. Additionally, we verified the observed cytotoxicity potential of highly expressing CD33 AML cells in a lowly expressing CD33 AML cell line, OCI-AML3 (around 30000 molecules per MOLM-13 cell versus around 3000 molecules per OCI-AML3 cell). We obtained very similar values for half-maximal effective doses of individual liCAD molecules. Subsequently we analyzed the number of CD47 molecules on MOLM-13 and OCI-AML3 cells and obtained comparable values (around 40000 molecules per MOLM-13 cell versus around 50000 molecules per OCI-AML3 cell). Therefore, the data cannot be explained by increased CD47 expression on OCI-AML3 cells compensating for decreased CD33 expression. The minor killing potential of SirpIg.αCD16 in both experiments indicates the non-targeting property of the SirpIg domain alone, due to its low affinity for CD47. For the bispecific control αCD33.αCD16 we demonstrate that the more CD33 is expressed on the tumor cell the better killing is induced. However, liCADs have regardless of CD33 antigen expression very similar induction

DISCUSSION

potential. Consistent with these observations we have come up with two different hypotheses. The first is that liCADs induce a dual targeting effect, but only upon bringing the effector cell into close proximity to the tumor cell. The second, more likely, possibility is, that crosslinking of the NK cell with the target cell leads to either a co-stimulatory effect on the NK cell or a pro-apoptotic stimulus on the tumor cell via CD47 binding. Our second hypothesis is supported by literature because, at least for T cells, it has been shown that CD47 binding (via Sirp α on DCs or mABs) has a co-stimulatory effect on T cell activation (Reinhold et al., 1997; Seiffert et al., 2001). Furthermore, in a multiple melanoma cell model it has been reported that anti-CD47 scFvs induce apoptosis of tumor cells (Kikuchi et al., 2005). Therefore, further experiments analyzing NK cell activation markers, such as CD107a, or apoptosis markers, such as annexin V, will have to be performed. Additionally, cytotoxicity assays using target cells that do not express CD47 will need to be performed to clarify if SirpIg within the liCAD acts on the target cell or on the NK cell. Through this one could determine if the obtained specific lysis of target cells incubated with the bispecific control SirpIg. α CD16 is tumor cell related or due to a co-stimulatory activation of NK cells.

We also performed effector to target cell ratio titrations to shed light on the potential of liCADs to induce serial lysis of effector cells. We saw that the specific lysis of MOLM-13 cells decreased with decreasing effector to target ratios. This indicates that liCADs may not have the potential to induce serial killing of tumor cells by NK cells. In contrast to cytotoxic T cells, it might be the case that only IL-2 stimulated, pre-activated NK cells are capable of serial killing, as previously reported in literature (Bhat and Watzl, 2007).

5.4. LiCADs increase phagocytic uptake of tumor cells in macrophages

A major goal of this thesis was to determine the ability of SirpIg to block the naturally occurring CD47-Sirp α interaction inducing phagocytosis in macrophages. In order to avoid donor-specific variations, which could easily lead to diverse results, we first wanted to establish a cell line based assay that facilitates on one hand reproducibility and on the other hand faster access to macrophages. Furthermore, working in an autologous setting is always preferred to an allogeneic setting, since background phagocytosis may be reduced. We therefore made use of the possibility to differentiate THP-1 cells to macrophages and

DISCUSSION

incubate them together with undifferentiated THP-1 cells. However, sustained results showed an unusual strong unspecific increase in phagocytosis and an especially high increase in phagocytosis by blocking only the CD47-Sirp α interaction. We also realized that THP-1 macrophages express very little CD16 on their surface, which makes them also a poor model system to test molecules containing an anti-CD16 scFv as an effector-recruiting domain.

We consequently switched to primary monocytes that we differentiated to M2 macrophages, which are commonly known as the CD16 expressing subset of macrophages (Italiani and Boraschi, 2014). Incubation of macrophages with SirpIg.SirpIg. α CD16. α CD33 effectively increased phagocytic uptake of MOLM-13 cells in all experiments, however SirpIg. α CD16. α CD33 showed only a slight increase compared to the bispecific control α CD33. α CD16. This was certainly also donor related since some macrophages responded with larger increase and other with same increase rates as the control. In contrast to the cell line based system, we did not see an increase in phagocytosis induced by the SirpIg domain alone. This is in agreement with the literature, which reports that Sirp α blockade alone is not sufficient to induce phagocytosis (Weiskopf and Weissman, 2015). Even though M2 macrophages are known to be the CD16 expressing subpopulation, we aimed to analyse only CD16⁺ cells by flow cytometry. We included a CD16 staining step in our analysis, but were only rarely able to detect CD16⁺ events. The reason for this might be the internalization of the CD16 receptor on the surface of macrophages upon ligation. In control wells, where we did not add liCAD protein, we could detect CD16 expression. As soon as we added liCAD, however, CD16 expression was hard to detect. Thus, we were not able to obtain reliable data sets and did not include these data in our evaluation. In order to limit analysis to CD16 expressing macrophages, an intracellular staining of CD16 would have to be performed. However, we aimed to avoid the intracellular staining of macrophages since it is a time-demanding procedure and includes fixation and permeabilization steps that might cause artefacts in the assay.

As most of the studies carried out by the Weissman group demonstrated a beneficial effect of the blockade of CD47 in tumor cell phagocytosis, we included the same clone they used for blocking (B6H12) in our assays to approximately correlate our liCADs with the mAb. Again, we could show that SirpIg.SirpIg. α CD16. α CD33 performed better than the anti-CD47 mAb

DISCUSSION

B6H12, which is however unsurprising since the liCAD molecule combines tumor cell targeting and checkpoint inhibition. It would therefore be better to compare liCADs with a combination of two mAbs, one that targets in our case CD33 and the other one that blocks the CD47 interaction.

5.5. LiCADs preferentially kill CD47/CD33 positive tumor cells

CD47 is expressed ubiquitously on all cells of the human body, which increases the likelihood of side effects if it is targeted. However, since the CD47 binding component in the liCAD molecule is the naturally occurring extracellular domain of Sirp α , which only weakly interacts with CD47, we hypothesize that liCAD molecules would preferentially target tumor cells that express CD33 but not other non-CD33 expressing cells.

Thus, we performed a cytotoxicity assay with a mixed target cell population of CD47 single positive and CD47/CD33 double positive cells. To this end, we made use of the Flp-INTM 293 HEK cell system, which enabled us to stably integrate full length human CD33. Since those cells are of human origin they express CD47, which is thus also expressed on untransduced cells. Analyzing dose response curves we could demonstrate that the CD47 control liCADs SirpIg_CV1. α CD16. α CD33 and α CD47. α CD16. α CD33 killed both cell populations to a very similar extent. In contrast, SirpIg.SirpIg. α CD16. α CD33 and SirpIg. α CD16. α CD33 had far higher half maximal effective dose values for Flp-INTM 293 HEK cells compared to CD33 Flp-INTM 293 HEK cells. This indicates, that at same concentrations, we induce in case of SirpIg. α CD16. α CD33 63-times higher and in case of SirpIg.SirpIg. α CD16. α CD33 even more impressively, 138-times higher specific lysis of CD33 Flp-INTM 293 HEK cells compared to Flp-INTM 293 HEK cells. We suggest this range as the therapeutic window in which the liCAD produces a therapeutic response without causing significant side effects in patients.

To confirm these data we performed additional cytotoxicity assays using either the maximal or half maximal effective concentrations of individual liCADs with Flp-INTM 293 HEK cells or, in a less artificial system, a mixture of MOLM-13 and OCI-AML3 cells. With the Flp-INTM 293 HEK cells we could again verify the preferential killing potential of low affinity liCADs SirpIg. α CD16. α CD33 as well as SirpIg.SirpIg. α CD16. α CD33. Both preferentially

DISCUSSION

killed CD33 Flp-IN™ 293 HEK cells whereas the CD47 control liCADs did not, at least at the maximal effective concentrations used. In experiments carried out with the half maximal effective concentrations of liCADs we observed a background killing of Flp-IN™ 293 HEK cells of around 10% that was visualized by the bispecific control α CD33. α CD16, which should not target CD33 negative cells. These results might be explained by variations in NK cell donors.

In order to translate the beneficial effect of liCADs from HEK cells to tumor cell lines, we performed cytotoxicity assays using MOLM-13 cells that highly express CD33 and OCI-AML3 cells that express CD33 at a low level. Even though both cell lines express CD33, we could observe that the higher expressing cell line, MOLM-13, was preferentially killed. We could not detect as many differences as in case of the Flp-IN™ 293 HEK cell system but, due to the mentioned CD33 expression levels as well as differences in CD47 expression, this was expected.

Taken together, we observed the huge and very impressive potential of our novel liCAD format to preferentially kill CD47/CD33 double positive cells in *in vitro* cytotoxicity assays, which puts hope into further clinical use of these molecules. We suggest that these trispecific Abs have a beneficial outcome and display decreased side effects compared to antibodies that target CD47 with high affinity.

5.6. LiCADs induce NK cell mediated killing of primary AML patient samples

We successfully demonstrated the potential of liCADs to induce effector cell mediated killing of various tumor cell lines as well as non-tumor cell lines, which indicates there may also be a high possibility of cytotoxicity behavior when used with AML patient samples. In order to confirm this hypothesis, our collaboration partner Prof. Marion Subklewe performed *in vitro* NK cell mediated cytotoxicity assays with primary AML patient cells. Her research group previously showed that CD33 expression on AML blasts is highly diverse (Krupka et al., 2014), which certainly influences outcome of mAb therapy. It was also shown that CD47 is highly overexpressed on AML blast samples compared to healthy hematopoietic cells (unpublished data), which is consistent with published data from the Weissman group (Majeti et al., 2009).

DISCUSSION

We could show that incubation of AML blasts with SirpIg.SirpIg.αCD16.αCD33 induced stronger NK cell mediated killing of blasts after 24 hours when compared to the bispecific control αCD33.αCD16. Furthermore, we observed a stronger downregulation of CD16 on the NK cells after SirpIg.SirpIg.αCD16.αCD33 incubation, which is indicative of stronger NK cell activation. At present we cannot rule out that the detected CD16 downregulation is due to an overlap of the binding epitopes of the anti-CD16 scFv and FACS antibody used. Though, the differences in mean fluorescence intensity of CD16 expression between NK cells incubated with SirpIg.SirpIg.αCD16.αCD33 and αCD33.αCD16 speak against this possibility. Certainly further investigations are necessary to verify these first hints on increased NK cell activation, like interferon γ secretion or staining for the activation marker CD107a. In addition to SirpIg.SirpIg.αCD16.αCD33, we will also test SirpIg.αCD16.αCD33 for killing and NK cell activation potential. Nevertheless, we are confident that the novel liCAD format has the potential to induce NK cell mediated killing of AML patient cell samples *in vitro* by improved NK cell activation compared to the bispecific molecule that does not have the SirpIg domain. Thus, these data strongly support our hypothesis about the increased NK cell activation by the SirpIg-CD47 interaction. However, we will have to rule out unspecific NK cell activation caused by CD47 ligation, since this would probably lead to undesired side effects and damage of healthy tissue, respectively.

5.7. Future directions for liCAD molecules

During this study we successfully demonstrated that the simultaneous targeting of CD33 on tumor cells and blockade of the CD47-Sirp α interaction results in increased effector cell functions in NK cells as well as macrophages. All of our performed experiments were *in vitro* studies thus *in vivo* efficacy must be tested. To date, a routinely used preclinical test of a new compound includes injections into animals. In the case of liCADs it certainly is very challenging to find a relevant mouse model, since the CD47-Sirp α interaction is species specific and a molecule targeting human antigens consequently cannot interact with mouse CD47. One of the main questions important to ask, that is to say the question about side effects due to ubiquitous expression of CD47, can therefore not be addressed by the accepted transplantable as well as spontaneous tumor mouse models. Therefore, one possibility would be to generate a CD47 humanized immunodeficient mouse, which is certainly challenging.

DISCUSSION

Cynomolgus monkeys could alternatively be used instead of mouse models. In a pre-clinical study it has been shown that a humanized anti-CD47 mAb was able to bind to monkey CD47 (Liu et al., 2015). For *in vivo* studies in general, half-life of liCAD proteins would have to be analysed, which might be optimized by different buffer formulations. Thus long-term stability tests as well as detailed serum-stability tests should be performed to reduce possible protein degradation *in vivo*.

Another interesting aspect would be to compare the liCAD format to conventional combination therapy, which combines two mAb against an immune checkpoint and a tumor target. It would be interesting to see if the liCAD performs similarly or even better than the combination of mAbs, since this could decrease therapy costs as well as possible side effects due to Fc mediated systemic immune system activation. Moreover, one could transfer the idea of locally blocking the CD47-Sirp α interaction by SirpIg to a conventional mAb and compare side-by-side the effects of liCADs and these engineered mAbs in order to investigate advantages and disadvantages of recruiting specific effector cells via scFvs or any Fc γ expressing immune cell.

6. REFERENCES

Adams, G.P., Schier, R., McCall, A.M., Crawford, R.S., Wolf, E.J., Weiner, L.M., and Marks, J.D. (1998). Prolonged in vivo tumour retention of a human diabody targeting the extracellular domain of human HER2/neu. *Br J Cancer* 77, 1405-1412.

Adams, J.C. (2001). Thrombospondins: multifunctional regulators of cell interactions. *Annu Rev Cell Dev Biol* 17, 25-51.

Aigner, M., Feulner, J., Schaffer, S., Kischel, R., Kufer, P., Schneider, K., Henn, A., Rattel, B., Friedrich, M., Baeuerle, P.A., *et al.* (2013). T lymphocytes can be effectively recruited for ex vivo and in vivo lysis of AML blasts by a novel CD33/CD3-bispecific BiTE antibody construct. *Leukemia* 27, 1107-1115.

Angov, E., Aufiero, B.M., Turgeon, A.M., Van Handenhove, M., Ockenhouse, C.F., Kester, K.E., Walsh, D.S., McBride, J.S., Dubois, M.C., Cohen, J., *et al.* (2003). Development and pre-clinical analysis of a Plasmodium falciparum Merozoite Surface Protein-1(42) malaria vaccine. *Mol Biochem Parasitol* 128, 195-204.

Arndt, C., Feldmann, A., von Bonin, M., Cartellieri, M., Ewen, E.M., Koristka, S., Michalk, I., Stamova, S., Berndt, N., Gocht, A., *et al.* (2014). Costimulation improves the killing capability of T cells redirected to tumor cells expressing low levels of CD33: description of a novel modular targeting system. *Leukemia* 28, 59-69.

Arndt, C., von Bonin, M., Cartellieri, M., Feldmann, A., Koristka, S., Michalk, I., Stamova, S., Bornhauser, M., Schmitz, M., Ehninger, G., *et al.* (2013). Redirection of T cells with a first fully humanized bispecific CD33-CD3 antibody efficiently eliminates AML blasts without harming hematopoietic stem cells. *Leukemia* 27, 964-967.

Barclay, A.N., and Brown, M.H. (2006). The SIRP family of receptors and immune regulation. *Nat Rev Immunol* 6, 457-464.

REFERENCES

- Barclay, A.N., and Van den Berg, T.K. (2014). The interaction between signal regulatory protein alpha (SIRPalpha) and CD47: structure, function, and therapeutic target. *Annu Rev Immunol* 32, 25-50.
- Bargou, R., Leo, E., Zugmaier, G., Klinger, M., Goebeler, M., Knop, S., Noppeney, R., Viardot, A., Hess, G., Schuler, M., *et al.* (2008). Tumor regression in cancer patients by very low doses of a T cell-engaging antibody. *Science* 321, 974-977.
- Bernstein, I.D. (2000). Monoclonal antibodies to the myeloid stem cells: therapeutic implications of CMA-676, a humanized anti-CD33 antibody calicheamicin conjugate. *Leukemia* 14, 474-475.
- Bhat, R., and Watzl, C. (2007). Serial killing of tumor cells by human natural killer cells--enhancement by therapeutic antibodies. *PLoS One* 2, e326.
- Brooke, G., Holbrook, J.D., Brown, M.H., and Barclay, A.N. (2004). Human lymphocytes interact directly with CD47 through a novel member of the signal regulatory protein (SIRP) family. *J Immunol* 173, 2562-2570.
- Bross, P.F., Beitz, J., Chen, G., Chen, X.H., Duffy, E., Kieffer, L., Roy, S., Sridhara, R., Rahman, A., Williams, G., *et al.* (2001). Approval summary: gemtuzumab ozogamicin in relapsed acute myeloid leukemia. *Clin Cancer Res* 7, 1490-1496.
- Caron, P.C., Co, M.S., Bull, M.K., Avdalovic, N.M., Queen, C., and Scheinberg, D.A. (1992). Biological and immunological features of humanized M195 (anti-CD33) monoclonal antibodies. *Cancer Res* 52, 6761-6767.
- Chames, P., and Baty, D. (2009). Bispecific antibodies for cancer therapy. *Curr Opin Drug Discov Devel* 12, 276-283.

REFERENCES

- Chames, P., Van Regenmortel, M., Weiss, E., and Baty, D. (2009). Therapeutic antibodies: successes, limitations and hopes for the future. *Br J Pharmacol* 157, 220-233.
- Chao, M.P., Alizadeh, A.A., Tang, C., Myklebust, J.H., Varghese, B., Gill, S., Jan, M., Cha, A.C., Chan, C.K., Tan, B.T., *et al.* (2010). Anti-CD47 antibody synergizes with rituximab to promote phagocytosis and eradicate non-Hodgkin lymphoma. *Cell* 142, 699-713.
- Chen, L.F., Cohen, E.E., and Grandis, J.R. (2010). New strategies in head and neck cancer: understanding resistance to epidermal growth factor receptor inhibitors. *Clin Cancer Res* 16, 2489-2495.
- Chung, J., Gao, A.G., and Frazier, W.A. (1997). Thrombospondin acts via integrin-associated protein to activate the platelet integrin α IIb β 3. *J Biol Chem* 272, 14740-14746.
- Collins, A.V., Brodie, D.W., Gilbert, R.J., Iaboni, A., Manso-Sancho, R., Walse, B., Stuart, D.I., van der Merwe, P.A., and Davis, S.J. (2002). The interaction properties of costimulatory molecules revisited. *Immunity* 17, 201-210.
- Corces-Zimmerman, M.R., Hong, W.J., Weissman, I.L., Medeiros, B.C., and Majeti, R. (2014). Preleukemic mutations in human acute myeloid leukemia affect epigenetic regulators and persist in remission. *Proc Natl Acad Sci U S A* 111, 2548-2553.
- Couzin-Frankel, J. (2013). Breakthrough of the year 2013. Cancer immunotherapy. *Science* 342, 1432-1433.
- Curran, M.A., Montalvo, W., Yagita, H., and Allison, J.P. (2010). PD-1 and CTLA-4 combination blockade expands infiltrating T cells and reduces regulatory T and myeloid cells within B16 melanoma tumors. *Proc Natl Acad Sci U S A* 107, 4275-4280.

REFERENCES

- Dohner, H., Weisdorf, D.J., and Bloomfield, C.D. (2015). Acute Myeloid Leukemia. *N Engl J Med* 373, 1136-1152.
- Ecker, D.M., Jones, S.D., and Levine, H.L. (2015). The therapeutic monoclonal antibody market. *MAbs* 7, 9-14.
- Elgert, K.D. (1998). Antibody structure and function. In *Immunology: Understanding the immune system* (John Wiley & Sons), pp. 58-78.
- Estey, E., and Döhner, H. (2006). Acute myeloid leukaemia. *The Lancet* 368, 1894-1907.
- Feldman, E.J., Brandwein, J., Stone, R., Kalaycio, M., Moore, J., O'Connor, J., Wedel, N., Roboz, G.J., Miller, C., Chopra, R., *et al.* (2005). Phase III randomized multicenter study of a humanized anti-CD33 monoclonal antibody, lintuzumab, in combination with chemotherapy, versus chemotherapy alone in patients with refractory or first-relapsed acute myeloid leukemia. *J Clin Oncol* 23, 4110-4116.
- Freeman, G.J., Long, A.J., Iwai, Y., Bourque, K., Chernova, T., Nishimura, H., Fitz, L.J., Malenkovich, N., Okazaki, T., Byrne, M.C., *et al.* (2000). Engagement of the PD-1 immunoinhibitory receptor by a novel B7 family member leads to negative regulation of lymphocyte activation. *J Exp Med* 192, 1027-1034.
- Fujioka, Y., Matozaki, T., Noguchi, T., Iwamatsu, A., Yamao, T., Takahashi, N., Tsuda, M., Takada, T., and Kasuga, M. (1996). A novel membrane glycoprotein, SHPS-1, that binds the SH2-domain-containing protein tyrosine phosphatase SHP-2 in response to mitogens and cell adhesion. *Mol Cell Biol* 16, 6887-6899.
- Gardai, S.J., McPhillips, K.A., Frasch, S.C., Janssen, W.J., Starefeldt, A., Murphy-Ullrich, J.E., Bratton, D.L., Oldenborg, P.A., Michalak, M., and Henson, P.M. (2005). Cell-surface calreticulin initiates clearance of viable or apoptotic cells through trans-activation of LRP on the phagocyte. *Cell* 123, 321-334.

REFERENCES

- Gasiorowski, R.E., Clark, G.J., Bradstock, K., and Hart, D.N. (2014). Antibody therapy for acute myeloid leukaemia. *Br J Haematol* *164*, 481-495.
- Goardon, N., Marchi, E., Atzberger, A., Quek, L., Schuh, A., Soneji, S., Woll, P., Mead, A., Alford, K.A., Rout, R., *et al.* (2011). Coexistence of LMPP-like and GMP-like leukemia stem cells in acute myeloid leukemia. *Cancer Cell* *19*, 138-152.
- Grimwade, D., and Freeman, S.D. (2014). Defining minimal residual disease in acute myeloid leukemia: which platforms are ready for "prime time"? *Blood* *124*, 3345-3355.
- Grosso, J.F., Goldberg, M.V., Getnet, D., Bruno, T.C., Yen, H.R., Pyle, K.J., Hipkiss, E., Vignali, D.A., Pardoll, D.M., and Drake, C.G. (2009). Functionally distinct LAG-3 and PD-1 subsets on activated and chronically stimulated CD8 T cells. *J Immunol* *182*, 6659-6669.
- Hatherley, D., Graham, S.C., Turner, J., Harlos, K., Stuart, D.I., and Barclay, A.N. (2008). Paired receptor specificity explained by structures of signal regulatory proteins alone and complexed with CD47. *Mol Cell* *31*, 266-277.
- Hess, C., Venetz, D., and Neri, D. (2014). Emerging classes of armed antibody therapeutics against cancer. *MedChemComm* *5*, 408-431.
- Hidalgo, M., Tourneau, C.L., Massard, C., Boni, V., Calvo, E., and al., e. (2014). Results from the first-in-human (FIH) phase I study of RO5520985 (RG7221), a novel bispecific human anti-Ang-2/anti-VEGF-A antibody, administered as an intravenous infusion to patients with advanced solid tumors. American Society of Clinical Oncology Annual Meeting.
- Hills, R.K., Castaigne, S., Appelbaum, F.R., Delaunay, J., Petersdorf, S., Othus, M., Estey, E.H., Dombret, H., Chevret, S., Ifrah, N., *et al.* (2014). Addition of gemtuzumab ozogamicin to induction chemotherapy in adult patients with acute myeloid leukaemia: a meta-

REFERENCES

analysis of individual patient data from randomised controlled trials. *Lancet Oncol* 15, 986-996.

Holliger, P., Prospero, T., and Winter, G. (1993). "Diabodies": small bivalent and bispecific antibody fragments. *Proc Natl Acad Sci U S A* 90, 6444-6448.

Hornig, N., Kermer, V., Frey, K., Diebolder, P., Kontermann, R.E., and Muller, D. (2012). Combination of a bispecific antibody and costimulatory antibody-ligand fusion proteins for targeted cancer immunotherapy. *J Immunother* 35, 418-429.

Ishida, Y., Agata, Y., Shibahara, K., and Honjo, T. (1992). Induced expression of PD-1, a novel member of the immunoglobulin gene superfamily, upon programmed cell death. *EMBO J* 11, 3887-3895.

Ishikawa-Sekigami, T., Kaneko, Y., Okazawa, H., Tomizawa, T., Okajo, J., Saito, Y., Okuzawa, C., Sugawara-Yokoo, M., Nishiyama, U., Ohnishi, H., *et al.* (2006). SHPS-1 promotes the survival of circulating erythrocytes through inhibition of phagocytosis by splenic macrophages. *Blood* 107, 341-348.

Italiani, P., and Boraschi, D. (2014). From Monocytes to M1/M2 Macrophages: Phenotypical vs. Functional Differentiation. *Front Immunol* 5, 514.

Jaiswal, S., Jamieson, C.H., Pang, W.W., Park, C.Y., Chao, M.P., Majeti, R., Traver, D., van Rooijen, N., and Weissman, I.L. (2009). CD47 is upregulated on circulating hematopoietic stem cells and leukemia cells to avoid phagocytosis. *Cell* 138, 271-285.

Jiang, P., Lagenaur, C.F., and Narayanan, V. (1999). Integrin-associated protein is a ligand for the P84 neural adhesion molecule. *J Biol Chem* 274, 559-562.

Jin, L., Lee, E.M., Ramshaw, H.S., Busfield, S.J., Peoppl, A.G., Wilkinson, L., Guthridge, M.A., Thomas, D., Barry, E.F., Boyd, A.,

REFERENCES

et al. (2009). Monoclonal antibody-mediated targeting of CD123, IL-3 receptor alpha chain, eliminates human acute myeloid leukemic stem cells. *Cell Stem Cell* 5, 31-42.

Johansson, D.X., Drakenberg, K., Hopmann, K.H., Schmidt, A., Yari, F., Hinkula, J., and Persson, M.A. (2007). Efficient expression of recombinant human monoclonal antibodies in *Drosophila* S2 cells. *J Immunol Methods* 318, 37-46.

Jones, P.T., Dear, P.H., Foote, J., Neuberger, M.S., and Winter, G. (1986). Replacing the complementarity-determining regions in a human antibody with those from a mouse. *Nature* 321, 522-525.

Jordan, C.T., Upchurch, D., Szilvassy, S.J., Guzman, M.L., Howard, D.S., Pettigrew, A.L., Meyerrose, T., Rossi, R., Grimes, B., Rizzieri, D.A., *et al.* (2000). The interleukin-3 receptor alpha chain is a unique marker for human acute myelogenous leukemia stem cells. *Leukemia* 14, 1777-1784.

Kharitonov, A., Chen, Z., Sures, I., Wang, H., Schilling, J., and Ullrich, A. (1997). A family of proteins that inhibit signalling through tyrosine kinase receptors. *Nature* 386, 181-186.

Kienast, Y., Klein, C., Scheuer, W., Raemsch, R., Lorenzon, E., Bernicke, D., Herting, F., Yu, S., The, H.H., Martarello, L., *et al.* (2013). Ang-2-VEGF-A CrossMab, a novel bispecific human IgG1 antibody blocking VEGF-A and Ang-2 functions simultaneously, mediates potent antitumor, antiangiogenic, and antimetastatic efficacy. *Clin Cancer Res* 19, 6730-6740.

Kikuchi, Y., Uno, S., Kinoshita, Y., Yoshimura, Y., Iida, S., Wakahara, Y., Tsuchiya, M., Yamada-Okabe, H., and Fukushima, N. (2005). Apoptosis inducing bivalent single-chain antibody fragments against CD47 showed antitumor potency for multiple myeloma. *Leuk Res* 29, 445-450.

REFERENCES

- Kim, Y.K., Shin, H.S., Tomiya, N., Lee, Y.C., Betenbaugh, M.J., and Cha, H.J. (2005). Production and N-glycan analysis of secreted human erythropoietin glycoprotein in stably transfected *Drosophila* S2 cells. *Biotechnol Bioeng* 92, 452-461.
- Kohler, G., and Milstein, C. (1975). Continuous cultures of fused cells secreting antibody of predefined specificity. *Nature* 256, 495-497.
- Konarev, P.V., Petoukhov, M.V., Volkov, V.V., and Svergun, D.I. (2006). ATSAS 2.1, a program package for small-angle scattering data analysis. *Journal of Applied Crystallography* 39, 277-286.
- Koreth, J., Schlenk, R., Kopecky, K.J., Honda, S., Sierra, J., Djulbegovic, B.J., Wadleigh, M., DeAngelo, D.J., Stone, R.M., Sakamaki, H., *et al.* (2009). Allogeneic stem cell transplantation for acute myeloid leukemia in first complete remission: systematic review and meta-analysis of prospective clinical trials. *JAMA* 301, 2349-2361.
- Krupka, C., Kufer, P., Kischel, R., Zugmaier, G., Bogeholz, J., Kohnke, T., Lichtenegger, F.S., Schneider, S., Metzeler, K.H., Fiegl, M., *et al.* (2014). CD33 target validation and sustained depletion of AML blasts in long-term cultures by the bispecific T-cell-engaging antibody AMG 330. *Blood* 123, 356-365.
- Kugler, M., Stein, C., Kellner, C., Mentz, K., Saul, D., Schwenkert, M., Schubert, I., Singer, H., Oduncu, F., Stockmeyer, B., *et al.* (2010). A recombinant trispecific single-chain Fv derivative directed against CD123 and CD33 mediates effective elimination of acute myeloid leukaemia cells by dual targeting. *Br J Haematol* 150, 574-586.
- Larkin, J., Hodi, F.S., and Wolchok, J.D. (2015). Combined Nivolumab and Ipilimumab or Monotherapy in Untreated Melanoma. *N Engl J Med* 373, 1270-1271.

REFERENCES

- Larson, R.A., Boogaerts, M., Estey, E., Karanes, C., Stadtmauer, E.A., Sievers, E.L., Mineur, P., Bennett, J.M., Berger, M.S., Eten, C.B., *et al.* (2002). Antibody-targeted chemotherapy of older patients with acute myeloid leukemia in first relapse using Mylotarg (gemtuzumab ozogamicin). *Leukemia* 16, 1627-1636.
- Latchman, Y., Wood, C.R., Chernova, T., Chaudhary, D., Borde, M., Chernova, I., Iwai, Y., Long, A.J., Brown, J.A., Nunes, R., *et al.* (2001). PD-L2 is a second ligand for PD-1 and inhibits T cell activation. *Nat Immunol* 2, 261-268.
- Lee, W.Y., Weber, D.A., Laur, O., Severson, E.A., McCall, I., Jen, R.P., Chin, A.C., Wu, T., Gernert, K.M., and Parkos, C.A. (2007). Novel structural determinants on SIRP alpha that mediate binding to CD47. *J Immunol* 179, 7741-7750.
- Lindberg, F.P., Bullard, D.C., Caver, T.E., Gresham, H.D., Beaudet, A.L., and Brown, E.J. (1996). Decreased resistance to bacterial infection and granulocyte defects in IAP-deficient mice. *Science* 274, 795-798.
- Lindberg, F.P., Lublin, D.M., Telen, M.J., Veile, R.A., Miller, Y.E., Donis-Keller, H., and Brown, E.J. (1994). Rh-related antigen CD47 is the signal-transducer integrin-associated protein. *J Biol Chem* 269, 1567-1570.
- Lindhofer, H., Mocikat, R., Steipe, B., and Thierfelder, S. (1995). Preferential species-restricted heavy/light chain pairing in rat/mouse quadromas. Implications for a single-step purification of bispecific antibodies. *J Immunol* 155, 219-225.
- Linenberger, M.L. (2005). CD33-directed therapy with gemtuzumab ozogamicin in acute myeloid leukemia: progress in understanding cytotoxicity and potential mechanisms of drug resistance. *Leukemia* 19, 176-182.

REFERENCES

- Liu, J., Wang, L., Zhao, F., Tseng, S., Narayanan, C., Shura, L., Willingham, S., Howard, M., Prohaska, S., Volkmer, J., *et al.* (2015). Pre-Clinical Development of a Humanized Anti-CD47 Antibody with Anti-Cancer Therapeutic Potential. *PLoS One* 10, e0137345.
- Liu, Y., Merlin, D., Burst, S.L., Pochet, M., Madara, J.L., and Parkos, C.A. (2001). The role of CD47 in neutrophil transmigration. Increased rate of migration correlates with increased cell surface expression of CD47. *J Biol Chem* 276, 40156-40166.
- Loureiro, L.R., Carrascal, M.A., Barbas, A., Ramalho, J.S., Novo, C., Delannoy, P., and Videira, P.A. (2015). Challenges in Antibody Development against Tn and Sialyl-Tn Antigens. *Biomolecules* 5, 1783-1809.
- Lowenberg, B. (2013). Sense and nonsense of high-dose cytarabine for acute myeloid leukemia. *Blood* 121, 26-28.
- Mack, M., Riethmuller, G., and Kufer, P. (1995). A small bispecific antibody construct expressed as a functional single-chain molecule with high tumor cell cytotoxicity. *Proc Natl Acad Sci U S A* 92, 7021-7025.
- Majeti, R., Chao, M.P., Alizadeh, A.A., Pang, W.W., Jaiswal, S., Gibbs, K.D., Jr., van Rooijen, N., and Weissman, I.L. (2009). CD47 is an adverse prognostic factor and therapeutic antibody target on human acute myeloid leukemia stem cells. *Cell* 138, 286-299.
- Mandelboim, O., Malik, P., Davis, D.M., Jo, C.H., Boyson, J.E., and Strominger, J.L. (1999). Human CD16 as a lysis receptor mediating direct natural killer cell cytotoxicity. *Proc Natl Acad Sci U S A* 96, 5640-5644.
- Mardiros, A., Dos Santos, C., McDonald, T., Brown, C.E., Wang, X., Budde, L.E., Hoffman, L., Aguilar, B., Chang, W.C., Bretzlaff, W., *et al.* (2013). T cells expressing CD123-specific chimeric antigen receptors exhibit specific cytolytic effector functions and antitumor

REFERENCES

effects against human acute myeloid leukemia. *Blood* 122, 3138-3148.

Mawby, W.J., Holmes, C.H., Anstee, D.J., Spring, F.A., and Tanner, M.J. (1994). Isolation and characterization of CD47 glycoprotein: a multispinning membrane protein which is the same as integrin-associated protein (IAP) and the ovarian tumour marker OA3. *Biochem J* 304 (Pt 2), 525-530.

Maynard, J., and Georgiou, G. (2000). Antibody engineering. *Annu Rev Biomed Eng* 2, 339-376.

McCracken, M.N., Cha, A.C., and Weissman, I.L. (2015). Molecular Pathways: Activating T Cells after Cancer Cell Phagocytosis from Blockade of CD47 "Don't Eat Me" Signals. *Clin Cancer Res* 21, 3597-3601.

Moretta, L., Bottino, C., Pende, D., Vitale, M., Mingari, M.C., and Moretta, A. (2004). Different checkpoints in human NK-cell activation. *Trends Immunol* 25, 670-676.

Neuberger, M.S., Williams, G.T., Mitchell, E.B., Jouhal, S.S., Flanagan, J.G., and Rabbitts, T.H. (1985). A hapten-specific chimaeric IgE antibody with human physiological effector function. *Nature* 314, 268-270.

Nimmerjahn, F., and Ravetch, J.V. (2008). Fcγ receptors as regulators of immune responses. *Nat Rev Immunol* 8, 34-47.

NovImmune (2015). NI-170: A bispecific antibody that empowers the immune system to kill malignant B cells.

O'Donnell, M.R., Abboud, C.N., Altman, J., Appelbaum, F.R., Arber, D.A., Attar, E., Borate, U., Coutre, S.E., Damon, L.E., Goorha, S., *et al.* (2012). Acute myeloid leukemia. *J Natl Compr Canc Netw* 10, 984-1021.

REFERENCES

- Oates, J., and Jakobsen, B.K. (2013). ImmTACs: Novel bi-specific agents for targeted cancer therapy. *Oncoimmunology* 2, e22891.
- Ockenhouse, C.F., Angov, E., Kester, K.E., Diggs, C., Soisson, L., Cummings, J.F., Stewart, A.V., Palmer, D.R., Mahajan, B., Krzych, U., *et al.* (2006). Phase I safety and immunogenicity trial of FMP1/AS02A, a *Plasmodium falciparum* MSP-1 asexual blood stage vaccine. *Vaccine* 24, 3009-3017.
- Oldenborg, P.A. (2004). Role of CD47 in erythroid cells and in autoimmunity. *Leuk Lymphoma* 45, 1319-1327.
- Oldenborg, P.A. (2013). CD47: A Cell Surface Glycoprotein Which Regulates Multiple Functions of Hematopoietic Cells in Health and Disease. *ISRN Hematol* 2013, 614619.
- Oldenborg, P.A., Zheleznyak, A., Fang, Y.F., Lagenaur, C.F., Gresham, H.D., and Lindberg, F.P. (2000). Role of CD47 as a marker of self on red blood cells. *Science* 288, 2051-2054.
- Pardoll, D.M. (2012). The blockade of immune checkpoints in cancer immunotherapy. *Nat Rev Cancer* 12, 252-264.
- Pasquini, M.C., Devine, S., Mendizabal, A., Baden, L.R., Wingard, J.R., Lazarus, H.M., Appelbaum, F.R., Keever-Taylor, C.A., Horowitz, M.M., Carter, S., *et al.* (2012). Comparative outcomes of donor graft CD34+ selection and immune suppressive therapy as graft-versus-host disease prophylaxis for patients with acute myeloid leukemia in complete remission undergoing HLA-matched sibling allogeneic hematopoietic cell transplantation. *J Clin Oncol* 30, 3194-3201.
- Petersdorf, S., Kopecky, K., Stuart, R.K., Larson, R.A., Nevill, T.J., Stenke, L., Slovak, M.L., Tallman, M.S., Willman, C.L., Erba, H., *et al.* (2009). Preliminary Results of Southwest Oncology Group Study S0106: An International Intergroup Phase 3 Randomized Trial Comparing the Addition of Gemtuzumab Ozogamicin to Standard

REFERENCES

Induction Therapy Versus Standard Induction Therapy Followed by a Second Randomization to Post-Consolidation Gemtuzumab Ozogamicin Versus No Additional Therapy for Previously Untreated Acute Myeloid Leukemia. *Blood* 114, 326-327.

Piccione, E.C., Juarez, S., Liu, J., Tseng, S., Ryan, C.E., Narayanan, C., Wang, L., Weiskopf, K., and Majeti, R. (2015). A bispecific antibody targeting CD47 and CD20 selectively binds and eliminates dual antigen expressing lymphoma cells. *MAbs* 7, 946-956.

Reinhold, M.I., Lindberg, F.P., Kersh, G.J., Allen, P.M., and Brown, E.J. (1997). Costimulation of T cell activation by integrin-associated protein (CD47) is an adhesion-dependent, CD28-independent signaling pathway. *J Exp Med* 185, 1-11.

Reinhold, M.I., Lindberg, F.P., Plas, D., Reynolds, S., Peters, M.G., and Brown, E.J. (1995). In vivo expression of alternatively spliced forms of integrin-associated protein (CD47). *J Cell Sci* 108 (Pt 11), 3419-3425.

Reusch, U., Burkhardt, C., Fucek, I., Le Gall, F., Le Gall, M., Hoffmann, K., Knackmuss, S.H., Kiprijanov, S., Little, M., and Zhukovsky, E.A. (2014). A novel tetravalent bispecific TandAb (CD30/CD16A) efficiently recruits NK cells for the lysis of CD30+ tumor cells. *MAbs* 6, 728-739.

Sakuishi, K., Apetoh, L., Sullivan, J.M., Blazar, B.R., Kuchroo, V.K., and Anderson, A.C. (2010). Targeting Tim-3 and PD-1 pathways to reverse T cell exhaustion and restore anti-tumor immunity. *J Exp Med* 207, 2187-2194.

Sanford, M. (2015). Blinatumomab: first global approval. *Drugs* 75, 321-327.

Scheinberg, D.A., Lovett, D., Divgi, C.R., Graham, M.C., Berman, E., Pentlow, K., Feirt, N., Finn, R.D., Clarkson, B.D., Gee, T.S., *et al.* (1991). A phase I trial of monoclonal antibody M195 in acute

REFERENCES

myelogenous leukemia: specific bone marrow targeting and internalization of radionuclide. *J Clin Oncol* 9, 478-490.

Schneider, H., Downey, J., Smith, A., Zinselmeyer, B.H., Rush, C., Brewer, J.M., Wei, B., Hogg, N., Garside, P., and Rudd, C.E. (2006). Reversal of the TCR stop signal by CTLA-4. *Science* 313, 1972-1975.

Schubert, I., Kellner, C., Stein, C., Kugler, M., Schwenkert, M., Saul, D., Mentz, K., Singer, H., Stockmeyer, B., Hillen, W., *et al.* (2011). A single-chain triplebody with specificity for CD19 and CD33 mediates effective lysis of mixed lineage leukemia cells by dual targeting. *MAbs* 3, 21-30.

Schwartz, R.H. (1992). Costimulation of T lymphocytes: the role of CD28, CTLA-4, and B7/BB1 in interleukin-2 production and immunotherapy. *Cell* 71, 1065-1068.

Seiffert, M., Brossart, P., Cant, C., Cella, M., Colonna, M., Brugger, W., Kanz, L., Ullrich, A., and Buhring, H.J. (2001). Signal-regulatory protein alpha (SIRPalpha) but not SIRPbeta is involved in T-cell activation, binds to CD47 with high affinity, and is expressed on immature CD34(+)CD38(-) hematopoietic cells. *Blood* 97, 2741-2749.

Shlush, L.I., Zandi, S., Mitchell, A., Chen, W.C., Brandwein, J.M., Gupta, V., Kennedy, J.A., Schimmer, A.D., Schuh, A.C., Yee, K.W., *et al.* (2014). Identification of pre-leukaemic haematopoietic stem cells in acute leukaemia. *Nature* 506, 328-333.

Singer, H., Kellner, C., Lanig, H., Aigner, M., Stockmeyer, B., Oduncu, F., Schwemmlein, M., Stein, C., Mentz, K., Mackensen, A., *et al.* (2010). Effective elimination of acute myeloid leukemic cells by recombinant bispecific antibody derivatives directed against CD33 and CD16. *J Immunother* 33, 599-608.

REFERENCES

- Slee, J.B., Christian, A.J., Levy, R.J., and Stachelek, S.J. (2014). Addressing the Inflammatory Response to Clinically Relevant Polymers by Manipulating the Host Response Using ITIM Domain-Containing Receptors. *Polymers (Basel)* 6, 2526-2551.
- Spasevska, I., Duong, M.N., Klein, C., and Dumontet, C. (2015). Advances in Bispecific Antibodies Engineering: Novel Concepts for Immunotherapies. *J Blood Disord Transfus* 6.
- Stoute, J.A., Gombe, J., Withers, M.R., Siangla, J., McKinney, D., Onyango, M., Cummings, J.F., Milman, J., Tucker, K., Soisson, L., *et al.* (2007). Phase 1 randomized double-blind safety and immunogenicity trial of *Plasmodium falciparum* malaria merozoite surface protein FMP1 vaccine, adjuvanted with AS02A, in adults in western Kenya. *Vaccine* 25, 176-184.
- Subramanian, S., Parthasarathy, R., Sen, S., Boder, E.T., and Discher, D.E. (2006). Species- and cell type-specific interactions between CD47 and human SIRPalpha. *Blood* 107, 2548-2556.
- The Cancer Genome Atlas Research, N. (2013). Genomic and Epigenomic Landscapes of Adult De Novo Acute Myeloid Leukemia. *The New England journal of medicine* 368, 2059-2074.
- Thol, F., Schlenk, R.F., Heuser, M., and Ganser, A. (2015). How I treat refractory and early relapsed acute myeloid leukemia. *Blood* 126, 319-327.
- Timms, J.F., Swanson, K.D., Marie-Cardine, A., Raab, M., Rudd, C.E., Schraven, B., and Neel, B.G. (1999). SHPS-1 is a scaffold for assembling distinct adhesion-regulated multi-protein complexes in macrophages. *Curr Biol* 9, 927-930.
- Tomasello, E., Cant, C., Buhring, H.J., Vely, F., Andre, P., Seiffert, M., Ullrich, A., and Vivier, E. (2000). Association of signal-regulatory proteins beta with KARAP/DAP-12. *Eur J Immunol* 30, 2147-2156.

REFERENCES

- Tsai, K.K., and Daud, A.I. (2015). Nivolumab plus ipilimumab in the treatment of advanced melanoma. *J Hematol Oncol* 8, 123.
- van Beek, E.M., Cochrane, F., Barclay, A.N., and van den Berg, T.K. (2005). Signal regulatory proteins in the immune system. *J Immunol* 175, 7781-7787.
- Veillette, A., Thibaudeau, E., and Latour, S. (1998). High expression of inhibitory receptor SHPS-1 and its association with protein-tyrosine phosphatase SHP-1 in macrophages. *J Biol Chem* 273, 22719-22728.
- Vellenga, E., van Putten, W., Ossenkoppele, G.J., Verdonck, L.F., Theobald, M., Cornelissen, J.J., Huijgens, P.C., Maertens, J., Gratwohl, A., Schaafsma, R., *et al.* (2011). Autologous peripheral blood stem cell transplantation for acute myeloid leukemia. *Blood* 118, 6037-6042.
- Wang, L., Hu, H., Yang, J., Wang, F., Kaisermayer, C., and Zhou, P. (2012). High yield of human monoclonal antibody produced by stably transfected *Drosophila schneider* 2 cells in perfusion culture using wave bioreactor. *Mol Biotechnol* 52, 170-179.
- Webster, R.M. (2014). The immune checkpoint inhibitors: where are we now? *Nat Rev Drug Discov* 13, 883-884.
- Weiner, G.J. (2010). Rituximab: mechanism of action. *Semin Hematol* 47, 115-123.
- Weiskopf, K., Ring, A.M., Ho, C.C.M., Volkmer, J.-P., Levin, A.M., Volkmer, A.K., Özkan, E., Fernhoff, N.B., van de Rijn, M., Weissman, I.L., *et al.* (2013). Engineered SIRP α Variants as Immunotherapeutic Adjuvants to Anticancer Antibodies. *Science* 341, 88-91.
- Weiskopf, K., and Weissman, I.L. (2015). Macrophages are critical effectors of antibody therapies for cancer. *MAbs* 7, 303-310.

REFERENCES

- Wolf, E., Hofmeister, R., Kufer, P., Schlereth, B., and Baeuerle, P.A. (2005). BiTEs: bispecific antibody constructs with unique anti-tumor activity. *Drug Discov Today* 10, 1237-1244.
- Yamao, T., Noguchi, T., Takeuchi, O., Nishiyama, U., Morita, H., Hagiwara, T., Akahori, H., Kato, T., Inagaki, K., Okazawa, H., *et al.* (2002). Negative regulation of platelet clearance and of the macrophage phagocytic response by the transmembrane glycoprotein SHPS-1. *J Biol Chem* 277, 39833-39839.
- Zeidler, R., Mysliwietz, J., Csanady, M., Walz, A., Ziegler, I., Schmitt, B., Wollenberg, B., and Lindhofer, H. (2000). The Fc-region of a new class of intact bispecific antibody mediates activation of accessory cells and NK cells and induces direct phagocytosis of tumour cells. *Br J Cancer* 83, 261-266.
- Zeidler, R., Reisbach, G., Wollenberg, B., Lang, S., Chaubal, S., Schmitt, B., and Lindhofer, H. (1999). Simultaneous activation of T cells and accessory cells by a new class of intact bispecific antibody results in efficient tumor cell killing. *J Immunol* 163, 1246-1252.
- Zhu, C., Anderson, A.C., Schubart, A., Xiong, H., Imitola, J., Khoury, S.J., Zheng, X.X., Strom, T.B., and Kuchroo, V.K. (2005). The Tim-3 ligand galectin-9 negatively regulates T helper type 1 immunity. *Nat Immunol* 6, 1245-1252.

7. ABBREVIATIONS

ADCC	Antibody-dependent cellular cytotoxicity
ADCP	Antibody-dependent cellular phagocytosis
AML	Acute myeloid leukemia
Ang2	Angiopoietin 2
APC	Antigen presenting cell
ASXL1	Additional sex combs-like 1
BiTE	Bispecific T cell engager
bsAbs	Bispecific antibodies
CD	Cluster of differentiation
CDC	Complement-dependent cytotoxicity
CDR	Complementarity-determining region
CEA	Carcinoembryonic antigen
CEBPA	CCAAT/enhancer-binding protein alpha
CTLA-4	Cytotoxic T-lymphocyte antigen 4
DAP12	DNAX activation protein 12
DC	Dendritic cell
DNA	Deoxyribonucleic acid
DNMT3A	DNA methyltransferase 3A
DVD	Dual-Variable-Domain
EMA	European Medicines Agency
EpCAM	Epithelial cell adhesion molecule
FAK	Focal adhesion kinase
FcγR	Fc gamma receptor
FDA	Food and Drug Administration
FLT3	FMS-related tyrosine kinase 3
FYB	FYN-binding protein

ABBREVIATIONS

GRB2	Growth-factor-receptor-bound protein 2
GVHD	Graft-versus-host disease
GVL	Graft-versus-leukemia
HCT	Hematopoietic-cell transplantation
HLA	Human leukocyte antigen
HSCs	Hematopoietic stem cells
IAP	Integrin-associated protein
IDH1	Isocitrate dehydrogenase 1
Ig	Immunoglobulin
IgSF	Immunoglobulin superfamily
IMAC	Immobilised metal affinity chromatography
ImmTACs	Immune mobilising monoclonal TCRs Against Cancer
ITIMs	Immunoreceptor tyrosine-based inhibitory motifs
ITAMs	Immunoreceptor tyrosine-based activating motifs
K _D	Dissociation constant
KIR	Killer cell immunoglobulin-like receptor
Lag 3	Lymphocyte activation gene 3
liCAD	Local inhibitory checkpoint antibody derivative
LSCs	Leukemia stem cells
mAb	Monoclonal antibody
MHC	Major histocompatibility complex
NHL	Non-Hodgkin's lymphoma
NK cells	Natural killer cell
NPM1	Nucleophosmin family, member 1
PD-1	Programmed death-1
PDL1	Programmed death ligand1
PTPNS1	Protein tyrosine phosphatase, non-receptor type substrate 1
RBC	Red blood cell

ABBREVIATIONS

scFv	Single chain fragment variable
SH2	Src homology 2
SHP-1	Src homology region 2 domain-containing phosphatase-1
SHP-2	Src homology region 2 domain-containing phosphatase-2
Sirp α	Signal regulatory protein alpha
SCAP2	SRC-family-associated phosphoprotein 2
TCR	T cell receptor
TET2	Tet oncogene family, member 2
Tim3	T cell membrane protein 3
TSP-1	Thrombospondin-1
VEGF	Vascular endothelial growth factor
WT	Wilms' tumor gene 1

8. ACKNOWLEDGEMENTS

First of all I would like to thank my supervisor Prof. Dr. Karl-Peter Hopfner for giving me the opportunity to work in the extremely interesting field of antibody engineering and immunotherapy. I am especially thankful for him giving me the freedom in designing my experiments and project. Thank you for your support and ideas.

I also would like to thank Prof. Dr. Marion Subklewe and Christina Krupka for the collaboration and time spent on scientific discussions.

Special thanks go to Prof. Dr. Kirsten Lauber together with Anne Ernst, who invested a lot of time and scientific advice in teaching me how to handle macrophages. It was a very fruitful cooperation and I certainly appreciated your honest interest in my PhD project. Thank you also together with PD Dr. med. Sebastian Kobold, for being a member of my thesis advisory committee.

I am thankful to Prof. Dr. Klaus Förstemann for being the second examiner of this thesis.

I am very grateful to Christian Schiller for his patient advices in protein purification, Martina Müller and Christian Linke-Winnebeck for help with SAXS data analysis, Robert Byrne for proof-reading and especially Nadja Fenn for supporting me with the patent application process and various other things. The whole Hopfner group and former members deserve particular gratitude for the friendly and most enjoyable working atmosphere in the lab. Special thanks go to the antibody subgroup fellows Alex, Moni, Laia and Claudia for their help. I really enjoyed working together with you.

Tommy, you have been my support through every aspect of life. I can't express how important you are to me. Without you everything is stupid. I am so much looking forward to our next adventures together with XX. You complete me.

Zuletzt möchte ich mich bei meinen Eltern, Brüdern, Cousinen, Freunden, sowie Charly und Doris bedanken. Ihr alle habt wesentlich dazu beigetragen, dass ich so erfolgreich durch diese anstrengende Zeit gekommen bin.

9. CURRICULUM VITAE

Personal Data

Name Nadine Moritz

Nationality Austria

Education

Since 12/2012 **Gene Center, Ludwig Maximilian University Munich**, Germany

PhD thesis in the group of Prof. Dr. Karl-Peter Hopfner.

April 9th, 2010 **University of Vienna**, Graduation

Diploma thesis: “The role of type I interferon in V-abl induced leukemia” (In the group of Dr. Dagmar Stoiber-Sakaguchi / Prof. Dr. Veronika Sexl)

2004 – 2010 **University of Vienna**, Diploma study of biology, specialized in genetics/microbiology

1996– 2004 **Gymnasium Werndlpark**, Steyr, Austria

Work experience

10/2011 – 10/2012 **Helmholtz Center Munich - Research unit Stem Cell Dynamics**, Munich, Germany

Scientist in the group of Dr. Timm Schroeder. “Lineage choice in hematopoiesis: transcription factor networks.”

09/2010 – 8/2011 **Dana-Farber Cancer Institute**, Boston, USA

Emil-Boral fellow in the group of Prof. A. Thomas Look. “Modelling myelodysplastic syndromes in zebrafish.”